Annual Report FY1999

平成 11 年度 活動報告

Institute for Geothermal Sciences

Graduate School of Science

Kyoto University

京都大学

大学院理学研究科

附属地球熱学研究施設

Institute for Geothermal Sciences
Graduate School of Science
Kyoto University

京都大学大学院理学研究科
附属地球熱学研究施設

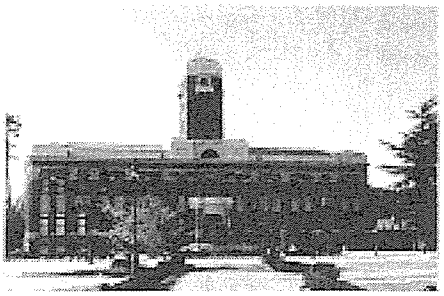

Beppu Geothermal Research Laboratory
Noguchibaru, Beppu 874-0903, Japan
Telephone: +81-977-22-0713
Facsimile : +81-977-22-0965
別府
〒874-0903　大分県別府市野口原
電話　　: 0977-22-0713
ファックス: 0977-22-0965
Homepage: http://www.vgs.kyoto-u.ac.jp

Aso Volcanological Laboratory
Choyo, Aso, Kumamoto 869-1404, Japan
Telephone: +81-9676-7-0022
Facsimile : +81-9676-7-2153
阿蘇（火山研究センター）
〒869-1404　熊本県阿蘇郡長陽村
電話　　: 09676-7-0022
ファックス: 09676-7-2153
Homepage:
http://www.kugi.kyoto-u.ac.jp/avl.html

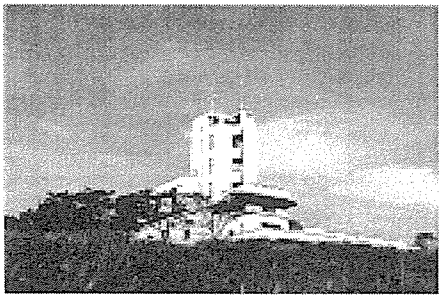

Front Cover Image:
The strombolian explosion in the 1st crater of Mt. Nakadake, Aso volcano in October 1979.
（Photograph: M. Sako）
表紙の写真:
1979 年 10 月の阿蘇中岳第 1 火口のストロンボリ式噴火の様子
（迫幹雄撮影）

Editorial compilation by S. Ohsawa
Printing by Nisshin Printing House, Inc.
May 2000

目次　Contents

序

地球熱学研究施設構成員各位のご努力により、施設発足第３年次に当たる平成 11（1999）年度も、研究活動はもちろんのこと、さまざまな活動が活発に行われました。ここに、その記録をとりまとめた年報を発行できることを喜びたいと思います。

平成 13 年４月現在、本施設には 11 名の教官が所属しておりますが、欠員１名については、早急に任用すべく手続きを進めているところです。これに加えて、日本学術振興会の特別研究員３名、文部省の特別予算による非常勤研究員３名、研修員１名、大学院生７名、さらに１名の留学生が施設に滞在して研究活動を行いました。また、外国人客員研究員には、平成 11 年４月１日から 12 年３月 31 日まで、John P. Matthews 教授が就任され、「高分解能リモートセンシングによる九州の火山及びその他の地球物理的現象に関する研究」のテーマで研究を行われました。

平成９年４月に本施設が発足して以来、地球物質科学に関連した研究組織と実験設備の整備が進められてきましたが、第３年次においても、よりいっそうの充実が図られ、平成 12 年２月１日付けで山梨県環境科学研究所より柴田知之助手を迎えることができました。他方、火山研究の分野においても変化がありました。まず、平成３年より８年間にわたって主に火山地下構造の調査・研究に多くの貢献をされた筒井智樹助手が、平成 11 年 11 月１日付けで秋田大学工学資源学部に助教授としてご栄転されました。ついで、田中良和助教授が平成 13 年１月１日付けで教授に昇任されました。

行政職では、昭和 32 年から 42 年間余りの長きにわたって、阿蘇における観測と施設の維持・管理を支援していただいた増田秀晴技官が、平成 12 年３月 31 日をもって定年により退官なさいました。また、同日付けで、別府の事務を担当していただいた佐野きよか・中野ちはる両事務補佐員が退職されました。これらの方々に、深く感謝を申し上げる次第です。

研究経費については、一般校費に加えて、科学研究費補助金を始めとする研究費が支給され、また、国内外における共同研究も行なわれました。

施設発足後３年が経過し、研究を始めとする諸活動が活発化しつつありますが、よりいっそうの発展が望まれます。大学法人化という流れの中で、施設のあり方にも変革が迫られるのは必至でありましょう。こうした内外の状況のもと、私たちはさらなる努力を傾けなければなりません。この活動報告が、施設全員の相互理解と研鑽の拠り所として活用されることを願います。施設外の方々には、この報告を通して私たちの活動をご理解いただき、ご指導ご助言をたまわりますよう、お願い申し上げます。

平成12年４月

地球熱学研究施設長

由佐　悠紀

Preface

It is my great pleasure to present the third issue of the annual report from the Institute for Geothermal Sciences, Graduate School of Science, Kyoto University, describing our activities in fiscal year 1999, which covered the period between April 1999 and March 2000.

At present, there are 11 faculty members at the institute; we are currently in the process of filling one vacant faculty position. In addition to the regular faculty members, three JSPS research fellows, three special research fellows, one visiting researcher, seven graduate students and one foreign student worked at the Beppu and/or the Aso facilities. From 1 April 1999 to 31 March 2000, Dr. John Matthews joined as Visiting Professor in Beppu working on an investigation entitled "Study of Kyushu volcanoes and other geophysical phenomena using high spatial resolution remote sensing techniques."

Several changes in staff are to report: Since the Institute was established in April 1997, we have been putting emphasis on strengthening the branch of earth material sciences. As part of this effort, Dr. T. Shibata joined us on 1 February, 2000, as Assistant Professor at Beppu, coming from the Yamanashi Institute of Environmental Sciences. Some changes in staff occurred also in the branch of volcanology. Firstly, Dr. T. Tsutsui, Assistant Professor at Aso, accepted a position as Associate Professor at Akita University as of 1 November, 1999. Since 1991, he had made many contributions to the Institute by furthering the study of subsurface structure beneath volcanic areas. Secondly, Dr. Y.Tanaka was promoted to Professor at Aso on 1 January, 2000.

Mr. H.Masuda, Technician, retired from Kyoto University by reaching retirement age on 31 March 2000. Over the last 42 years, he has made many important contributions to various observations and to the maintenance of the facilities at the Aso Laboratory. On the same day, Ms. K. Sano and Ms. T. Nakano, Secretaries, left the Beppu Laboratory. I would like to express my cordial gratitude to all of them.

In addition to the regular budget, we were supported by funds from a variety of other sources, including Grants in Aid for Scientific Research from the Ministry of Education, Science, Sports and Culture of Japan; many successful collaborations with national and international researchers have also taken place.

Research and other activities have progressed steadily since the establishment of the Institute, and the Institute is expected to develop further in the future. The new policy of juridical personalization of national universities will, however, cause a significant change in the organization of the Institute. Under these changing circumstances inside and outside the Institute, we must strengthen our efforts even more. I hope that this annual report will contribute to the mutual understanding among the members of the Institute, as well as present their activities to a broader audience. I would like to invite all people to investigate our activities through this report and am looking forward to hearing comments and advise concerning the further development of the Institute.

Beppu, April 2000
Yuki Yusa, Professor/Director

構成員　Member

教授　Professors

田中良和　Yoshikazu Tanaka
巽　好幸　Yoshiyuki Tatsumi
由佐悠紀　Yuki Yusa 〔施設長 Director〕

助教授　Associate Professors

古川善紹　Yoshitsugu Furukawa
大沢信二　Shinji Ohsawa
須藤靖明　Yasuaki Sudo

助手　Assistant Professors

橋本武志　Takeshi Hashimoto
川本竜彦　Tatsuhiko Kawamoto
小野博尉　Hiroyasu Ono
柴田知之　Tomoyuki Shibata
鈴木勝彦　Katsuhiko Suzuki
筒井智樹　Tomoki Tsutsui
〔平成11年11月秋田大学に転出〕

外国人研究員　Visiting Faculty

John P. Matthews
〔平成12年4月地球物理学教室へ転出〕

技官　Technical Professionals

外　輝明　Teruaki Hoka
増田秀晴　Hideharu Masuda
〔平成12年3月退職〕
馬渡秀夫　Hideo Mawatari
迫　幹雄　Mikio Sako
吉川　慎　Shin Yoshikawa

研究員　Research Associates

熊谷一郎　Ichiro Kumagai
坂中伸也　Shin'ya Sakanaka
〔平成12年4月秋田大学へ転出〕
佐野貴司　Takashi Sano
〔平成12年4月富士常葉大学へ転出〕
下田　玄　Gen Shimoda
宇津木充　Mitsuru Utsugi
芳川雅子　Masako Yoshikawa

研修員・客員研究員　Visiting Researcher

大上和敏　Kazutoshi Oue
Iskandar Zulkarnain

大学院生　Graduate students

相澤義高　Yoshitaka Aizawa
〔平成12年3月修了〕
網田和宏　Kazuhiro Amita
長谷英彰　Hideaki Hase
可児智美　Tomomi Kani
John Makario Londono
森　健彦　Takehiko Mori
中坊　真　Makoto Nakaboh
吉川美由紀　Miyuki Yoshikawa

研究支援職員　Technical Assistant

Bogdan S. Vaglarov

事務補佐員　Secretaries

佐野きよか　Kiyoka Sano
〔平成12年3月退職〕
今村町子　Machiko Imamura
中野ちはる　Chiharu Nakano
〔平成12年3月退職〕

臨時用務員　Temporal Assistant

山崎咲代　Sakiyo Yamasaki

研 究 活 動　Research Activities

研究報告　Scientific Reports

Experimental determination of compressional wave velocities of olivine aggregate up to 1000°C at 1 GPa

Yoshitaka Aizawa[1], Kazuhiko Ito[2], and Yoshiyuki Tatsumi[3]

[1]Graduate School of Human and Environmental Studies, Kyoto University, Kyoto 606-8501, Japan

[2]Faculty of Business Administration, Southern Osaka University, Osaka 587-8555, Japan

[3]Institute for Geothermal Sciences, Graduate School of Science, Kyoto University, Beppu 874-0903, Japan

The velocity of the compressional wave (V_P) was measured for olivine aggregates at temperatures up to 1000°C at 1 GPa using a piston-cylinder high-pressure apparatus. The samples used in the present study were hot-pressed olivine aggregates with uniform chemical composition. The value of V_P at 1 GPa and an ambient temperature is 8.42 km/s, which is identical to that in previous measurements of olivine single-crystals. The temperature derivative of V_P ($\partial V_P / \partial T$= -5.8 x 10^{-4} km·s^{-1}·K^{-1}) obtained from the present experiments at 1 GPa is slightly higher than the previously reported value at an ambient pressure. The temperature gradient for constant velocity $(dT/dZ)_c$ is calculated to be 7°C/km. Taking the temperature gradient in the upper mantle into account (15°C/km within the lithosphere and 0.6°C/km within the asthenosphere), it is suggested that the low velocity zone in the upper mantle could be caused by a drastic change in the temperature gradient at the lithosphere/asthenosphere boundary.

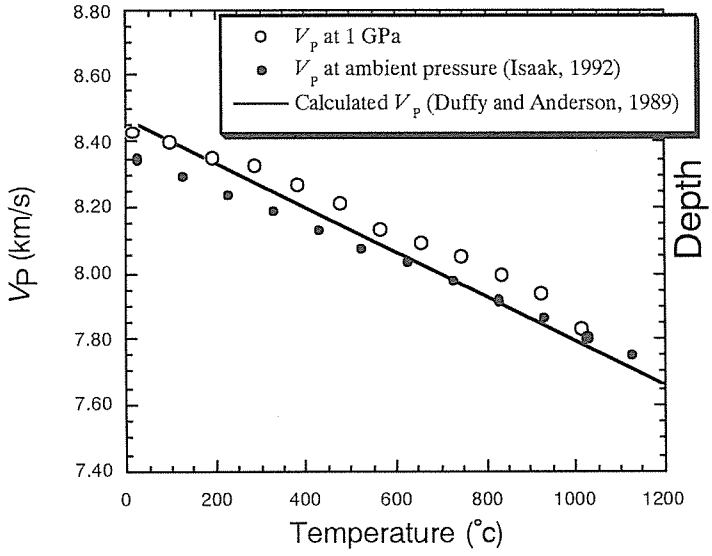

Fig. 1. V_P as a function of temperature at 1 GPa obtained from this study, together with previous measurements of a single crystal at an ambient pressure [Isaak, 1992]. The thick line represents the calculated velocities based on the procedures of Duffy and Anderson (1989).

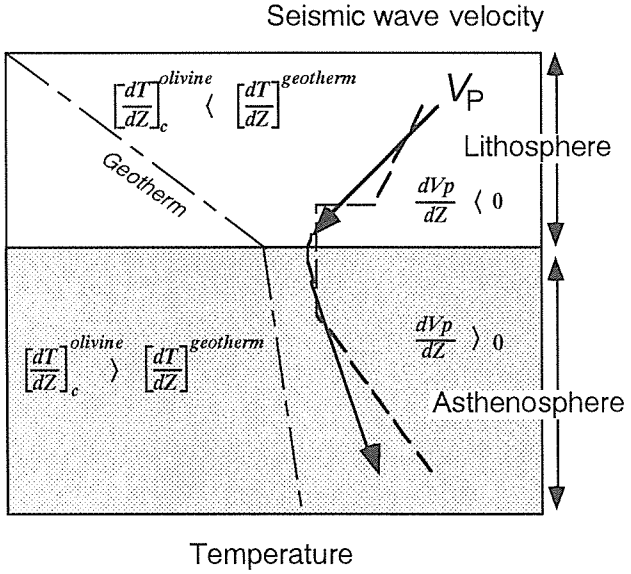

Fig. 2. Relationship between a geotherm estimated by the plate model [McKenzie, 1967] and seismic wave velocity of olivine (upper mantle) as a function of depth. According to the temperature gradient, (dVP/dZ) may change from negative to positive at the lithosphere/asthenosphere boundary, causing a low velocity zone. Seismic studies determine the average velocities of the lithosphere and the asthenosphere (dashed line), although the real velocity may change continuously.

Resistivity structure of upflow zone of geothermal fluid in Beppu geothermal field

Amita, K., Ohsawa, S., Hase, H., Sakanaka, S.,
Oue, K., Shimoda, G., Hashimoto, T., Yusa, Y.

Beppu hotspring at the eastern end of Central Kyushu, is one of the biggest geothermal fields in Japan, in which fumarolic and hotspring activity spreads out up from the Tsurumi volcanic group down to the eastern coast, over a 5 km (E-W) by 8 km (N-S) range. Flow rate of the hotspring water including fumarolic steam and heat flow amounts to 50,000 tons/day and 350 MW, respectively. The aim of this study is to localize the upflow zone of the parent geothermal fluid as a pattern of contrast in the electrical conductivity. On May and June 1999, broadband MT surveys were performed around the Tsurumi volcano group.

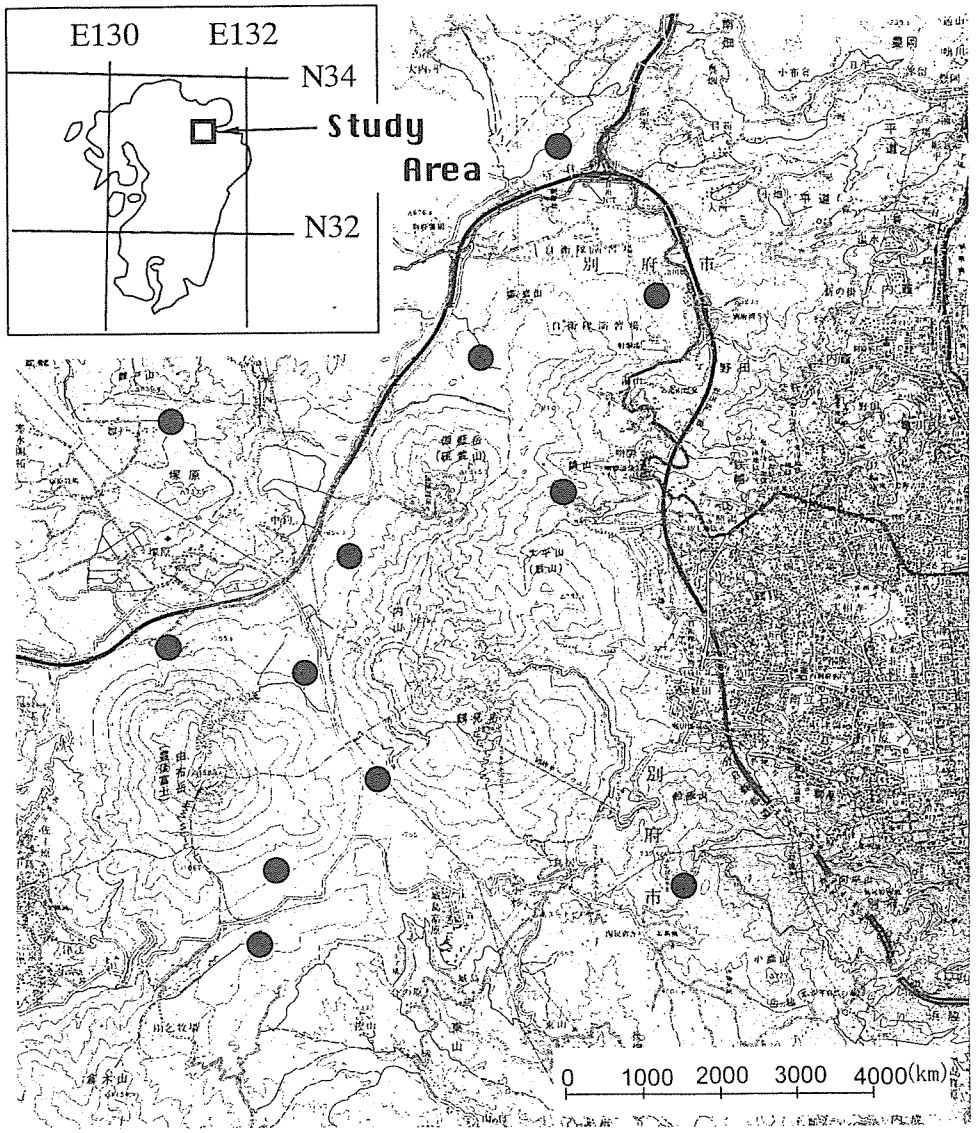

Fig.1. Location of Beppu geothermal field and the distribution of magnetotelluric sites.

WATER PARTITIONING AMONG MANTLE PHASES

Bolfan-Casanova, N.[1], Keppler, H.[1], Kawamoto, T., and Rubie, D. C.[1]

[1] Bayerisches Geoinstitut, Universität Bayreuth, D-95440 Bayreuth, Germany

The atmosphere and oceans formed by degassing of the Earth's mantle. However, considerable amounts of water could still be stored in the mantle in the form of hydroxyl point defects in nominally anhydrous minerals (NAMs) such as olivine, pyroxene, garnet and their high-pressure polymorphs. Such dissolved water plays a key role in the geodynamics of the Earth because it affects melting behaviour and transport properties of minerals, such as deformation, diffusion and electrical conduction. In the recent years data on the solubility of water in NAMs of the upper mantle have become available (Bell and Rossman, 1992; Kohlstedt et al., 1996). In addition, considerable progress has been achieved in determining the stability of dense hydrous magnesium silicates (DHMS) (Thompson, 1992; Frost and Fei, 1998). DHMS may play an important role in carrying water back into the mantle by subduction processes whereas NAMs will be responsible for the storage of water in the mantle itself. However, little is known about the partitioning of water among these phases. This is particularly important for the recycling of water by subduction and convection in the mantle.

We conducted multi-anvil experiments in the MgO-SiO_2-H_2O system to study partitioning of water at P-T conditions of the transition zone and top of the lower mantle. The water contents of synthetic phases were measured with FTIR spectroscopy. The results show, as illustrated in Fig. 1, that among all NAMs (1) magnesium silicate perovskite is the only phase which does not dissolve any detectable amount of water, and (2) minerals having Mg_2SiO_4 composition, namely wadsleyite and ringwoodite, can incorporate up to 3 % wt H_2O, and (3) the polymorphs of $MgSiO_3$, namely clinoenstatite, ilmenite and majorite, only dissolve up to 2500 ppm wt H_2O. The partitioning coefficients of water among these phases suggest that recycling of water by dehydration of subducting slabs and redistribution by convection should be particularly effective in the upper mantle and transition zone. Based on these results, recycling of water in the lower mantle appears to be much more difficult because only very small amounts of water partition into perovskite. However, the presence of transition metal cations and other elements such as Al may enhance water solubility, especially in perovskite, and may affect the above conclusions. We therefore are currently examining samples synthesised in wet peridotitic compositions (e.g. KLB-1).

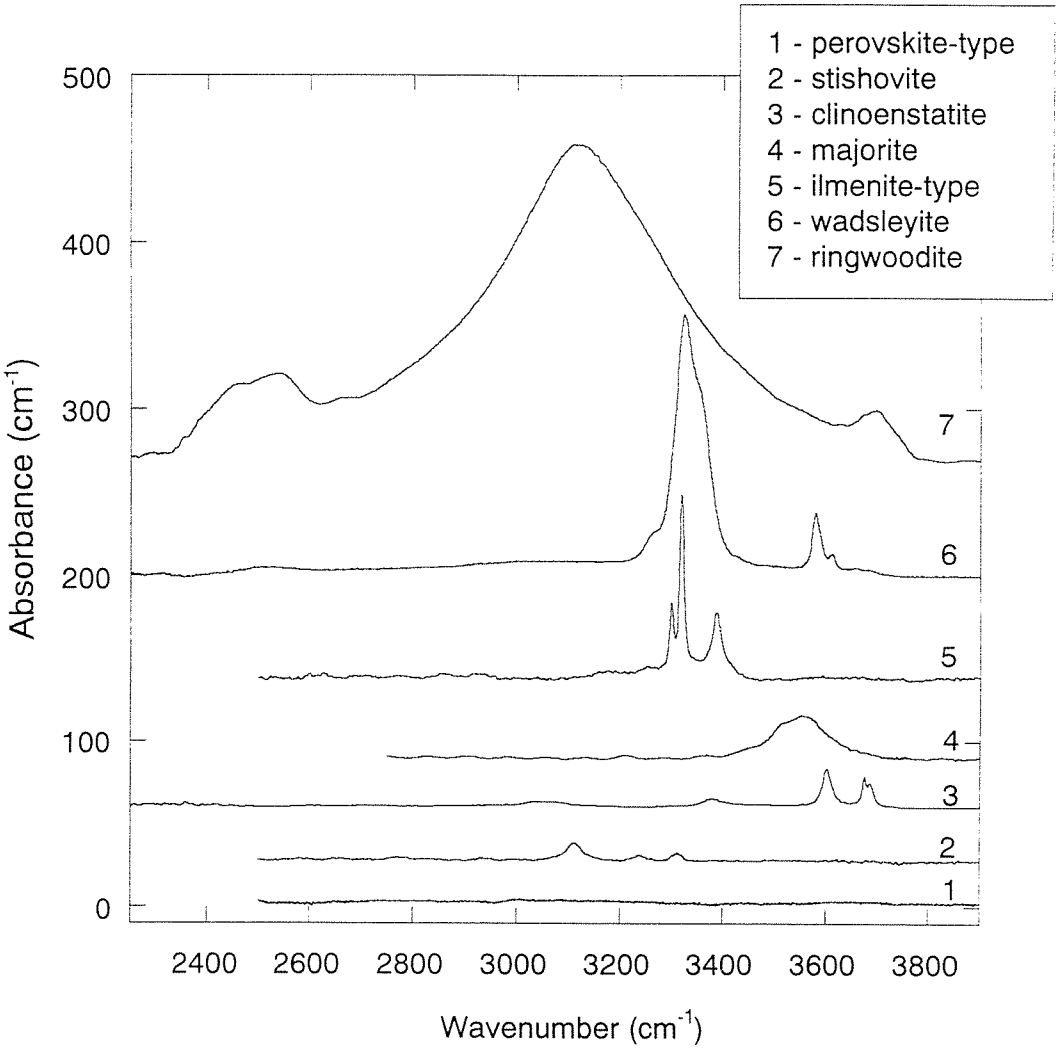

Figure 1. Unpolarized IR spectra in the OH stretching region of high-pressure nominally anhydrous silicates synthesized in the MgO- SiO_2-H_2O system.

References

Bell D. R. and Rossman G. R. (1992), Water in Earth´s mantle: the role of nominally anhydrous minerals, *Science* 255: 1391-1397

Kohlstedt D.L., Keppler H. and Rubie D.C. (1996), Solubility of water in the _, _ and _ phases of $(Mg,Fe)_2SiO_4$, *Contribution to Mineral Petrology* 123: 345-357

Thompson A. B. (1992), Water in the Earth´s upper mantle, *Nature* 238: 295-302

Frost D. J. and Fei Y. (1998), The stability of phase D at high pressure and high temperature, *Journal of Geophysical Research*, 103: 7463-7474.

Interplate coupling and deformation in the accretionary prism in the Southwest Japan subduction zone

Furukawa, Y.

In subduction zones interplate thrust earthquakes have been repeatedly occurred, which is caused by the frictional coupling between the overlying and the subducting plates. Temperature structure in subduction zones has been estimated, and the relation between temperature and the depth extent of the seismogenic zone has been discussed: A critical temperature is proposed to limit the landward extent of the seismogenic zone at the plate interface, while depth extent of dehydration reactions in the subducting oceanic crust is also suggested to control the depth of the seismogenic fault.

In most of subduction zones accretionary prism has been developed. In the accretionary prism many folds and thrusts are commonly observed; the deformation is likely to be caused by the frictional stress at the base of the prism. The deformation in the prism then reflects the strength of the frictional coupling at the base of the prism, and gives information about the frictional coupling.

In the Southwest Japan subduction zone accretionary prism is well developed, and the accretion of sediments is presently active. The macroscopic flow of accreted materials in the prism was suggested from observed surface heat flow data . In this subduction zone temperature structure has been estimated. In the previouses timates, however, deformation in the accretionary prism was not considered.

In this study temperature structure and deformation in the accretionary prism in the Southwest Japan subduction zone are simulated using a two-dimensional isoviscous corner flow model. Using surface heat flow data the average interplate frictional stress and the effective viscosity of the prism are estimated to be 2~30MPa and $10^{20\sim21}$Pa·s, respectively. The low stress value is probably due to high pore pressures caused by dehydration reactions in the subducting crust. Estimated temperature of the landward limit of the seismogenic zone is 350~500°C; when the frictional stress is considered, the temperature becomes ~100°C higher than that of the onset of plasticity of granitic rocks (350°C). The brittle-plastic transition of gabbroic rocks might control the depth extent of the seismogenic zone in lower crustal depths. Flow velocity at the bottom of the prism is estimated to be ~0.01m/yr, indicating that ~25% of the conversion has been consumed by the deformation of the accretionary prism in this subduction zone.

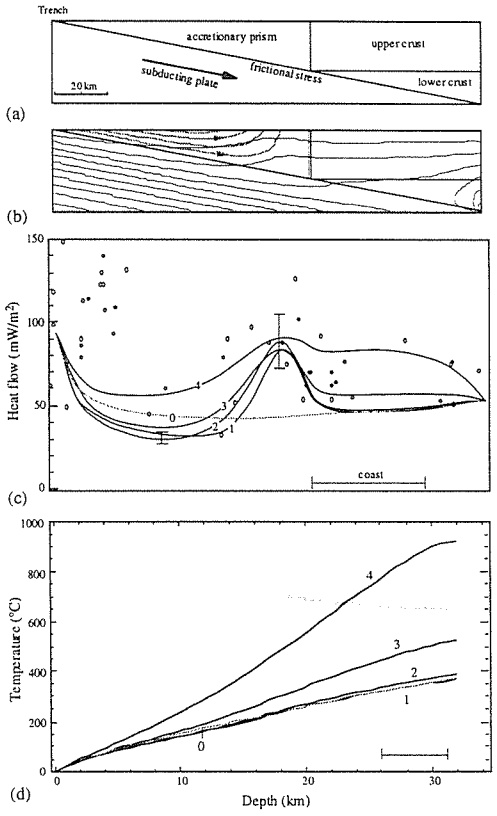

Figure Model geometry and calculation results. Locations of the trench are aligned and the same horizontal scale is used for these figures. (a) Model geometry; (b) Calculated temperature and flow structures at present: Isotherms with the interval of 100°C (solid lines) and stream lines (hatched lines). Arrows indicate the flow direction. (c) Calculated surface heat flow profiles for the frictional stress gradient and the effective viscosity of 0: no-flow; 1: (0.015MPa/km,10^{19}Pa·s); 2: (0.3,10^{20}); 3: (2.0,10^{21}); 4: (7.0,10^{22}). Two vertical bars indicate the calculated heat flow range for the case 2, when the stress gradient varies in the range of 0.2~0.4 MPa/km. Observed heat flow data (open circles) and the expected heat flow range in the landward side (hatched box) are also shown. The horizontal bar denotes the coastal range. (d) Calculated temperature profiles at the plate inter face for the five cases. The hatched line and the horizontal bar denote the wet solidus of basalts and the landward limit of the seismogenic zone, respectively.

Infrasonic precursors to a Vulcanian eruption at Sakurajima Volcano, Japan

M. Garcés, M. Iguchi, K. Ishihara, M. Morrissey, ***Y. Sudo,*** *and* ***T. Tsutsui***

Ten infrasonic stations, ten seismometers, and video images were utilized to monitor the May 17-19, 1998 eruption sequence of Sakurajima Volcano. During this seismo-acoustic experiment, we recorded hundreds of infrasonic tremor and long-period events associated with seismic signals, and observed a transition from almost complete quiescence to a mild Vulcanian eruption (VEI 2). Throughout the experiment, we noted a change in the character and number of infrasonic events with increasing volcanic activity, and this trend prompted the prolongation of the experiment for two additional days. This decision was fortuitous, as at 22:17 of May 19, 1998, the Japan Meteorological Agency released an eruption report. This eruptive event, which released ash and gases to a height of 2 km over the vent, was recorded continuously by one infrasonic and two seismic stations. We present the experimental setup as well as the procedure through which infrasonic signals may be incorporated into future eruption monitoring and forecasting algorithms of open-vent volcanic systems. In addition, our recordings suggest that infrasonic signals are more representative of processes occurring within the volcanic interior than seismic signals, which are strongly altered by diffraction and scattering in the volcanic edifice.

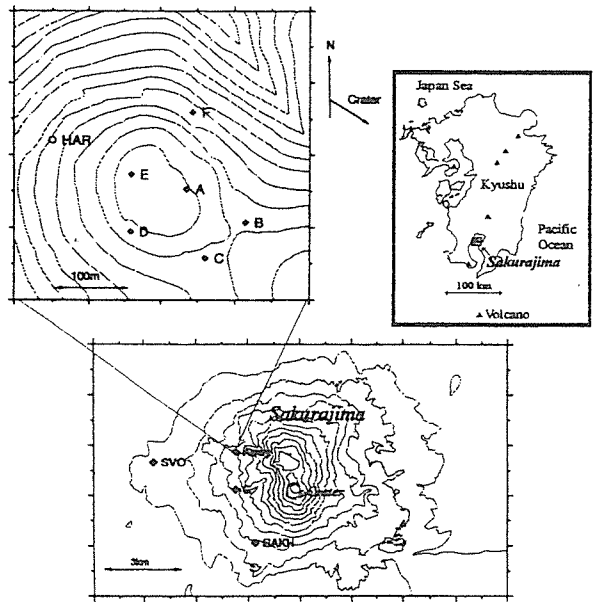

Figure 1. Experimental layout and location of network and array sites. The inset shows the six-element seismo-acoustic array configuration. All instruments in the array (stations A-F) were identical: three-component, Mark L-22 2 Hz seismometers, Setra model 270 absolute pressure microbarometers, and Hakusan digital recorders. Three 2-Hz vertical component seismometers were co-located with two Bruel and Kjaer (stations G and H) and one ACO (station I) low-frequency microphones. Station I was located close to E for calibration of the Setras. All pressure sensors have a flat frequency response in the 0.1-20 Hz bandwidth. An additional ACO microphone is located at the Sakurajima Volcanological Observatory (SVO), and one borehole 1 Hz seismometer (HAR) is located near the array site (after Sakai et al., 1996).

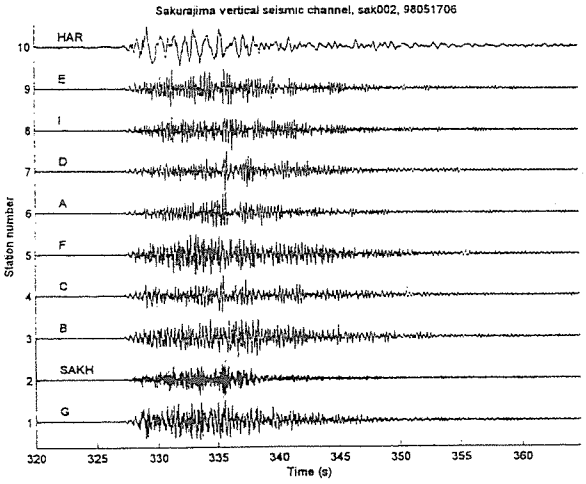

Figure 3. Normalized vertical seismic waveforms for the volcanic explosion of May 17, 1998. The amplitude of the seismic wave at station G is 0.1 micrometers/s.

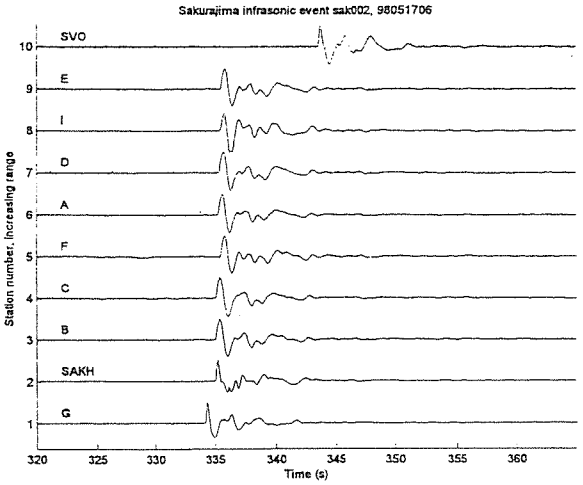

Figure 2. Normalized waveforms for the volcanic explosion of May 17, 1998. The maximum amplitude of the pressure wave at station G is 25.3 Pascals.

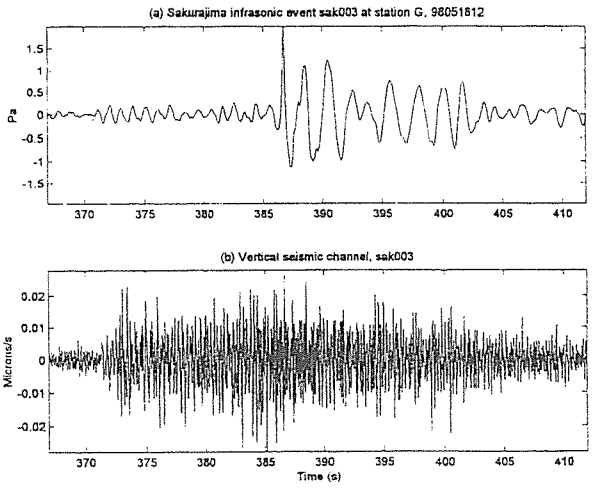

Figure 4. Acoustic and seismic waveforms for a tremor and LP event, recorded at station G on May 18, 1998.

Electrical studies on Mt.Kishima and Mt.Ojo, central cones of Aso Volcano

Hase, H. and Ustugi, M.

Mt.Kishima and Mt.Ojo are located at the northwestern side of the central cones of Aso Volcano. They were formed about three thousand years ago and two thousand years ago, respectively. They are younger than most of other cones belonging to Aso Volcano. We have conducted self-potential survey (SP) in the central cones of Aso Volcano since 1998. The authors detected baffling positive SP anomalies on Mt.Kishima and Mt. Ojo. Positive SP anomalies are often observed around fumarolic areas or thermal zones. However, we can not recognize any signs of fumarole or thermal areas on Mt.Kishima and Mt.Ojo. We suspect that the shallow electrical structure can provide an important information to clarify the mechanism causing positive SP anomalies there. We consider that a contrast of resistivity is one of the possible causes of the SP anomalies.

Some electric surveys have been previously attempted to clarify the electrical structure in Aso caldera, and the electrical structure of Aso caldera has been roughly revealed. However, no survey has ever focused on especially Mt.Kishima and Mt.Ojo. Hence, shallow geoelectrical information including Mt.Kishima and Mt.Ojo was not still enough. Accordingly we conducted bipole-dipole survey on Feb. 23 and 24 in 2000. In our experiment we injected alternative direct current up to 8A into the earth with a period of 20 seconds. We deployed a bipole source with its length of 1.9km. Bipole-dipole survey receives two horizontal components of telluric signal. On the method we use DC amplitude and vector direction of received electric fields to infer the conductivity of the earth. The data analysis of this survey is under processing. We are going to build a forward 1-D resistivity model at first.

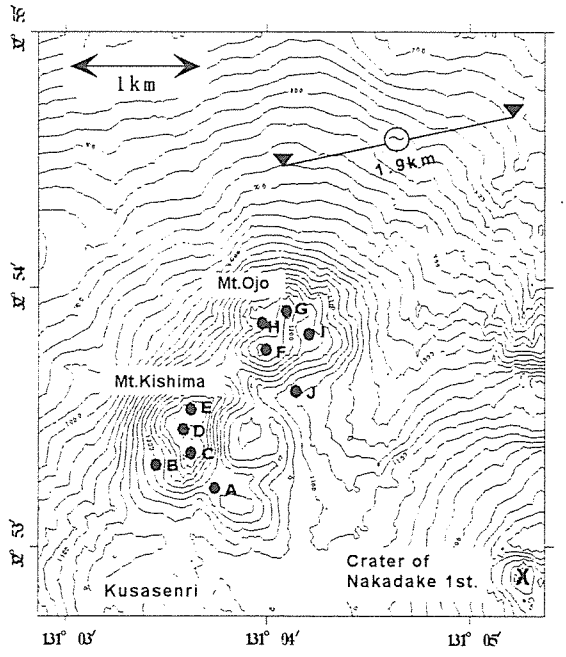

Fig.1 Location of bipole-dipole site
(●:receiving point, ▼:injection point of direct current)

Self-potential measurements on Iwate Volcanoes

Hase, H., Sakanaka, S., Tanaka, Y., *Goto, A.* and Taniguchi, H.**

**CNEAS, Tohoku University*

Iwate Volcano is one of the active volcanoes in northeastern Japan arc, which showed some symptoms of an eruption such as the action of seismicity, inflation of its edifice, and changes in fumarolic contents, in 1998. Mt. Ubakura is one of the cones belonging to Iwate Volcanic series, where geothermal activity on the ground surface can be seen in the vicinity of the summit. We conducted a self-potential (SP) survey on Mt.Ubakura on Nov. 13 and 14, 1999 in order to clarify if there is any electrical signature of geothermal fluid flow associated with volcanic activity. The survey line, which is almost 5km long, extends from the western flank of Mt.Inukura to Ohanabatake which is located at the west of Mt.Iwate. As the result of the survey, we recognized two positive peaks at the western flank and at the summit of Mt.Ubakura. There is some geothermal activity of Mt.Ubakura in the vicinity of the SP anomalies. The electrokinetic potential produced by subsurface fluid flow is a promising candidate for the cause of these SP anomalies. Accordingly, we consider these two peaks to correspond to upflow of geothermal fluid.

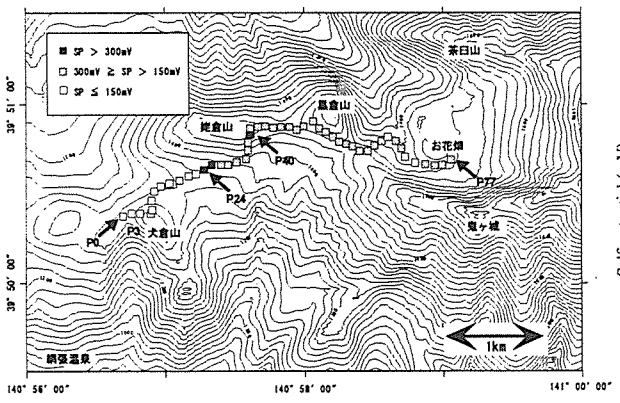

Fig. 1 Survey line of self-potential (SP) around Mt. Ubakura. The survey was conducted on Nov. 13 and 14 in 1999. P0 is the reference point. Topographic effect removed.

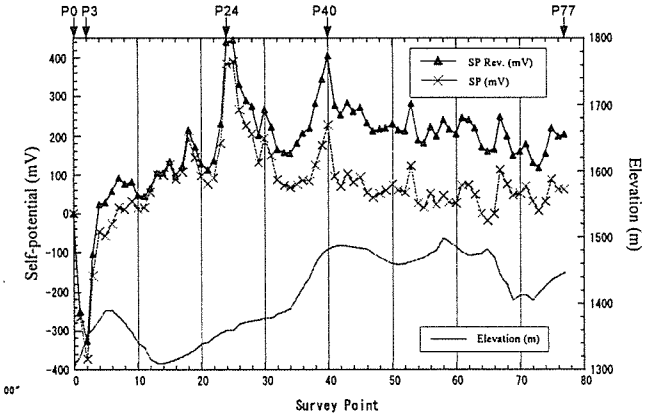

Fig. 2 Self-potential(mV) and Elevation(m) around Mt. Ubakura (×: raw data, ▲:revised value with topographic elevation (-1.0mV/m))

Self-potential measurements on the central cones of Aso Volcano (2)

Hase, H., Hashimoto, T., Sakanaka, S. and Tanaka, Y.

We have been conducted self-potential (SP) surveys since 1998 in the central cones of Aso Volcano, southwestern Japan. The aim of this research is clarifying the features of SP distribution in whole central cones of Aso Volcano, including hot spring areas and an active crater of Nakadake. We employed a pair of Cu-$CuSO_4$ non-polarized electrodes and a portable digital voltmeter with internal impedance of more than 10M-ohm.

As a result of the survey, we detected three characteristic positive anomalies: (i) a regional anomaly which centers on the Nakadake crater (+800mV); (ii) local anomalies around the hot spring areas (Jigoku-Tarutama, Yoshioka and Yunotani, +200mV); (iii) local anomalies around Mt.Kishima and Mt.Ojo (+300mV). Positive SP anomalies, which are often observed around fumarolic areas or thermal zones, are considered as a sign of subsurface hydrothermal activity. The most probable cause of these SP anomalies is thought to be the electrokinetic streaming potential produced by subsurface hydrothermal upflows. According to the electrokinetic theory, the source free flow across a boundary with different electrokinetic coupling coefficients causes electric charge on the boundary.

To explain the observed anomalies (i), we assume a dipole source that positive and negative poles located at 1km and at 10km in depth under the Nakadake crater, respectively. We also assume the resistivity of the ground as 100 ohm-m, the electric current as 85A. The result of one dimensional inversion of both MT and TDEM suggested the existence of low resistivity (less than 10 ohm-m) layer under about 1km deep. Also high resistivity layers were detected above and below the low resistive layer. Because of the strong contrast of resistivity, it is possible to assume that the positive charges are trapped at the boundary and the dipole source is formed by hydrothermal upflows up to 1km depth. We recognize the anomalies (ii) can be also explained by the same mechanism of (i). However, the mechanism that makes the anomaly (iii) is not clarified yet.

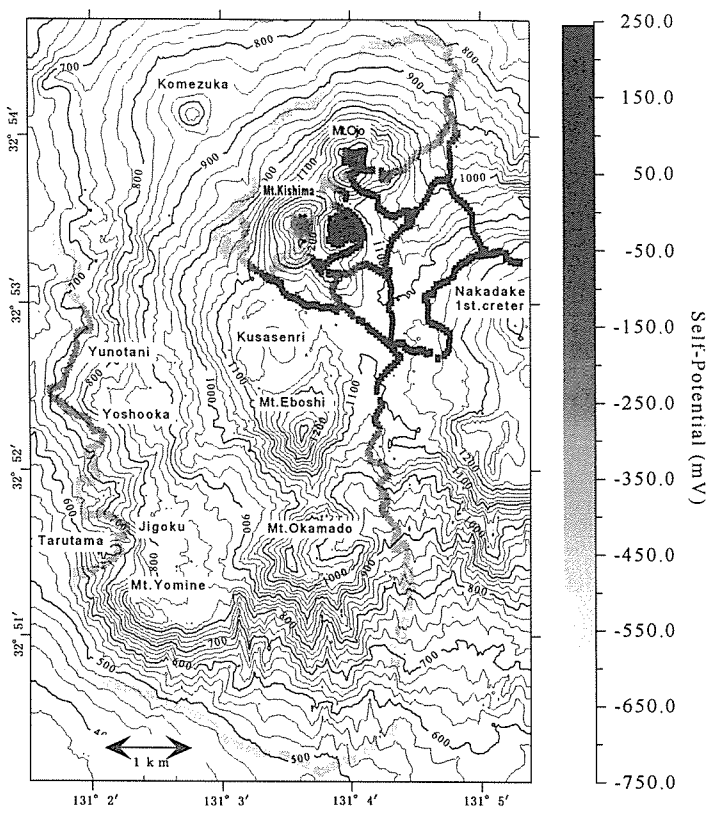

Fig.1 Survey line and data (revised value with topographic effect (-0.8mV/m)) of self-potential (SP) on the central cones of Aso Volcano

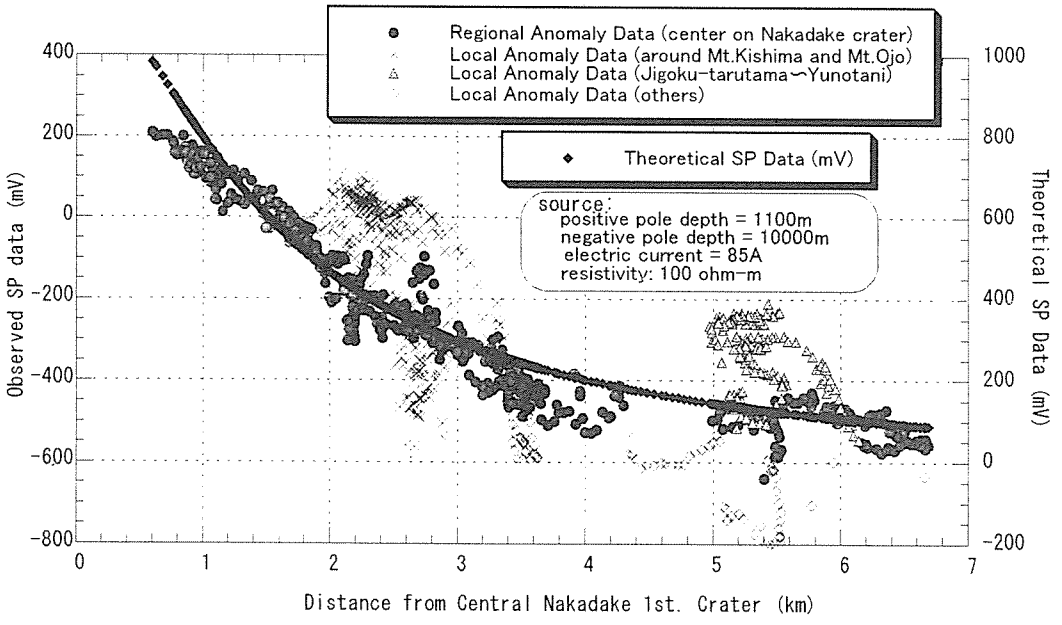

Fig.2 Observed SP data revised value with topographic effect (-0.8mV/m) and theoretical SP data (positive pole = 1100m, negative pole = 10000m, electric current = 85A, resistivity = 100 ohm-m)

Atmospheric electric fields associated with earthquakes that observed by corona current measurements

Hase, H., Tanaka, Y., Kamogawa, M.[1], Nagao, T.[2] and Uyeda, S.[3]

[1] Waseda Univ. [2] Earthquake Prediction Research Center, Tokai Univ.
[3] The Inst. Physical and Chemical Research (RIKEN)

Geoelectric potential changes in the earth's crust, electromagnetic wave seismo-electromagnetic emissions in atmosphere, and ionospheric disturbances have been well-known as the seismic electromagnetic phenomena. Although the measurements of electromagnetic wave emissions in the atmosphere have attracted the interests of researchers, there are few measurements of the atmospheric electric field, because a lot of noises and strong local effects prevent us from distinguishing signals and noises. However, we have tried the measurements of the atmospheric electric field by using corona current measurement that is relatively insensitive to noises, and we recognized that seismogenic electric field of the atmosphere on the earth's surface could be observed by using lightning warning devices called "Coronarm" that measures corona current. Corona current does not take place when the electric field is less than about 500 V/m, it is relatively easy to distinguish them from noises of meteorological origin such as lightning activity, rainfall and humidity by comparing seismic signals with neighboring meteorological data.

Coronarm has two types of sensors as shown in Fig. 1 (a). One is an antenna sensor for electric field changes, which is mainly for the detection of inductive and radiative electric field changes caused by distant lightning activity. The other is an electric field meter, which mainly measures the electric field caused by neighboring electrified thunderclouds by using the corona current. The lightning warning device gives us the warning information on cloud-ground lightning by combination of results of these two sensors. The antenna sensor and the electric field meter catch thundercloud activity from 20km to about 50km and within 10km, respectively. In this study, we mainly used the data of the electric field meter, namely, corona current.

Coronarm has been developed by Central Lightning Protection Co. Ltd. Coronarms have been set up at more than one thousand points all over the world, mostly in golf fields. Accordingly we have only to select a golf field which already have a Coronarm and to attach our recorder to it in order to install our observational station. In this study, we chose three golf fields (Aso golf club, Minami-Aso country club and Aso-Takamori golf club) inside the Aso Caldera for our stations. We also newly introduced the whole system of Coronarm at Ishihara station in Oita prefecture on 16 and 17 May in 1999 (Fig.2).

For the present, we have not yet obtained any coronal current events associated with earthquakes. One of the reason is that the adjustment of the sensors was not complete. We have to be very careful when we adjust a Coronarm sensor because the atmospheric electric field is easily changed by obstacles around the station such as mountains, trees or houses. Actually, the sensor of Aso-Takamori golf club had not worked properly because of the mis-adjustment of the sensor. We hope to obtain a clear event associated with an earthquake in the near future.

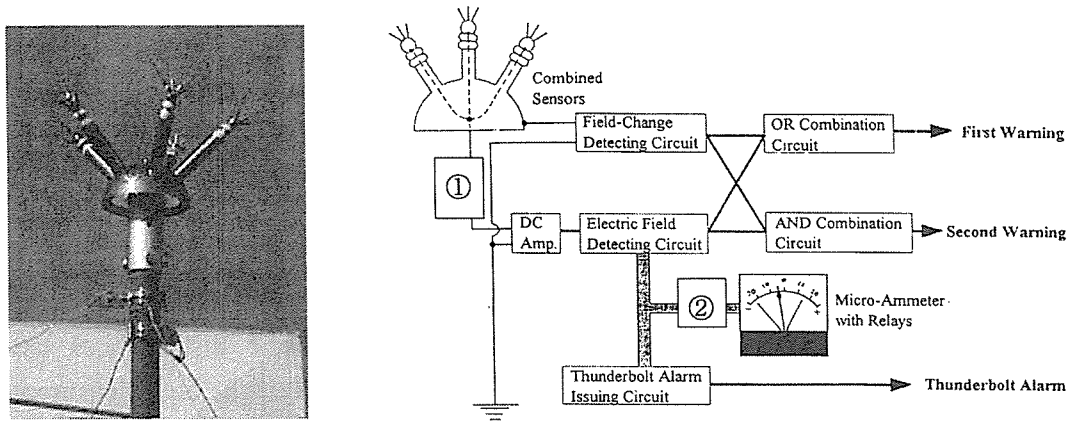

(a) (b)

Fig.1 Atmospheric electric field sensor. (a) Top of sensor has 30 sharp needles to obtain sensitive and extremely stable corona current. Half a ball of sensor is antenna sensor for an inductive and radiation electric field changes. (b) Schematic diagram of measurement system.

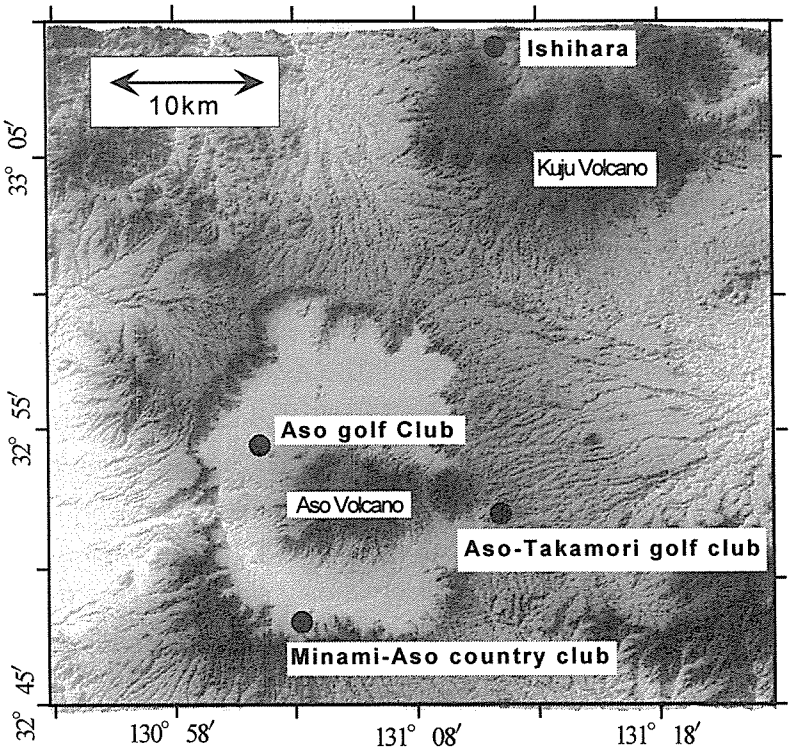

Fig.2 Location of Coronarm station

Self-Potential Variability of 10 Years Observed at Unzen Volcano

Hashimoto, T., Tanaka, Y. and Masuda, H.

The evolution of a hydrothermal system beneath Unzen Volcano, one of the dacitic volcanoes in southwestern Japan, has been investigated by self-potential (SP) monitoring for ten years since 1991. We detected a large and steep rise in SP before the formation of the summit lava dome in 1991. A concentric positive SP anomaly around the dome amounting more than 1000mV lasted throughout the eruptive stage to 1995. Besides the positive anomaly, we have observed the growth of a negative center adjacent to the dome during the eruptive period. The growth of such dipolar SP change is attributed to the streaming potential associated with shallow hydrothermal circulation which is driven by the onset of the magmatic eruption (Hashimoto, 1995).

Our ten-year monitoring has revealed that the concentric positive SP still exists and even shows a gradual growth at some stations after the eruptive period. This fact implies that a hydrothermal circulation will not easily disappear once it is set up. Spatial pattern of SP is basically stable throughout these ten years. However, we have also detected considerable decrease at the southwest of the dome since 1997 (after the eruptive period). This is the same area where we observed a sharp increase at the initial stage of the last eruption. At this moment we speculate this decreasing change implies the gradual dissipation of the hydrothermal system. We hope that the drilling project in 2000 will provide some crucial information on the mechanism of the SP change.

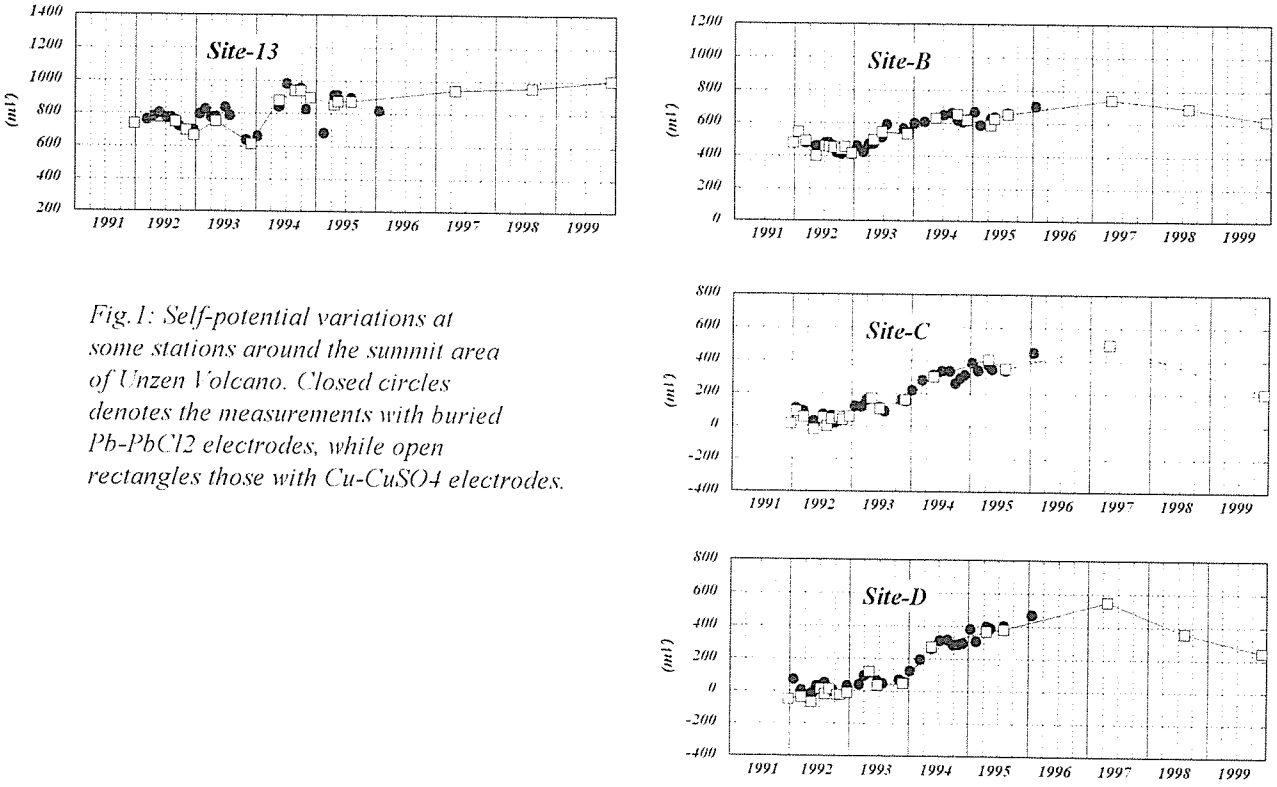

Fig. 1: Self-potential variations at some stations around the summit area of Unzen Volcano. Closed circles denotes the measurements with buried Pb-PbCl2 electrodes, while open rectangles those with Cu-CuSO4 electrodes.

Electromagnetic explorations in Aso Volcano (II)
—TDEM and MT—

Hashimoto, T., Tanaka, Y., Sakanaka, S., Hase, H., Amita, K., Masuda, H.,
Kanda, W. (DPRI, Kyoto Univ.),
Kagiyama, T., Munekane, H., Koyama, T., Ogawa, T. (ERI, Univ. Tokyo),
Mogi, T., Ikoma, Y., Djedi S., Widarto (Kyushu Univ.),
Handa, S. (Saga Univ.), Shimoizumi, M. (Polytech Coll. Kitakyushu)
and Takakura, S. (Geological Survey of Japan)

Electrical resistivity structure beneath Aso Volcano, southwestern Japan, was investigated with natural-source MT (magnetotelluric) and controlled-source TDEM (time-domain electromagnetics) methods. These experiments of TDEM and MT were conducted in December, 1998 and in May, 1999, respectively. We deployed 13 stations in a 4km-3km area including the active crater. One dimensional inversions of both MT and TDEM showed a common feature of horizontally layered structure with mid-low-high resistivity from surface to depth. The surface layer, indicating the resistivity values between 100 to 1000 ohm-m, corresponds to volcanic deposits. The second layer, indicating less than 10 ohm-m, is plausible to be an aquifer trapping volcanic gases, or an altered clay zone as the result of hydrothermal activity, In either case, we need much fluid within or adjacent to the layer. The third layer shows more than 1000 ohm-m, suggesting the basement rock of the caldera. Here, the structure beneath the central part of Aso Volcano shallower than 5km can be characterized by the water-bearing layer at a depth around 1km which lies between impermeable basement of the caldera and porous surface deposits.

We consider that the water-bearing layer of Aso plays an important role in heat discharging system of the volcano as a field of interaction between heat and water. The layer acs as an energy buffer when heat comes up from depth toward the surface. This process provides a reasonable explanation for some kinds of geophysical variability such as the rapid thermal (de)magnetization under the active crater (Tanaka, 1993), as well as the VLPT (very long period tremor) whose source is inferred to be a vibrating inclined crack around a depth of 1.0 to 1.5km (Yamamoto et al., 2000).

summary of 1-D MT inversion

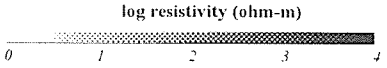

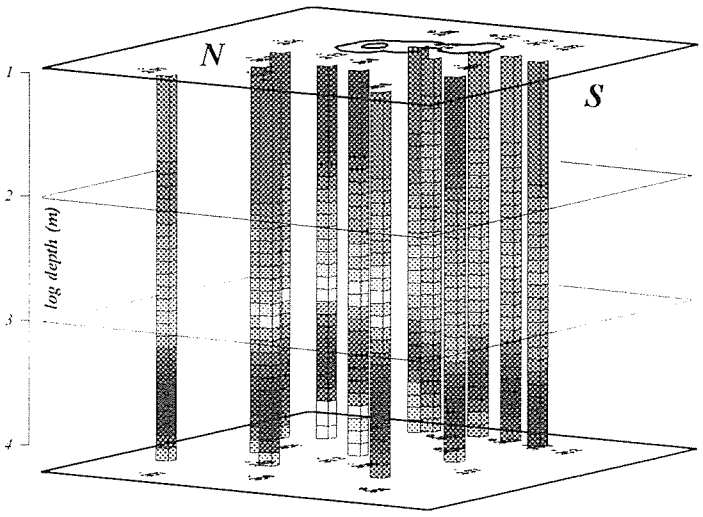

Origin of Carbon Dioxide Discharged from Nagayu Hot Spring, Oita Prefecture, Japan

Kazutoshi Iwakura, ***Shinji Ohsawa,*** *Nobuki Takamatus,*
Kazutoshi Oue, *Kenji Notus,* ***Yuki Yusa*** *and Masayuki Imahashi*

Chemical composition, $^{3}He/^{4}He$ ratio and $\delta\ ^{13}C$-value of CO_2 in free gases collected from Nagayu hot spring, Oita Prefecture, Japan, were determined to elucidate the origin of carbon dioxide (CO_2 in free gas + total dissolved CO_2). Main chemical constituent in the free gases was CO_2 and others were N_2, Ar and He in small amounts. Helium isotope ratio and corrected $\delta\ ^{13}C$-value of the carbon dioxide for isotopic fractionation between the gaseous and the dissolved CO_2 ranged from 6.27 to 6.82 R/R_{atm} and from –7.47 to -8.61‰, respectively. This result indicates that the carbon dioxide discharged from Nagayu is originated from magmatic fluid. Based on the $CO_2/^{3}He$ ratio and the corrected $\delta\ ^{13}C$-value of the discharged gases, quantitative estimate of mantle derived carbon, subducted marine limestone and organic sedimentary carbon are given as 4, 69 and 27%, respectively. (Submitted to J. Balneological Soc. Japan)

In-situ Determination of Melting Temperatures in the $Ca(OH)_2$ - $CaCO_3$ - H_2O System: Revisited With Externally Heated Diamond Anvil Cell

Kawamoto, T.

Univariant melting temperatures of the $Ca(OH)_2$ - $CaCO_3$ - H_2O system have been in-situ determined with an externally heated diamond anvil cell (DAC, Bassett et al., 1992 Rev Sci Instrum). $Ca(OH)_2$ crystals with a trace of $CaCO_3$ were placed in distilled and de-ionized water along with an air bubble in a Re gasket between diamond anvils. Under an optical microscope, he samples were heated by passing an electric current through Mo wires. Temperature was measured to ± 2 °C with two thermocouples attached to the diamonds. A homogenization temperature of air bubble and H_2O tells the pressure temperature path of the sample. The crystals were found to start melting at univariant melting temperature in the $Ca(OH)_2$ - $CaCO_3$ - H_2O system at 630 °C, 0.27 GPa, 622 °C, 0.42 GPa, and 623 °C, 0.6 GPa (Figure). The samples totally melted at temperatures lower than melting temperatures in the $Ca(OH)_2$-H_2O system.

The melting relations in the CaO - CO_2 - H_2O system were determined by temperature quench experiments using cold-sealed vessels up to 0.4 GPa (Wyllie and Tuttle, 1960, J Petrol, Wyllie and Raynor, 1965, Am Mineral). Because the melts in this system cannot be quenched to glasses during the decrease of temperature, it is necessary to interpret the textures observed in run products to determine the melting relations. The melting temperatures of $Ca(OH)_2$ with and without H_2O were also estimated up to 3.3 GPa by differential thermal analysis, DTA, using piston cylinder apparatus (Irvine et al., 1977 Am J Sci). The DTA data are concordant to those obtained by the quench experiments in a pressure range up to 0.4 GPa. DTA is a popular method to determine melting temperatures of unquenchable materials. The present in-situ observation of minimum melting temperatures of $Ca(OH)_2$ - $CaCO_3$ - H_2O system is in agreement with the values determined by quench experiments at 0.27 and 0.42 GPa (Figure, Wyllie and Tuttle, 1960, J Petrol, Wyllie and Raynor, 1965, Am Mineral). It is likely to suggest that externally heated DAC can be a useful tool for direct observation of melting reactions including unquenchable melts.

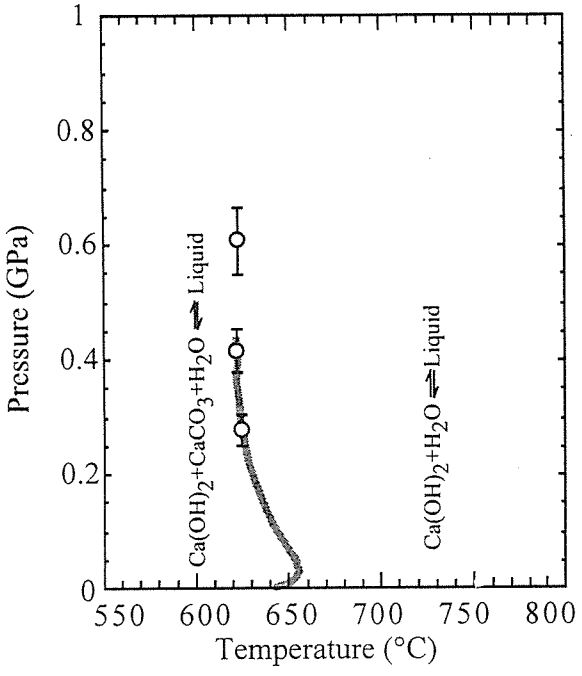

Figure Pressure and Temperature diagram showing univariant melting curves in the $Ca(OH)_2$ - $CaCO_3$ - H_2O (Wyllie and Tuttle, 1960, J Petrol, with a revision by Wyllie and Raynor, 1965, Am Mineral). and $Ca(OH)_2$ - H_2O systems (up to 0.4 GPa; Wyllie and Tuttle, 1960, J Petrol, Wyllie and Raynor, 1965, Am Mineral and 1 GPa; Irvine et al., 1977 Am J Sci). The present experimental results (circles) are in agreement with the previous data at 0.27 and 0.42 GPa.

Laminar entrainment and mixing in compositionally buoyant plumes: Effect of viscosity ratio

Kumagai, I.

Possibility for a laminar entrainment of starting plumes with a compositionally buoyancy has been explored in laboratory experiments. All starting plumes, within the range of the viscosity ratios of the ambient to the buoyant (source) fluids $10<\varepsilon_{as}<856$, entrain the heavier ambient fluid into their heads as they ascend. The degree of mixing in the plume head plays an important role in the ascent velocity of the plume head, which can be modeled by the Stokes velocity for a sphere.

Two modes of mixing between the ambient and the buoyant materials are identified and classified by the behavior of the toroidal flows within the plume head (circulation in a torus). The first (figure 1) is observed for a small viscosity ratio ($\varepsilon_{as}<11$), and can be characterized as the mixing throughout the single toroidal flow in the plume head. The entrained material in the plume head moves with the toroidal flow and forms a multi-layered and swirled structure. In contrast, the second mode (figure 2) occurs for a higher viscosity ratio ($104<\varepsilon_{as}<856$), and forms a gravitational stratified structure within the plume head. The buoyant fluid, which is supplied from the pipe flow, is stored at the upper part of the plume head and the entrained fluid forms a layer at the lower, then each stratum makes its own toroidal flow. The shear-flow at the interface between two superposed toroidal flows promotes the shear instability and forms a mixing layer. Finally both fluids in the plume head mingle together.

The mantle materials have a temperature dependent viscosity. Because the Pr number in the mantle is extremely high, the high temperature anomaly and the high viscosity contrast between a mantle plume and the ambient mantle are expected. Above characteristic anatomy of the second mode would be reflected in the spatial and the temporal variation of the geochemical data obtained from mantle plume products.

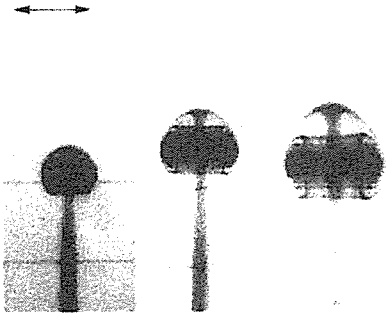

Figure 1. Typical experimental images of the starting plume head with swirled structure. Time interval is 500 sec. The viscosity ratio is about 10. The scale is 0.01 m.

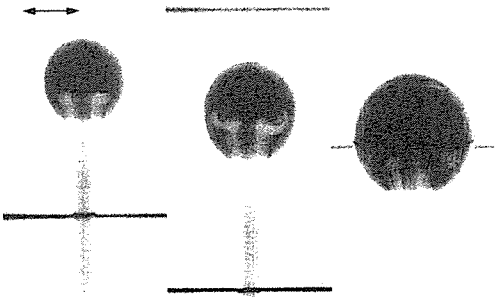

Figure 2. The viscosity ratio is about 100. The shear instability at the interface between the two layers causes the whole mixing. The above images are 0, 2100 and 7865 sec, respectively.

A low-F pegmatite-related, contact metasomatic Mo skarn from the southwestern Grenville Province, Ontario, Canada: petrogenetic and phase equilibium implications.

Lentz, D R. and ***Suzuki, K.***

The Hunt Mo skarn deposit is one of the best examples of a late-tectonic, granitic pegmatite-related, contact-metasomatic skarn system in the Grenville Province. A Re-Os age of 1069 ± 10.9 Ma was obtained from a molybdenite crystal (6.4 ppm Re) hosted in proximal skarn (sample 50 O) consistent with a contact metasomatic origin related to the granitic body. Although less evolved than other Grenvillian pegmatites, the Condon Lake granitic pegmatite is a low-temperature, A-type intrusion, with moderate redox characteristics. In contrast to many Mo-bearing skarns in the region, this deposit has low U, Th, REE, F, and P contents. The reduced marginal magnesian skarn is well zoned geochemically, mineralogically, and texturally from the contact outward into the dominant graphite-bearing calc-silicate-calcite-dolomite marble, which is locally intercalated with clinopyroxenite, orthoamphibolite and pyroxene-biotite quartzofeldspathic gneiss. A narrow zone of endoskarn [< 1m; scapolite(scp)-Kfs-cpx] is locally developed. This contrasts with the wider zoned exoskarn [< 10 m; scp-cpx (proximal), cpx-phl, cpx-trem-phl, trem-phl (distal), marble], that host the bulk of the primary molybdenite (+/- pyrrhotite) and minor secondary pyrite-pyrrhotite-molybdenite veins. In addition to the obvious Si, Fe, Ti, Mn, S, and Mo addition, Cu, Zn, Y, Nb, and Zr are also slightly enriched. The high $f(H_2O)/f(HF)$ ratios (138,000 to 204, 000) and moderate $f(H_2O)/f(HCl)$ ratios (2,200 to 11,000) at the Hunt deposit contrast with the lower fugacity ratios from other Mo-bearing U-Th-REE skarns in the region, indicating that Mo transport and deposition is principally related to an hydroxide complex.

(Submitted to Econ. Geol.)

The use of spectral analysis for identification of spatial seismic sources in Nevado del Ruiz Volcano, Colombia.

By: John. M. Londono.,*,** Yasuaki Sudo ,* Lorena Sanz **, J. Alonso Osorio **

Abstract

A spectral analysis of volcano-tectonic (VT) earthquakes was carried out at Nevado del Ruiz Volcano (NRV) for the period between 1985 and 1995 for several spatial seismic sources around the volcano, named North, East, West, South and Crater sources. The spectral analysis demonstrates that the spatial seismic sources in the NRV present very defined and different frequencies for each source. The North source presents two important peaks of frequency, in 4.7 Hz and 9.4 Hz. The East source also, presents two important peaks, in 4.3 and 11.4 Hz. The West source presents a peak in 3.9 Hz and another in 5.1 Hz. The South source presents two peaks, one in 4.5 Hz and another in 6.1 Hz. And the Crater source only showed an important peak in 12.1 Hz. This important peaks of frequency for each seismic source can be used as a tool to help to identify the possible location of VT earthquakes (that is, the spatial seismic source) during a volcanic crisis. Besides that each source presents characteristic peaks, which help to distinguish from the others, another different peaks were also observed in the spectra for each source. This suggests that, not only the source effect is important in these earthquakes but the path effect of the seismic waves are also an important factor in VT earthquakes at NRV. There was a direct relationship between the depth of the earthquakes and the frequency for the East, North and Crater seismic sources, and a contrary behavior for the South and West sources. Some temporary changes were observed in spectral parameters such as the frequency of the P and S waves, in the West and South seismic sources. Before the eruption on September 1, 1989, both P and S waves showed a similar frequencies for that seismic sources. But after that eruption, the frequencies of P and S waves showed a big scattering until today. This fact showed that inner conditions of NRV changed after the eruption on September 1, 1989, and probably it continues in the same way until now. It seems that, the south and western part of NRV is different from the east, north and crater area. Some geologic faults present in the area, can help to explain such differences.

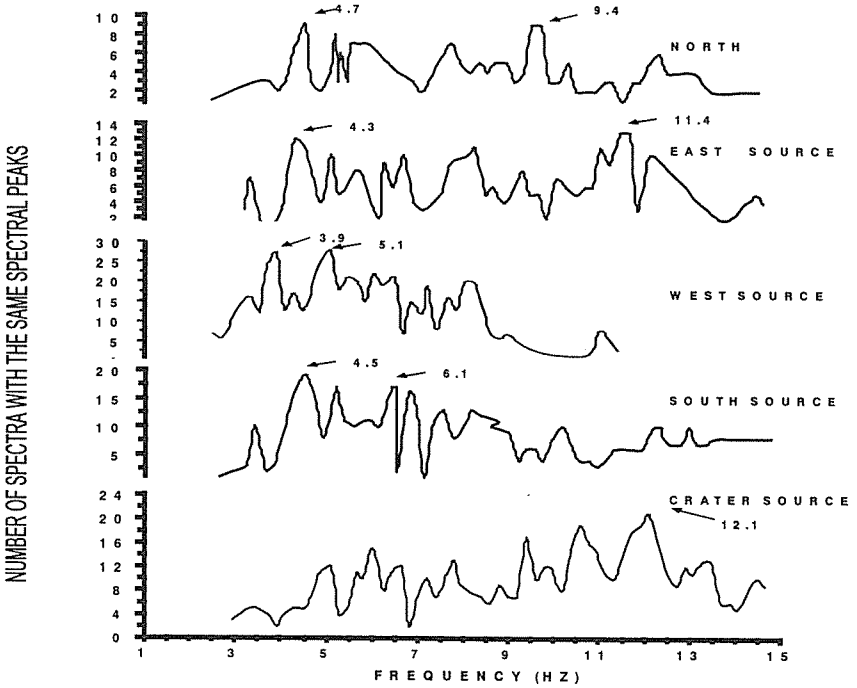

* Aso Volcanological Laboratory. Kyoto University
** Ingeominas. Volcanological and Seismological Observatory. Manizales.Colombia.

ANALYSIS OF THE TEMPORAL AND SPATIAL VARIATION OF THE SEISMIC ACTIVITY AND THE V_p/V_s RATIO OF VOLCANO-TECTONIC EARTHQUAKES AT NEVADO DEL RUIZ VOLCANO, COLOMBIA (1986 - 1996)

By John. M. Londono [*,**], Sudo Yasuaki.[*], Enrique Franco. [**]

ABSTRACT

An analysis of the temporal and spatial variation of the seismic activity, and the distribution of the V_p/V_s ratios for volcano-tectonic (VT) earthquakes at Nevado del Ruiz Volcano (NRV) was carried out for the period between 1986 and 1996. The seismic activity of NRV, which began their last eruptive period in December 1984, has behaved in a varied way in time and space. In the period of study at least six spatial seismic source were present. The Crater source and South source were the most active. A migration of the seismicity was observed from 1986 until before the eruption of September, 1989, with a tendency to have more shallow depths. From 1992 until now on, there is a stage with tendency to be more stable, being notorious in the energy liberated by VT earthquakes. The average magnitude of VT did not show any special tendency, having a maximum value in 1989.

Using the Wadati's method, the V_p/V_s ratio was calculated for more than 1500 high quality VT earthquakes located around the volcano. It was found that for the NRV, the V_p/V_s value, as half term, oscillates between 1.3 and 1.5. In some places, were found anomalous values regarding the previous ones, that suggest the presence of areas of materials with different properties in the NRV. An inverse relationship between the magnitude of the earthquakes and the V_p/V_s values for the whole time was found: when increasing the magnitude it tends to diminish the V_p/V_s ratio, and vice versa. It maybe due to changes in the property of the materials when being liberated energy. In the eruption of 1989 this tendency is observed to diminish. We suggest that the low V_p/V_s values found in NRV, are due to the presence of gas or steam inside the volcano. This supposition is in agreement with another studies of geochemistry and drilling surveys carried out at NRV.

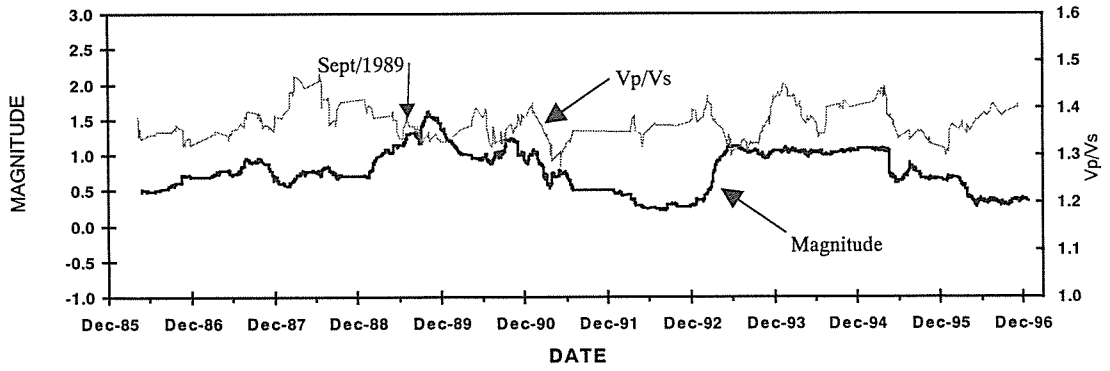

[*] Aso Volcanological Laboratory. Kyoto University
[**] Ingeominas. Volcanological and Seismological Observatory. Manizales.Colombia.

High Spatial Resolution Remote Sensing of Kyushu Volcanoes

Matthews, J

The application of new satellite remote sensing techniques to the study of earthquakes and volcanoes now forms an important part of the overall research strategy of the Geophysics community at Kyoto University.This project makes use of high spatial resolution images gathered by the LANDSAT, ERS-1 and JERS-1 satellites to examine surficial processes taking place in the vicinity of the active volcanoes of Kyushu. In the case of the recent activity at Unzen, which took place between 1990-94 , the synergistic use of LANDSAT with Synthetic Aperture Radar imagery gives new multiband image combinations which are interpreted with the aid of information gained by intensive aircraft survey data gathered at the time of the eruption. The satellite imagery clearly highlights, in a truly synoptic fashion, the effects of toxic releases from the volcano (gas and ash) on the alpine environment. At lower altitudes, the valley floors are subject to repeated re-surfacing by pyroclastic flows and the subsequent mudflows induced by heavy rainfall. The developmental sequence of these dangerous and destructive processes has been, in part, been revealed by the quantitative measurements offered by the satellite methods.

Source Mechanism of Pulsative Seismic Event "Heart Beat" at a Mud Volcano in Mt. Garan, Tsurumi Volcano

Takehiko MORI, Yasuaki SUDO, Tomoki TSUTSUI, Makoto NAKABOH and Shin YOSHIKAWA

In October 1995, a mud volcano formed in Mt. Garan, one of cones at Tsurumi Volcano. This produced characteristic seismic events named "Heart beats" with a constant time interval of 1.3s. Seismic observations were performed around the mud volcano to investigate the source mechanism of the "Heart beats" in April 1996. Assuming homogeneous half-space of Vp=300m/s based on seismic velocity survey around the mud crater. The source of the "Heart beats" was located at the eastern bottom of the mud volcano. This area was the most fumarolic active region in the crater. The source mechanism of "Heart beats" was determined by evaluating the moment tensor of the initial motion by waveform inversion. Two seismic sources were assumed in order to explain the initial motions and the following large dilatational phases of the "Heart beats." The "Heart beats" were initiated by normal faulting, and this was followed by volumetric contraction of $0.5 \times 10^{-4}m^3$.

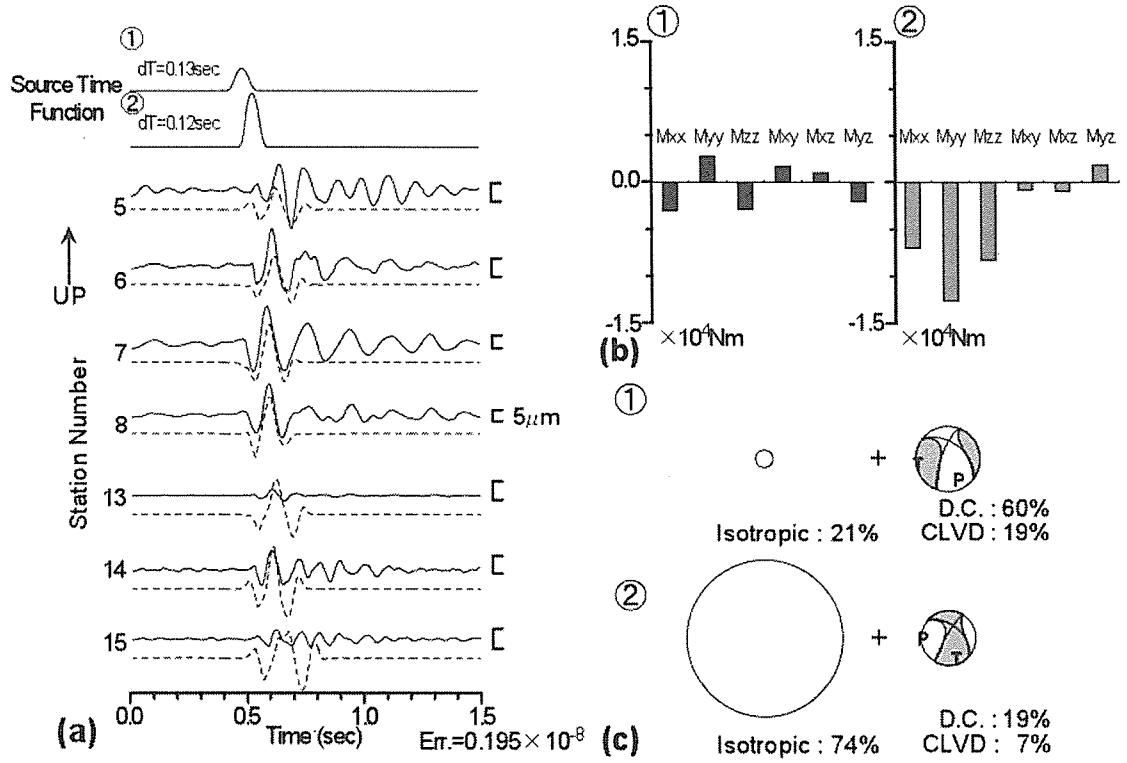

Figure Results of the moment tensor inversion by a double source. (a) Observed waveforms of "Heart beat" (solid curves) and synthetic waveforms (dashed curves). The top two trace shows the two components of the source time function. The pulse widths of the first and second sources are 0.13s and 0.12s, respectively. The time lag of the second event is 0.048s. (b) Best solution for the moment tensor of both sources. (c) Focal mechanism solution of the two sources projected on upper hemisphere.

Porphyritic high-Mg andesites in the Setouchi volcanic belt, SW Japan

Nakashima, T., ***Shimoda, G., and Tatsumi, Y.***

Porphyritic high-Mg andesites (PHMAs; SiO_2 ~55 wt.%; MgO ~7 wt.%) are found in the Miocene Setouchi volcanic belt, SW Japan. The PHMAs are characterized by the presence of plagioclase phenocrysts, whereas the rather aphyric, mantle-derived high-Mg "sanukitoid" andesites (HMAs) found in the region do not contain such phenocrysts. The following petrographic observations suggest a role for mixing in producing the PHMA magma: (1) reversely zoned pyroxene phenocrysts, both clino- and ortho-pyroxenes, are observed in PHMAs; (2) normally zoned clinopyroxene may be in equilibrium with olivine but not with normally zoned orthopyroxene in terms of Fe-Mg partitioning; (3) plagioclase displays a wide compositional range (An_{80-45}) with a bimodal distribution; (4) two types of olivine phenocrysts and spinel inclusions, one with compositions identical to those in HMA sanukitoids and the other identical to those in basalts, are recognized in terms of Ni-Mg and Cr-Al-Fe^{3+} relations, respectively. The above petrographic characteristics may be best explained by the presence of three end-member magmas, namely Mg-rich basalt and HMA sanukitoid magmas, both having olivine and clinopyroxene phenocrysts and a low-Mg, plagioclase-phyric andesite magma. Major, trace, and isotope compositions of these magmas may also support the magma-mixing origin for PHMAs. (*submitted to Bull. Volcanol. Soc. Jpn.*)

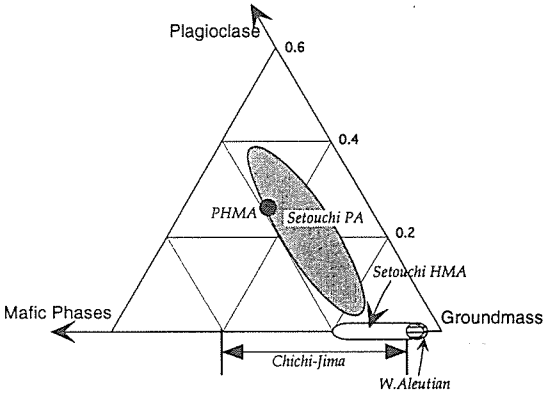

Fig. 1 Modal compositions of high-Mg andesites (HMAs) and Setouchi porphyritic andesites (PA). The present sample of a porphyritic high-Mg andesite (PHMA) contains far more phenocrysts than HMAs reported to date, and is characterized by the presence of plagioclase phenocryst.

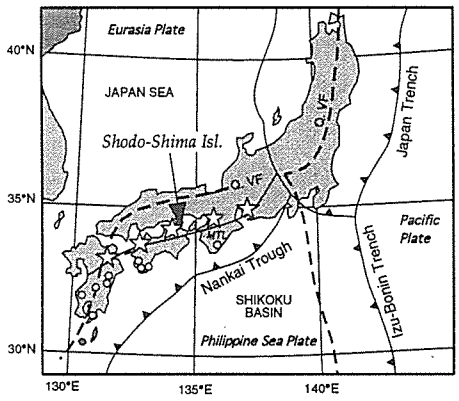

Fig. 2 A simplified tectonic map of the SW Japan arc. The Setouchi volcanic belt (stars) is located in the forearc region of the arc, i.e., in the trenchward region of the Quaternary volcanic front (Q.VF). In the outer zone of the SW Japan arc, i.e., to the south of the Median Tectonic Line (MTL), are distributed felsic volcano-plutonic complexes (open circles).

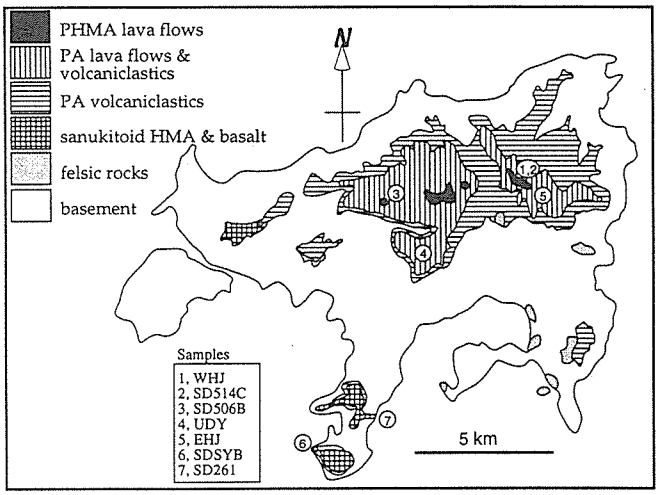

Fig. 3 A generalized geologic map of Shodo-Shima Island after Tatsumi (1983). Setouchi volcanic rocks on this island are divided into two groups, the older felsic rocks and the younger intermediate to mafic rocks including HMAs, porphyritic andesites, and basalts which form a composite volcano.

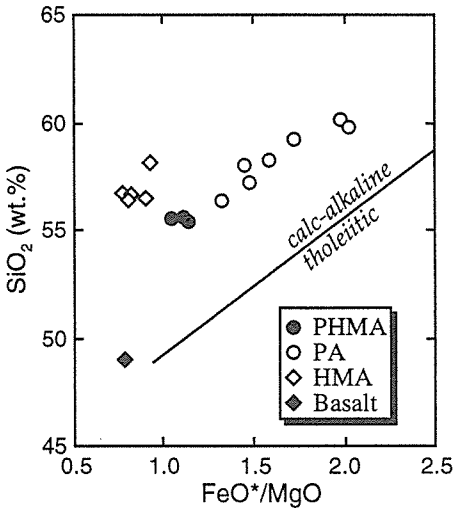

Fig. 4 FeO*/MgO vs. SiO2 for Setouchi volcanic rocks on Shodo-Shima Island. Porphyritic andesites and PHMAs form a typical calc-alkaline trend.

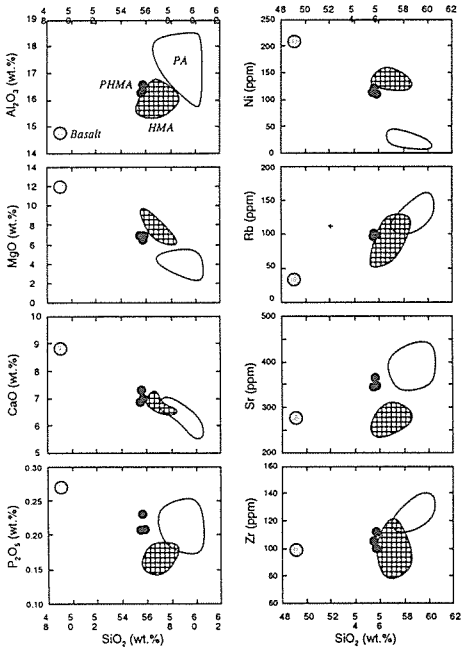

Fig. 5 Selected major and trace element compositions of Setouchi volcanic rocks on Shodo-Shima Island.

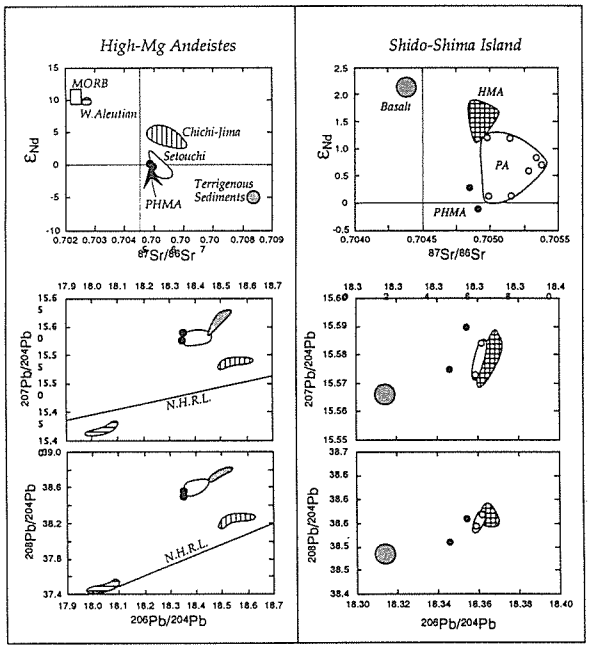

Fig. 7 Left, isotopic compositions of PHMAs, high-Mg andesites from three regions, and trench-fill terrigenous sediments at the Nankai Trough (Shimoda et al. 1998). Right, isotopic compositions of Setouchi volcanic rocks on Shodo-Shima Island.

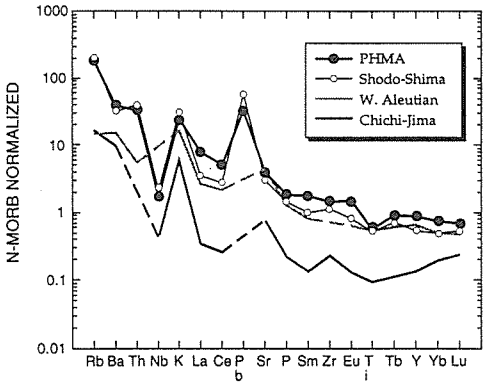

Fig. 6 N-MORB normalized (Sun and McDonough, 1989) incompatible element compositions of PHMAs and other HMAs from Shodo-Shima Island, W. Aleutian (Yogodzinski et al. 1994) and Chichi-Jima (Taylor et al. 1994).

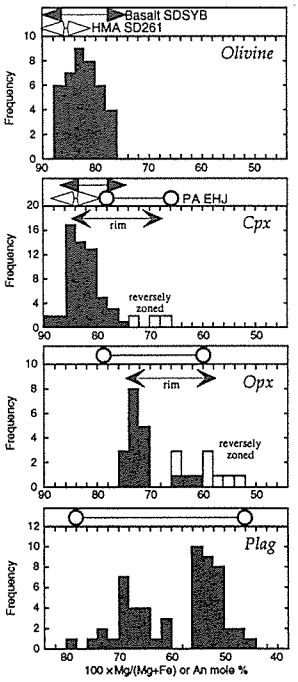

Fig. 8 Frequency distribution diagrams for Mg# or An mole% of phenocryst phases in PHMAs. The range of compositions of phenocrysts in basalt, HMA, and PA is also shown.

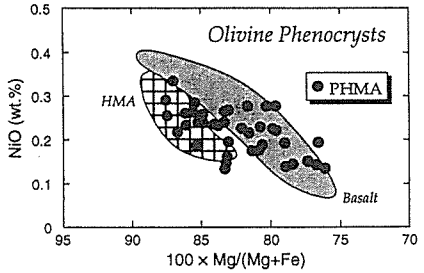

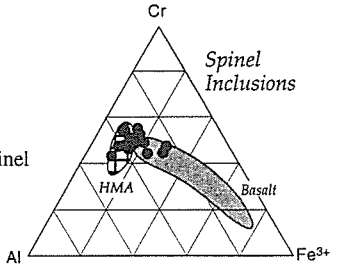

Fig. 9 Compositions of olivine phenocrysts and spinel inclusions in HMA, basalt, and PHMA.

Isotopic Characteristics of Rainwater from Two Major Japanese Typhoons

Shinji Ohsawa and Yuki Yusa

The stable isotope ratios of hydrogen and oxygen were measured for rainwaters from Typhoon No. 13 which struck Japan on September 1993 and Typhoon No. 6 which passed in July 1996. Rainwater was collected every hour over 2 - 3 day periods at Beppu, Japan (33°16′N, 131°29′E) which lies on or close to the typhoon routes. The deuterium excess parameters ($\delta D - 8 \cdot \delta^{18}O$) of the rainwaters vary over wide ranges from 19.22 to 1.52 for Typhoon No. 13, 1993 and from 6.02 to −8.10 for Typhoon No. 6, 1996, respectively. Rainwaters with higher d-values precipitated in the forward parts of the typhoons. This is ascribed to the possibility that the water vapors supplied by the bottom air currents from the front (rear) of the typhoons may be originally formed by rapid (gentle) evaporation of seawater. Symmetrical patterns of spatial δD and $\delta^{18}O$ distributions within the typhoon precipitations, as estimated from the variations in the isotope ratios of the typhoon rainwaters, should appear from a continuous isotopic fractionation of water vapors with the bottom air currents converging toward the typhoon center. Weighted means of δD and $\delta^{18}O$ of the typhoon precipitations are more negative than those of ordinary rainfall, suggesting that an isotopic influence of typhoon precipitation on surface waters, e.g. river, stream, lake and spring waters, may be important. (Submitted to Limnology)

Physical state and origins of constituents of Beppu geothermal fluid inferred from chemical and isotopic data of fumarolic discharges

Shinji Ohsawa

Chemical and isotopic data of steam condensate and gas samples collected from fumaroles and steam wells in Beppu express physical state (temperature, phase condition) and origins of constituents (H_2O, He, N_2, CO_2) of underground hydrothermal fluid of Beppu geothermal system as follows. (1) Steams of the fumarolic discharges are formed by boiling of meteoric hydrothermal waters of about 300℃ or below, inferred from the δ D and $\delta\,^{18}O$ values of the collected steam condensates. (2) Based on the H_2 ／Ar and CO_2／Ar ratios of the fumarolic discharges, maximum temperature of the hydrothermal waters is estimated to be about 300℃, which gaves good agreement with the values estimated from the hydrogen and oxygen isotope ratios of the evaporated steams and abundant ratios of cations in the hot spring waters. (3) From relative He－N_2 －Ar composition, the $^3He/^4He$－$^4He/^{20}Ne$ relation and $\delta\,^{12}C$ values of CO_2 (with the He isotope ratio), part of He, N_2 and CO_2 in the fumarolic discharges are indicated to be originated from magmatic emanation.

New subjects of inquiries as follows are brought up from this study. (Ⅰ) Why the hydrogen and oxygen isotope compositions do not state positively that magmatic steam mixes with the meteoric hydrothermal system of Beppu, although the He isotope ratio and the He－N_2－Ar composition clearly show that magmatic He and N_2 certainly contribute to formation of the sysytem? (Ⅱ) Where and how atmospheric He and N_2 in the fumarolic gases, which most probably are not derived by direct air－contamination on the gas－sampling, mix with the underground hydrothermal fluid? (Ⅲ) Original source of carbon in the magmatic CO_2 must be identified, which is an important awaiting solution together with the problem on the origin of chloride in the Beppu hydrothermal water.

Mixing of Volcanic CO_2 with Groundwater Originating in a Non-Volcanic Sedimentary Basin, Oita Plain, Middle Eastern Kyushu, Japan

Shinji Ohsawa, Kazutoshi Iwakura and Nobuki Takamatsu

The Oita plain (east-central Kyushu) is a sedimentary basin consisting of Pliocene and Pleistocene sedimentary rocks, which is bounded on the west by a Quaternary volcanic row. More than a hundred wells have been dug there in order to exploit the non-volcanic hot spring resources. Groundwaters at temperatures between 30 and 55℃ are obtained from wells drilled to 600 to 800m depth. Almost all the groundwaters are chemically classified as bicarbonate or chloride-bicarbonate types, and contain bicarbonate ions at concentrations of over several hundred mg/l (Kittkawa and Kitaoka, 1985).

The stable carbon isotope ratio ($\delta\ ^{13}C$) of total dissolved carbonate (TDC) of the groundwaters varies over a wide range: -3.3 to -20.2 ‰ (NEDO, 1989), and is inversely proportional to the reciprocal of the concentration of TDC ($\delta\ ^{13}C = -27.90 \times 1/[TDC] - 7.19$, $r^2 = 0.838$). This relationship indicates mixing of the two type groundwaters containing light TDC ($\delta\ ^{13}C$; ca. -20 ‰) and heavy TDC ($\delta\ ^{13}C$; ca. -5‰). The former corresponds to normal groundwater (Mizutani, 1995), whereas the latter isotope ratio falls within the range of volcanic gases in subduction zones (Sano, 1996). The light TDC is thought to originate from soil CO_2. On the other hand, the heavy TDC is probably derived from volcanic CO_2 because the helium isotope ratio ($^3He/^4He$) of gas accompanying the heavy TDC groundwater is high: 8.7×10^{-6} (NEDO, 1989). Therefore, it is likely that volcanic CO_2 exuding from greater depths is mixed with the groundwater system of the Oita non-volcanic sedimentary basin. (Submitted to WPGM2000)

Volcanic earthquakes near Naka-dake, Aso Volcano in 1999

H. Ono

Volcanic activity was calm at Naka-dake in 1999. The crater bottom of the first crater has been covered with hot water pool.

Volcanic earthquakes occurred under the first crater of Naka-dake and source distribution was similar to the distributions of usual year. The number of observed volcanic earthquakes was small and volcanic earthquake activity was calm. The source location and daily frequency distribution of volcanic earthquakes were showed in Fig. 1 and Fig. 2.

A felt volcanic earthquake (felt earthquake scale II) was observed on February 26. The location was at 1.5km below sea level under the first crater. It was a memorable event of this year.

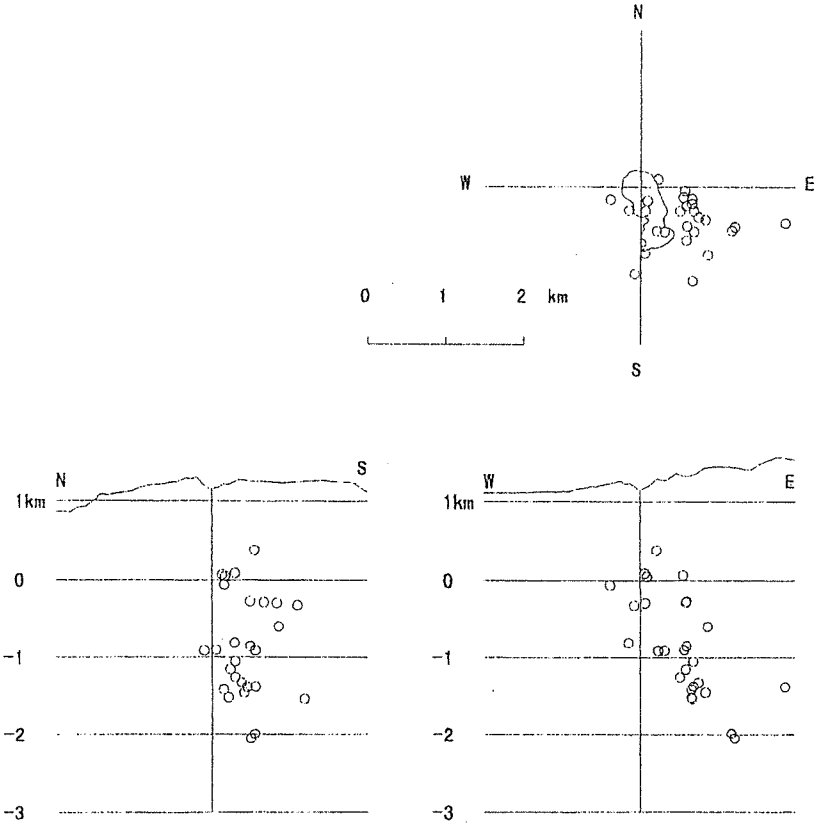

Figure 1. Source distribution of volcanic earthquakes near Naka-dake in 1999.

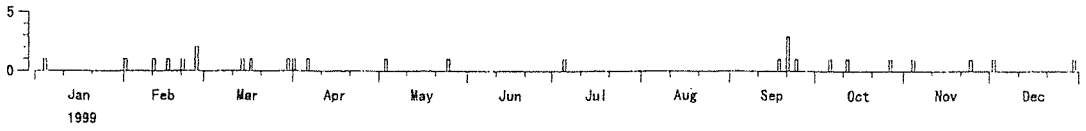

Figure 2. Daily frequency distribution of volcanic earthquakes in 1999.

Ground deformation near Naka-dake, Aso Volcano

Ono, H. and Sako, M.

The tunnel for ground deformation observation locates in 30m underground at about 1km south-west of Naka-dake crater and consists of horizontal tunnels forming equilateral right-angled triangle. Watertube tiltmeters of 25m span (WT1 and WT2) and extensometers of 20m span (E1 and E2) and 25m span (E3) have been installed.

The remarkable ground deformation has been detected on the records observed water tube tiltmeters till June of 1999. Southwest uplift of 8 μ radian in the latter half of 1998 continued to westward uplift of 5 μ radian from Jan. to June in 1999. This ground tilt indicate subsidence of crater side and is compatible with low activity of the first crater.

Extensometers recorded annual variation with strain amplitude of 10^{-6} order.

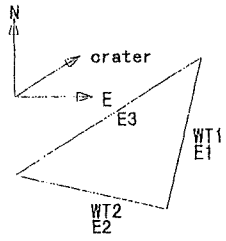

Figure 1. Tunnel and setting of watertube tiltmeters (WT1,WT2) and extesometers (E1,E2,E3)

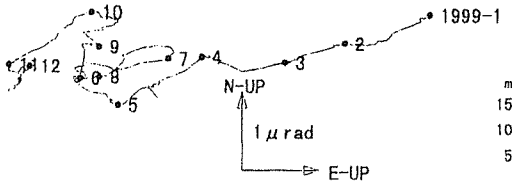

Figure 3. Upward vector from watertube tiltmeter observation. Attached numbers show months(1st day).

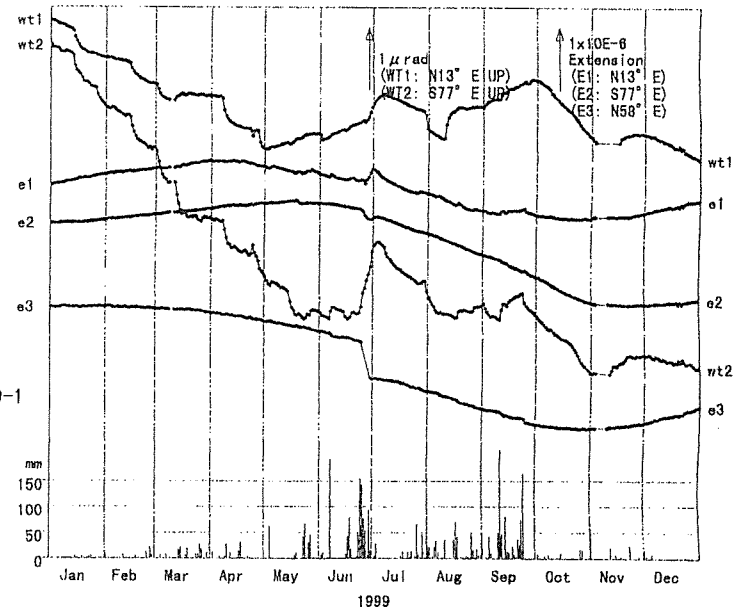

Figure 2. Ground deformation records in 1998. Lower is daily precipitation.

EDM survey network is shown in Fig. 4. Base line KAW2-KAE2 and SUN3-KAE2 over the crater tend to expand for last few years. The other base lines on the west flank of the crater tend to contract. It is inferred that source is shallow.

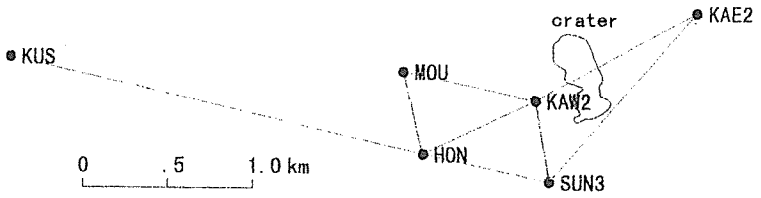

Figure 4. EDM survey network near Naka-dake.

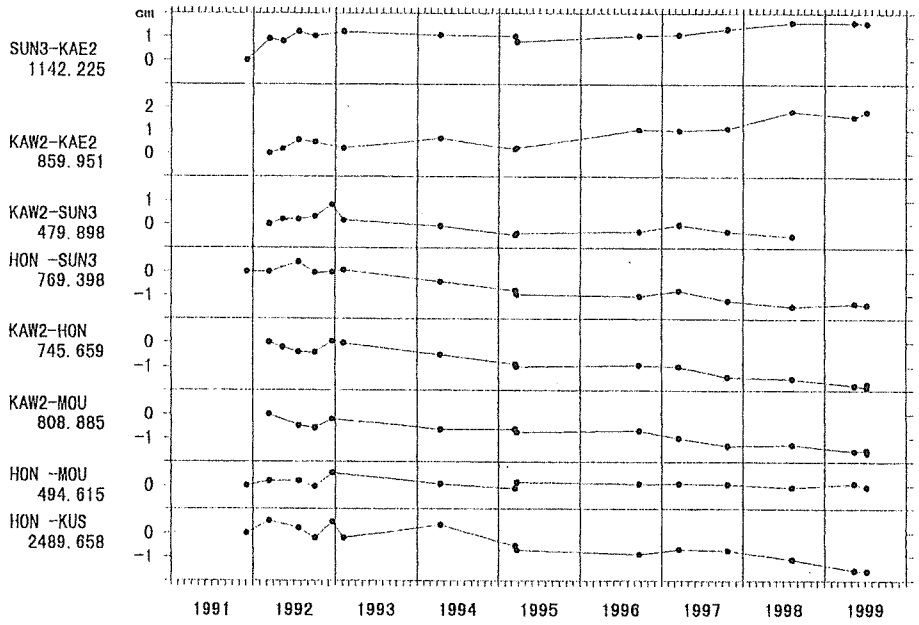

Figure 5. Variation of EDM base line distances.

Ground deformation of Kuju Volcano

Ono, H., Nakaboh, M., Sako

Ground deformation around Hossho-zan of Kuju Volcano have continued for 4.5 years after the eruption of 1995. EDM surveys have been carried out after the eruption. The base lines were shown in Fig. 1.

Distances along several base lines near the crater of 1995 activity showed contraction. For example, the contraction of baseline SGM-HSS (distance 1110m) was 34cm for 30months after eruption and 8cm in 1999. These were equivalent to -3×10^{-4} and -7×10^{-5} strain respectively. The source location of contraction computed by Mogi's model didn't change at about 500m beneath the crater.

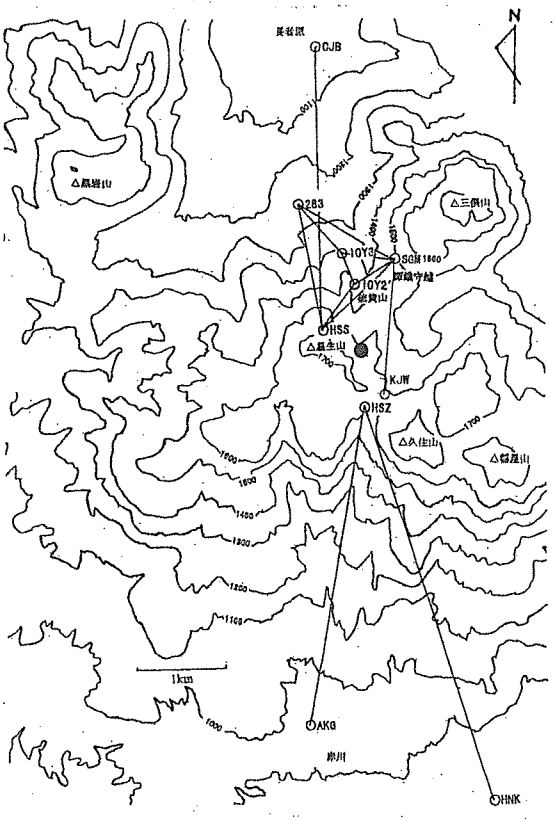

Figure 1. Location map of EDM base lines at Kuju Volcano and new crater indicated by ●.

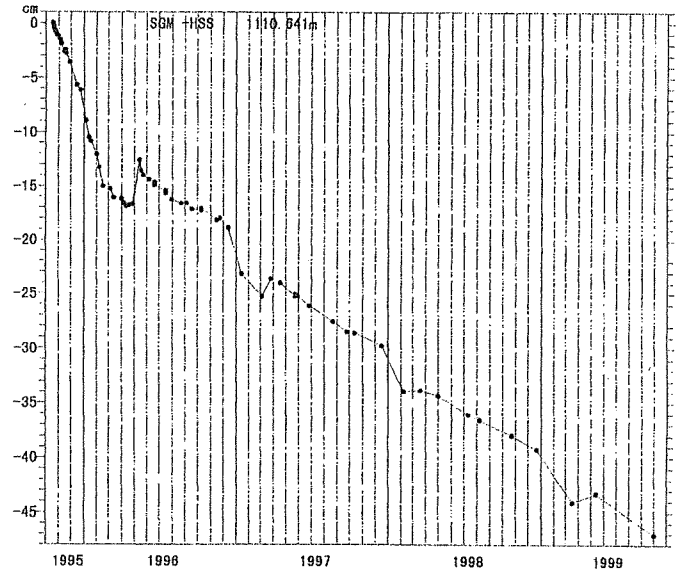

Figure 2. Variation of distance SGM-HSS.

Changes of the geomagnetic total intensity obtained by repeated survey at Kuju Volcano, Kyushu, Japan

Sakanaka,S., Tanaka,Y., Hashimoto,T. and Utsugi,M.

We have continued to conduct the geomagnetic observation at the thermal area called Kuju-Iwoyama in Kuju volcano, Japan. In October 1995, a moderate phreatic eruption occurred at the flank of Mt. Hossho on the south of Iwoyama area, which is one of the volcanic bodies of Kuju volcano. In addition to pre-existed fumaroles, new vents formed by 1995 eruption remain to be hydrothermally active even at present, in the beginning of 2000.

Just after the eruption, we installed six proton precession magnetometers for continuous observation of the total intensity. The prominent characteristics of magnetic changes at Kuju-Iwoyama are 1) constant rates of magnetic changes after 1995 eruption and 2) the total amount of changes more than 100nT at the vicinity of fumaroles. A thermally remagnetized virtual magnetic dipole explains observed magnetic changes at five continuous observation sites.

In order to confirm the cooling mechanism and visualize the shape of cooling area, we newly installed plastic pegs for repeated magnetic survey in the end of March in 1999. We have so far totally 35 repeated survey points within 2km around. In general, the results of repeated magnetic survey are subject to errors originated from the magnetic storm or the solar activity more than those of continuous magnetic observation. Together with continuous observation, however, the amount of errors included in the result of the repeated survey is able to be checked and possible to be corrected using continuous values. The rates of changes obtained at repeated survey points installed next to the continuous observation sites are well-consistent with those obtained at the continuous sites. We can infer that errors obtained by repeated survey around Kuju-Iwoyama are within 3nT.

The three candidates of mechanism of magnetic changes around Kuju-Iwoyama are thermomagnetic effect, piezomagnetic effect and electrokinetic effect. At the point of total amount of magnetic changes up to more than 100nT, hydrothermally cooling effect (thermomagnetic effect) is regarded to be most dominant.

The distribution pattern of the total intensity changes on the whole is as follows; positive changes appear in the southern area and negative changes in the northern area. A virtual magnetic dipole aligning the geomagnetic field can approximately explain the distribution of magnetic changes at repeated survey points. Strictly speaking, however, the predicted changes by the single magnetic dipole overestimate the amount of negative magnetic changes in the northern area.

Next we tried to explain the magnetic changes by two magnetic dipole sources. One of the best fit two sources is located at the depth of 200m just below C-region which is one of the pre-existed fumaroles. The other is at the depth of 700m and about 100m north of the shallower source. Both of sources indicate remagnetization. We think that a magnetic source including two virtual sources is favorable.

Hence we suggest an elongated magnetic source slightly inclined to the north which applausively reproduces the observed magnetic changes. The elongated magnetic source is a replica of the body being cooled by water vapor flowing.

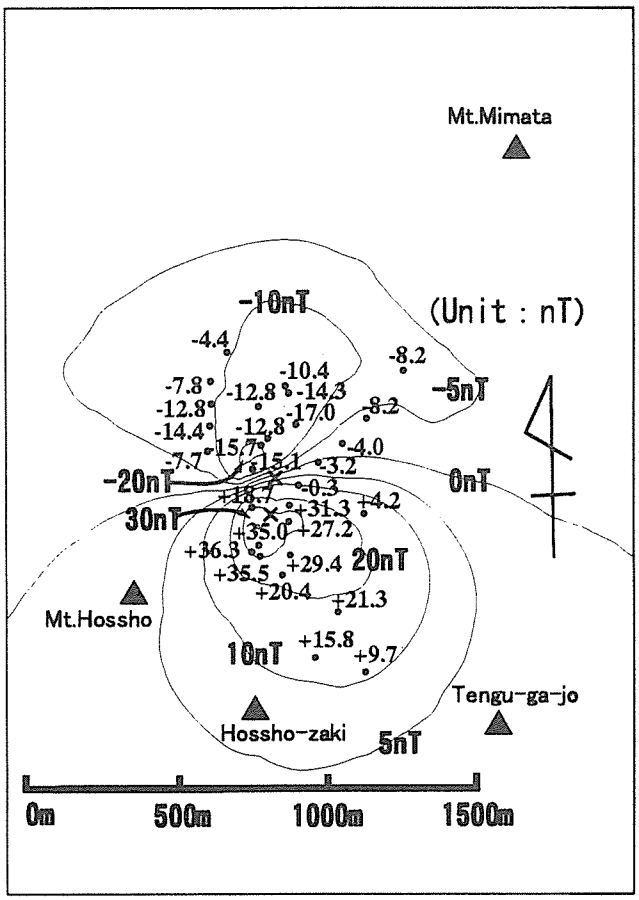

Fig.1 Magnetic changes at Kuju-Iwoyama obtained by repeated surveys. Changes in the total intensity are revealed as annual change rates during 1999. Contour lines show the changes in the total intensity predicted by best fit two magnetic dipole sources. The symbols × denote the centers of virtual magnetic sources.

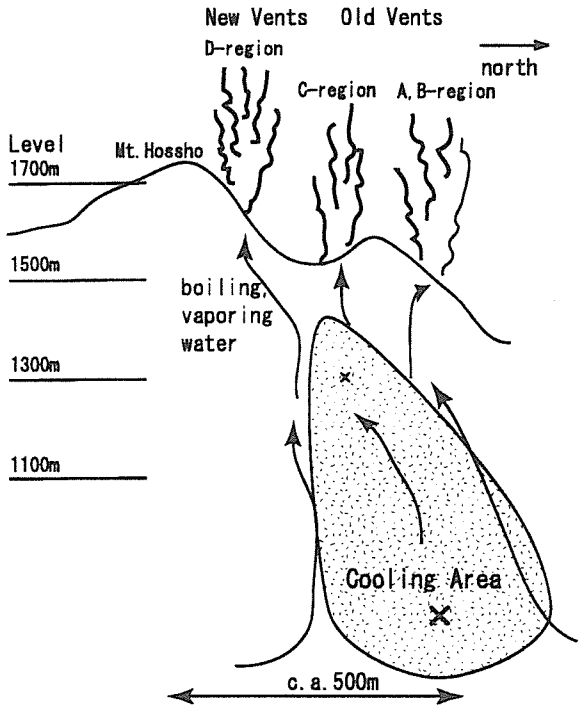

Fig.2 One of favorable shematic diagrams below Kuju-Iwoyama geothermal area. The Cooling body is inferred from the magnetic changes on the ground. The symbols × denote the centers of virtual magnetic sources.

Melting of recycled oceanic crust within a mantle plume head: Genesis of Deccan Trap basalts

Sano, T. and Fujii, T. (Univ. Tokyo)

Based on the major and trace element compositions of Deccan Trap rocks, we propose that melting of an hybrid mantle diapir composed of a fragmented, recycled oceanic crust and a host peridotite plume head can explain the genesis of Deccan Trap basalts (Fig. 1). This model can be supported on two counts. Firstly, most Deccan tholeiites possess MgO contents which are lower than those expected for high degree partial melts of the single peridotite plume normally considered in explanation of the large volume of Deccan magmas. Secondly, major and immobile trace element compositions of Deccan tholeiites can be reasonably explained by simple mixing of two member magmas. These should consist of an alkalic picritic basalt which may represent an inferred peridotite-derived melt, and a partial melt of oceanic crust. High pressure-temperature melting experiments of average mid-oceanic ridge basalt composition can generate such a partial melt under conditions identical to those inferred for the above alkalic picritic basalt. The inferred weight percent of the recycled oceanic crust in the plume head is 7–12 wt %. Potential temperatures calculated for the hybrid mantle plume head lie in the 1430–1445 °C and are lower than those for a simple peridotite plume head (≥ 1450 °C).

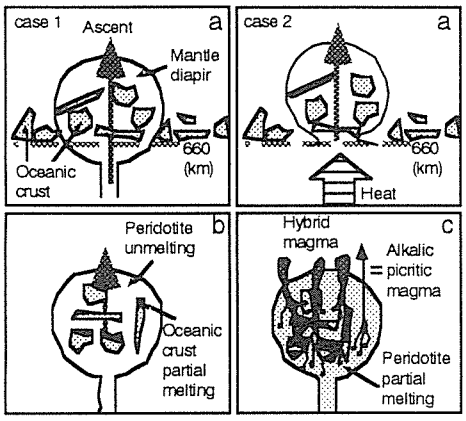

Fig. 1. Schematic diagrams based on the composite diapir model proposed by Yasuda et al. [1992, 1997] and Yasuda and Fujii [1998], showing the melting process of the composite diapir during its ascent. Two cases have been proposed for ascent of ancient subducted oceanic crust from the base of the upper mantle. In the first case, fragments of the subducted oceanic crust are entrained into the upwelling mantle diapir at the base of the upper mantle (Fig. 1a, case 1). In the second case, heat transfer from the lower mantle causes the temperature to rise until a part of upper mantle (depleted mantle) which include fragments of subducted oceanic crust becomes unstable (Fig. 1a, case 2). Whichever the case, we accept the composite diapir which consists of fragmented oceanic crust and host peridotite ascends adiabatically (Fig. 1a).

Fractionation of Deccan Trap Basalts: Contribution from Geochemistry and Experimental Petrology

Sano, T., Fujii, T. (Univ. Tokyo), Deshmukh, S.S. (Nagpur, India), Fukuoka, T. (Rissho Univ.) and Aramaki, S. (Nippon Univ.)

Deccan Trap basalts are generally highly contaminated, but a less contaminated component can be defined which contains little or no lithospheric material. Members of this sub-group possess distinctive geochemical characteristics such as Ba < 100 ppm, Sr = 190-240 ppm, TiO_2 = 2.0-4.0 wt %, Zr/Nb = 10-18. Analyses of 325 basalts, which were collected from 27 sections well distributed through the Deccan Traps, demonstrate that these less contaminated basalts are distributed widely throughout the study region. In order to understand the shallow-level fractionation processes of the Deccan Trap magmas, melting experiments were conducted at one atmosphere at both quartz-fayalite-magnetite (QFM) and nickel-nickel oxide (NNO) oxygen fugacities for three different Mg-rich basalts, one of which belongs to the less contaminated group. The results indicate that the QFM buffer can reasonably account for both the phenocryst assemblage and the chemical trend of the less contaminated basalts. From the results of these experiments we establish an empirical geothermometer based on the MgO content in experimental glasses, and estimate the pre-eruption temperature of less contaminated basalts to be 1150-1170 °C (Fig. 1).

(J. Petrol., submitted)

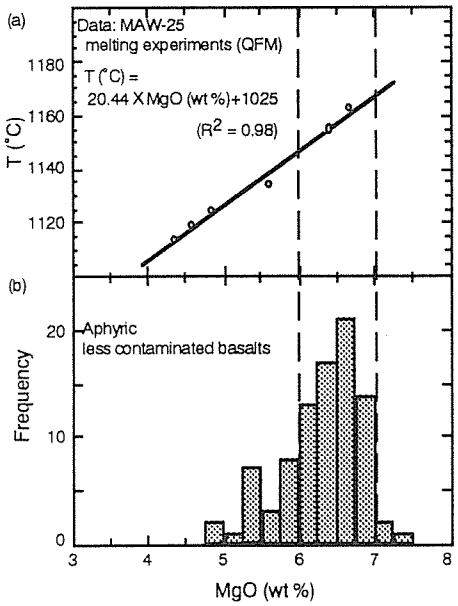

Fig. 1. (a) % wt MgO content in glass versus temperature produced by melting experiments for MA-W-25. (b) % wt MgO content versus frequency of aphyric less contaminated Deccan Trap basalts.

Re and Os System in Ophiolitic Complexes: Implications for Chromitite Formation and Ophiolite Paragenesis.

R.A. Santos, **K.Suzuki**, B. Takano, **Y. Tatsumi** Y. Miyata, and Y. Nozaki

Ultramafic rocks and some chromitites from two Philippine Ophiolite complexes, the Palawan and Dinagat ophiolite complexes, have been analyzed for its Re and Os isotopic compositions. Both complexes host chromitite pods and layers of economic quantities and are hosted by depleted mantle rocks (harzburgite) with dunite selvage. Lenses of dunite in harzburgite are discernible in both complexes and apparently increases in frequency as major zones of chromitite deposits are approached.

Prior to the use of the Carius tube digestion technique in the isotope dilution methodology two other digestion steps were taken into consideration: the microwave digestion and the fire-assay techniques. The former has the advantages of optimum homogenization of spikes in the sample and of faster digestion time; whereas the latter is efficient in the recovery of Os (and the PGEs- platinum group elements) but poor in Re recovery. The Carius tube technique with single-bead separation procedure is found to have the lowest blank contribution. Duplicate analysis of SARM7 standard rock is at the level of 98%.

The $^{187}Os/^{188}Os$ ratios of chromitite samples yield present-day values that are suprachondritic (0.1304 - .1570) whereas harzburgite at some distance from the chromitite zone have ratios mainly of sub-chondritic to chondritic (0.1197 - 0.1273) level. Regressing these ratios based on the chromitite isochron resulted in values suggestive of extensive melt depletion of the peridotite hosts. The chromitite Os ratios are suggestive of radiogenic Os introduction into the chromitite-producing system. An apparent "chromatographic effect" on $^{187}Os/^{188}Os$ ratios was delineated on samples proximal to chromitite and pyroxenite zones. These samples yield values (0.1325 – 0.1730) which are suggestive of radiogenic Os enrichment.

The chromitites in both complexes are generally Cr-rich (Cr# >68) though minor layers of chromitites are at the level of 55 to 60 (Cr#). Inclusion mineralogy and geochemistry show the dominance of pargasite and diopside with relative enrichment in Na, K and Ti in comparison with those in the peridotite matrix. Whole rock REEs of the chromitites revealed relative enrichment compared to the peridotite host.

The Os and Re systematics in combination with the peridotite and chromitite mineralogy and chemistry suggest for the possible formation of the Palawan and Dinagat ophiolite complexes in a supra-subduction setting. Chromitite formation might have resulted from the interaction of fluid-enriched melt derived from the dehydration of a subducting slab with depleted upper mantle rocks.

References:

[1] Shirey,S. and Walker,R. (1998), *Annu. Rev. Earth Planet. Sci.* **26**,423-500.[2]Brandon, A. et al. (1996), *Science* **272**, 861-864.

Chemical Separation of Pb, Sm and Nd for isotope analyses of Rock Samples

Shibata, T. and Yoshikawa, M.

The methods for chemical separation of Pb, Sm and Nd from rock samples are determined to be realized the multi-isotope analyses of Pb, Sm-Nd and Rb-Sr in BGRL. The separations are made by ion chromatography using ion-exchange resins following essentially Koide and Nakamura (1989), Shibata et al. (1989) and Shibata (1992). The procedure for chemical separation of Rb-Sr is described in Yoshikawa and Shibata (in this issue).

Chemical Separation of Pb

Rock sample was decomposed by HBr-HF mixed acid in a Teflon® jar on a hot plate at ≈ 100 °C. After dryness, 1.0 ml of 0.5 N HBr was added to the decomposed samples and centrifuged. The supernatant was loaded on to the column, which was charged 0.1 ml of anion-exchange resin (Muromac®; AG1X8) and conditioned by 0.6 ml of 0.5 N HBr. To remove the other elements, additional 2.0 ml of 0.5 N HBr was passed though the column. Finally, Pb was collected by 1.3 ml of H_2O. By this procedure, Pb was isolated from rock samples completely.

Chemical Separation of Sm and Nd

The procedure of removal of major elements is described Yoshikawa and Shibata (in this issue). The pH-controlled cation exchanged resin of AG 50W X8 was charged into a 0.3 ml of Teflon® column (3mm in diameter 40 mm in length). The resin was then conditioned by 0.6 ml of 0.2 M α-hydroxyisobutric acid (α-HIBA). The dried Sm and Nd fraction was dissolved in 0.1 ml of 0.06 N HCl. This solution was loaded onto the column as 3 fractions. 0.9 ml of 0.2 M a-HIBA was successively added to the column, and the first 0.5 ml was added as a fraction of 0.1 ml. Sm was collected by 0.9 ml of 0.2 M α-HIBA and 1.1 ml of 0.2 M α-HIBA was added. Nd was finally collected by 2.2 ml of 0.2 M α-HIBA. By this procedure, the pure fractions of Sm and Nd without any isobaric elements during thermal ionization mass spectrometry (TIMS) were obtained.

Multi-isotope analyses

The chemical procedures presented here and Yoshikawa and Shibata (in this issue) have made it possible to isolate Pb, Sm, Nd, Rb and Sr from rock sample. Although the further examinations, such as measurements by TIMS and procedural blanks for each element, and maintenance of chemical laboratory are necessary, multi-isotope analyses for Pb, Sm-Nd and Rb-Sr will be realized by these chemical procedures.

Behavior of subducting sediments beneath the arc under high geothermal gradient; implication for the progressive continental growth

Gen Shimoda

In order to evaluate the relation between sediments and Setouchi volcanic rocks, bulk rock chemistry of pelagic sediments from the Philippine Sea (GDP 15-12) and trench-filled sediments from the Nankai Trough (DSDP site 582) were determined with X-ray fluorescence (XRF) spectrometers. Incompatible element compositions of these pelagic sediments and especially for the elements Pb, Ba and Th were found to be much higher than those of terrigenous sediments. Mixing calculations using Pb/ Sr, Ba/Sr and Th/Zr ratios indicate that terrigenous rather than pelagic sediment plays a significant role to produce the high-Mg andesites (HMA) and basalts in the Setouchi volcanic belt in SW Japan arc. Pb/K_2O Pb/Rb, Ba/K_2O and Ba/Rb ratios on the MgO variation diagrams also suggest a similar contribution. The relatively minor presence of pelagic sediment can be explained by smaller amounts of pelagic sediment subducted beneath the SW Japan arc, due to young slab age (11 m.y.). The sediment melting would restrict crustal material recycling back into the mantle by the production of arc magmas under high geothermal conditions and may contribute to progressive continental growth and evolution of the depleted mantle during the Archean period.

(to be submitted to Chemical geology)

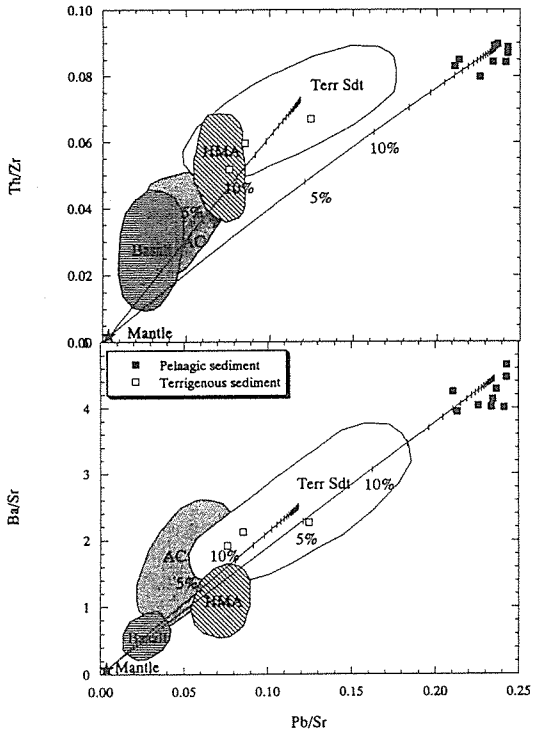

Fig. 1 Ba/Sr and Th/Zr vs. Pb/Sr diagrams for pelagic and terrigenous sediments. Composition of terrigenous ediment reported Shimoda et al., (1998) are abbreviate as Terr Sdt. HMA and basalt data from Shimoda et al., (1998) are also shown. Ratios of the average continental crust, data from Rundnick, (1995), Shaw et al., (1986), Wedepohl, (1994),Weaver and Tarney, (1984) and Taylor and McLennan, (1985), are abbreviate as AC.

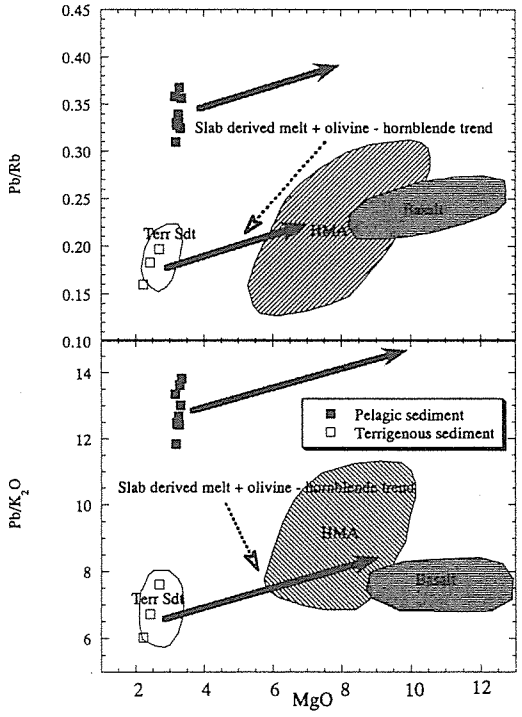

Fig. 2 MgO variation diagrams for Pb/K2O and Pb/Rb ratios for pelagic (filled squares) and terrigenous (open squares) sediments along with Setouchi HMA and basalt.

Fast separation of lead with low crosslinkage ion exchange resin for quantitative and isotopic analyses in geological materials.

Gen Shimoda

A separation scheme for lead with low crosslinkage ion exchange resin (AG1-X2) was described. A chemical characteristic of the resin, i.e., come to equilibrium more rapidly, enables to flow of medium at high rate (6 ml/min/cm^2). As a result, it took only about 20 minutes to isolate lead from other rock forming elements. A column with low ratio of height over inner diameter (ID 4 mm, H 10 mm) was employed in order to strip lead quickly from resin. Furthermore, 6 M HNO_3 was adopted as eluent in stead of commonly used 6 M HCl to achieve quantitative and rapid stripping. These enable to elute lead only 0.35 ml of 6 M HNO_3 and make it possible to separate lead from large amount of major elements such as magnesium, calcium, iron and sodium (correspond to 100 mg rock sample) with much smaller amount of total elution volume (1.95 ml). Recovery of the method obtained by single measurement was 95 % and total procedure blanks obtained by duplicated analyses were 13 and 15 pg, respectively. The evolved method should be suitable to separate lead for isotopic and abundance analyses from geological material with low concentration and/or small samples.

(to be submitted to Analytica Chimica Acta)

Application of strontium-specific extraction chromatographic method for isotopic and abundance analyses for geological samples

Gen Shimoda

Recently improved extraction chromatographic method was examined to separate strontium from geological samples for isotopic and abundance analyses. Trace amount of strontium (50 μg) can be separated from 100 mg of rock forming elements, such as calcium, magnesium, iron, sodium and potassium. The most of elements, including barium which can not be separated completely by previous works, were eluted with 15 ml of 7 M HNO_3 from a column containing 1 ml of Sr.Spec resin (inner diameter 6.4 mm, height 50 mm). Subsequently strontium can be recovered by 3 ml of H_2O rather than commonly used 0.05 M HNO_3. Although the resin can sharply separate strontium from other elements, change of solute, namely 7 M HNO_3 to H2O, elute small amount of rubidium (0.3 % of total amount). Thus further purification, e.g., duplicate separation, was required to isotopic analyses.

(to be submitted to Geostandard News Letter)

Seismic Activeity around Aso Caldera and Kuju Volcano in 1999

Sudo, Y.

A telemetrically seismic network around Aso Caldera and Kuju Volcano is composed of 10 stations. Several earthquake swarms have occurred at the western region of Aso Caldera and the northwestern side area of Kuju Volcano. From March to April and June in 1999, at the northwestern caldera floor big swarms occurred, some events were felt. On February and from October to November at the southwestern region outside Aso Caldera, many felt earthquakes occurred. At Kuju Volcano, many earthquakes occurred on April, May, June, and November. The mechanisms of their events indicate a combination of both normal and right lateral strike-slip type faults. The tension axis maintains a horizontal north-south orientation.

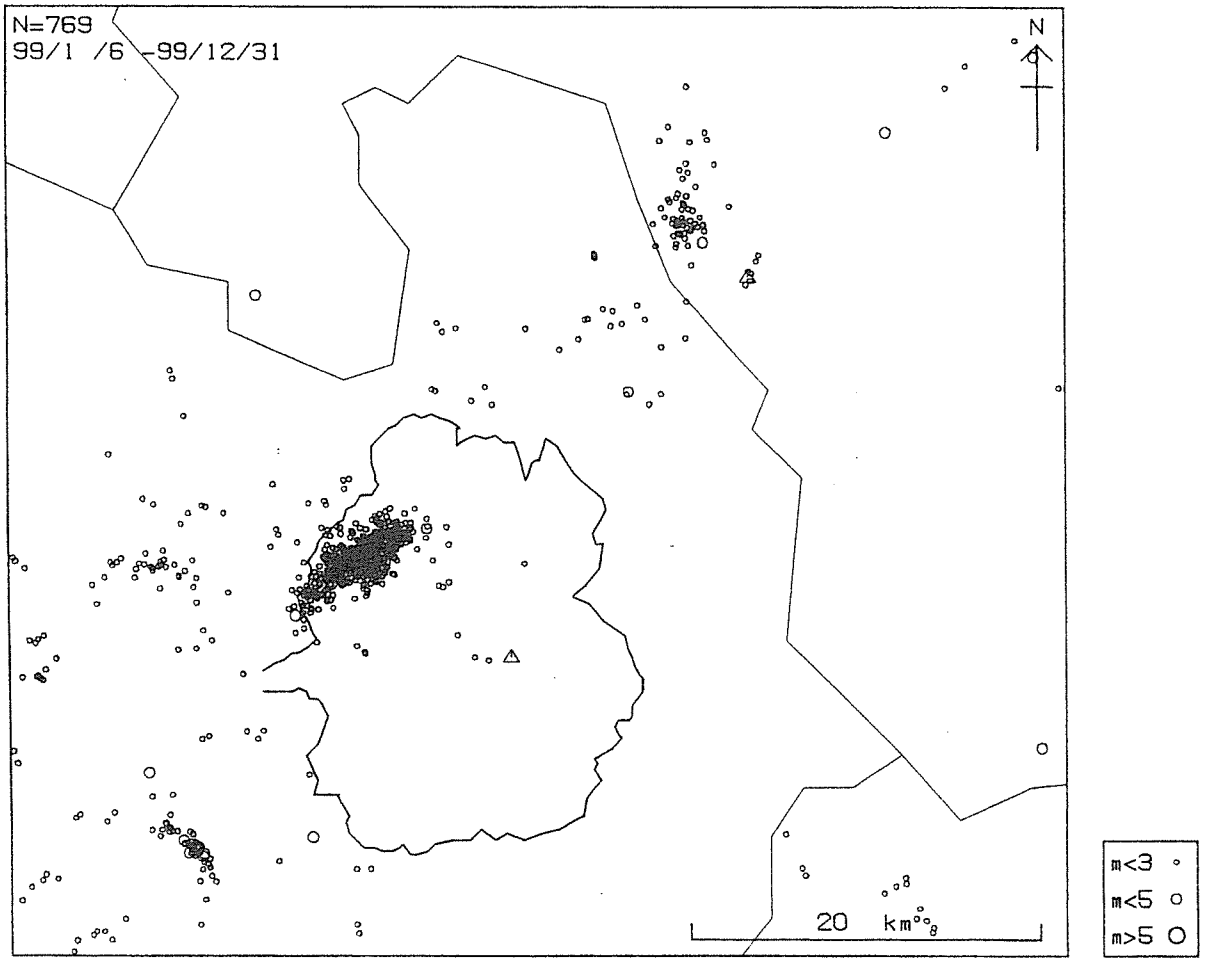

Figure 1: Distribution of epicenters around Aso Caldera and Kuju Volcano in 1999.

Decomposition method of geological sample for osmium analysis: Carius tube vs. closed PFA vessel.

Suzuki, K. and Tatsumi, Y.

Two representative digestion techniques for determination of Os (and Re) abundance and isotopic compositions, the Carius tube and closed PFA vessel decomposition, are compared with regard to precise quantitative analysis of Os. Osmium is volatile in oxidative environments and should be handled with care not to permit Os to escape before complete isotopic equilibration between Os derived from a sample and the added enriched isotopes (the spike) in the isotope dilution method. We found in Os standard calibration experiments that a PFA container more or less leaked around the lid, especially in case of the vessel half-filled with solution, which resulted in incomplete homogenization of Os (Fig. 1). On the other hand, the Carius tube digestion method, i.e., decomposition in a sealed glass tube at 220 – 240 °C, gives exceedingly reproducible results in the Os standard calibration experiment (Fig. 1), indicating complete isotopic equilibration of Os, which would lead to more robust determination of Os abundance in geological materials.

Analytical results of homogeneous molybdenite powder, HLP-5 (in-house standard of AIRIE, Colorado State Univ.), also shows contrast results. The Re-Os ages determined by the Carius tube digestion combined with liquid bromine-extraction, are exceedingly reproducible (0.61 %, 2 sigma). On the contrary, the Re-Os ages of HLP-5 obtained by the PFA vessel decomposition do not reproduce well. These results could be applied to analysis of other geological materials. Consequently, the Carius tube decomposition combined with bromine-extraction followed by micro-distillation allow us to determine more easily the accurate Os abundance in a geological sample.

(To be submitted to Chem. Geol.)

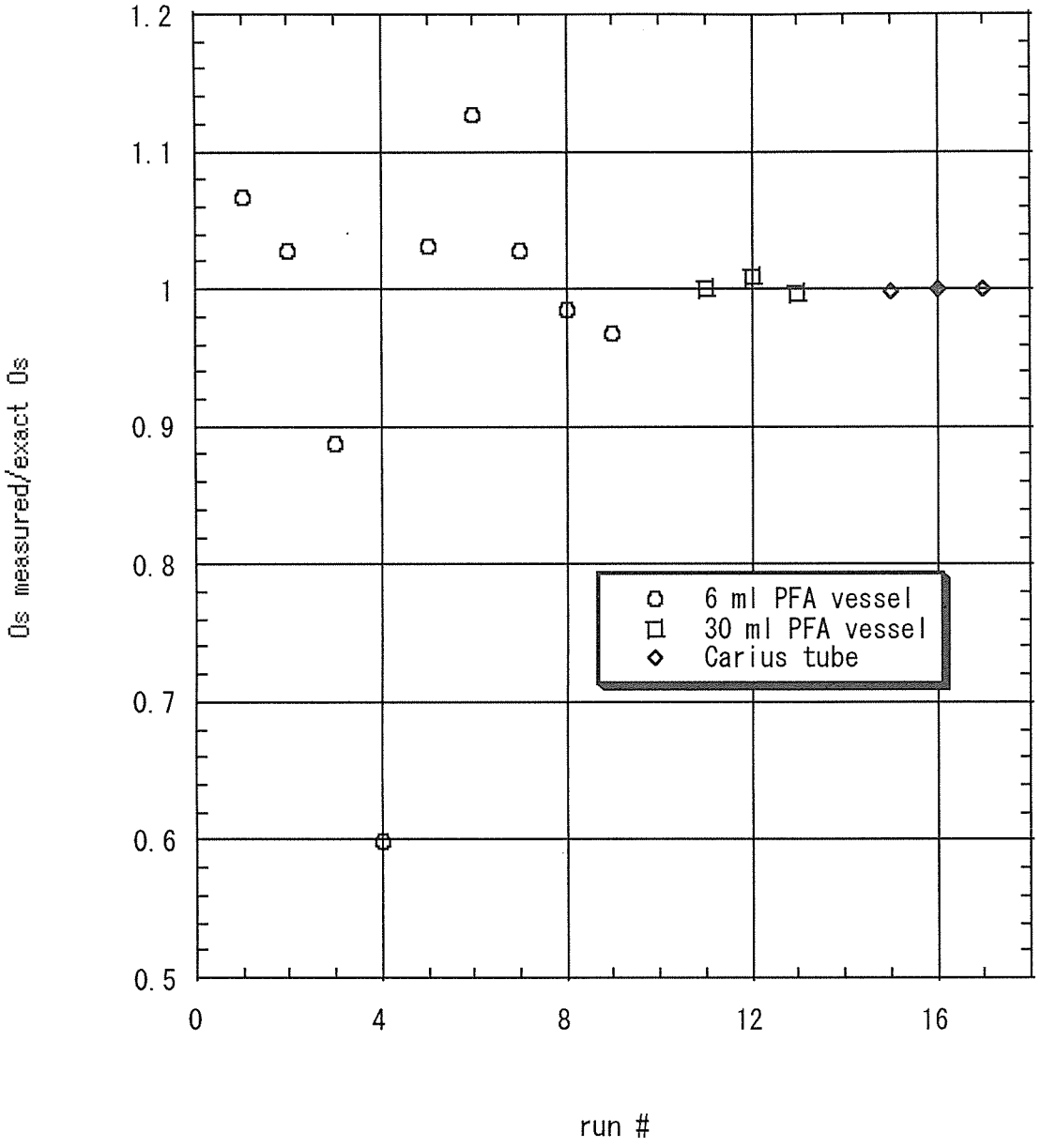

Fig. 1. Results of osmium standard calibration. Exact Os concentration is based on the calibration between our standard and the standard of University of Maryland. More reproducible results was obtained for the Carius tube digestion than the results obtained for the PFA vessel decomposition.

High resolution Re-Os age for molybdenite from Broken Hill ore deposits.

Suzuki, K., Skirrow, R. G. and **Tatsumi, Y.**

Highly reproducible Re-Os ages (2 sigma = 0.07 - 0.4 % in duplicate analysis) were obtained for molybdenites from the Olary region, Broken Hill, Australia (Table 1), employing the combined method of the modified Carius tube digestion and bromine-extraction technique. The obtained ages for molybdenites from 8 location in 4 ore deposits of the Olary region range from 1631 to 1612 Ma. This result indicates that continuous hydrothermal activity between 1631 - 1612 Ma may have occurred under the Olary region and hydrothermal fluids frequently approached the mineralization zone through cracks and faults. Although the application of the highly reproducible technique is limited only to molybdenite, the ages reported here provide so far the highest reproducibility in radiometric age determination, which may allow us depict the dynamic formation processes of molybdenite-bearing rocks at about 0.1 % resolution.

Table 1. Re-Os data of molybdenites from Olary, Broken Hill, Australia.

sample name	Re-Os age (Ma)
Kalkaroo 1	1631.7 +/- 4.9
duplicate	1628.2 +/- 1.6
Kalkaroo 2	1624.1 +/- 8.4
duplicate	1624.8 +/- 1.7
White Dam 1	1612.0 +/- 2.8
duplicate	1612.6 +/- 4.8
White Dam 2	1631.4 +/- 1.8
White Dam 3	1616.5 +/- 0.6
Portia 1	1615.0 +/- 8.4
Portia 2	1614.0 +/- 6.4
Portia 3	1616.3 +/- 1.8
Waukaloo	1613.4 +/- 5.4

(To be submitted to Science)

Re-Os isotopic composition of GSJ standard rocks, JB-1a, JA-2 and JP-1.

Suzuki, K. and Tatsumi, Y.

Rhenium-osmium isotopic compositions of standard rocks JB-1a, JA-2 and JP-1, distributed by Geological Survey of Japan (GSJ), were measured through negative thermal ionization mass spectrometry (NTI-MS). Duplicate analyses of each sample show heterogeneous distribution of Os and Re in the standard rocks. Inverse relationships between isotopic compositions and concentrations of Os reveal that the JB-1a and JA-2 are products of mixing between chondritic mantle and two distinct radiogenic material (Figure), probably derived from the subducting slab. In addition, the phases containing radiogenic and unradiogenic Os likely exist in both JB-1a and JA-2, which indicates incomplete isotopic equilibration of Os at their formation processes. On the other hand, JP-1, Horoman ultramafic complex, yields sub-chondritic Os isotopic composition and was therefore derived from the depleted mantle source.

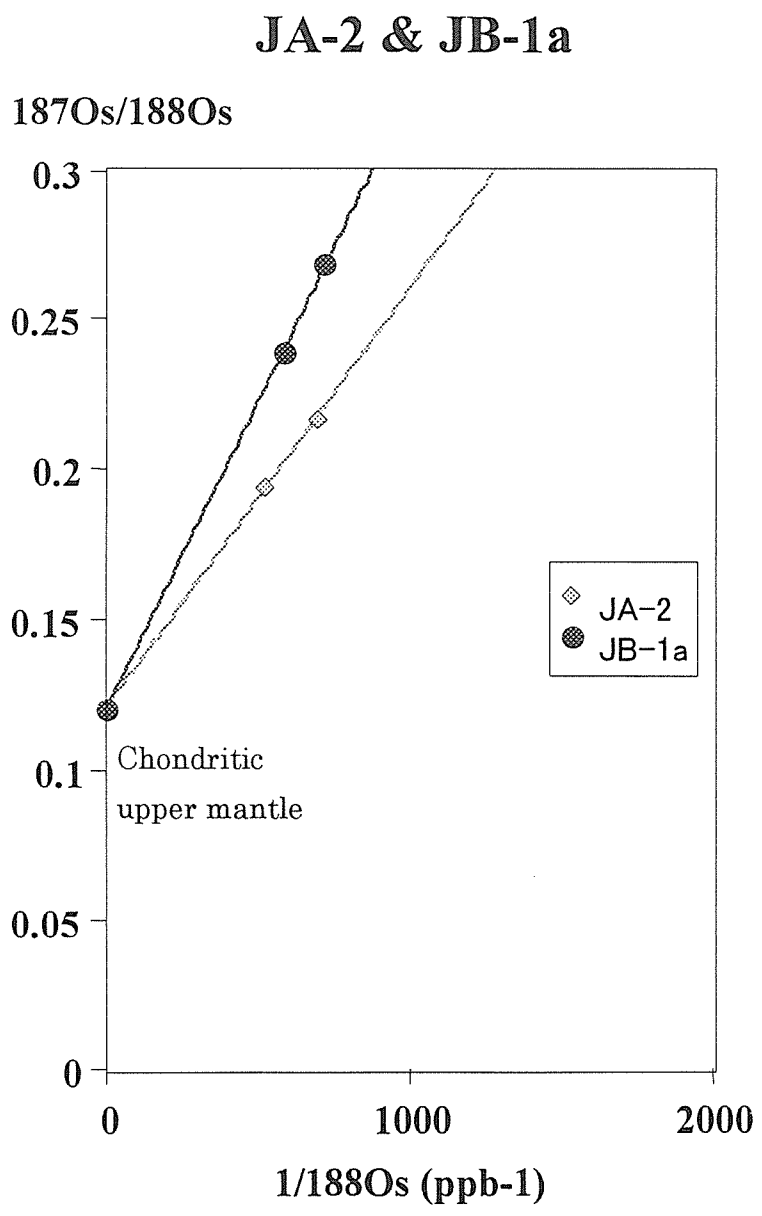

(To be submitted to Geochem. J.)

Re-Os systematics of molybdenite from Riviera, South Africa: Implications for mineralization and post-depositional alteration.

Suzuki, K., Scheepers, R. and Smit, C. M.

Re-Os ages of six molybdenites from Riviera in western Cape Province of South Africa were determined. Five molybdenites except one give Re-Os ages in agreement with each other within analytical uncertainties, whose weighted mean is 510 +/- 9 Ma. This age is consistent with the timing of intrusion of the I-type granitoids in the area, indicating that this intrusion is responsible for the formaiton of Riviera molybdenum ore deposits. On the contrary, duplicate analyses of the other molybdenite (Mo 10) yield the older and inconsistent Re-Os ages (566 Ma and 1093 Ma). Previously, Suzuki et al. (2000) experimentally showed that Re-Os system of molybdenite was disturbed in low concentration (<1 %) NaCl or $NaHCO_3$ solution at a temperature of 180 °C for 20 days. Smit et al. (1999) found that alteration with H_2O - CO_2 - rich fluid of temperature of 175 - 375 °C and of moderate salinity (ca. 8 eq. % NaCl) occurred after primary mineralization of molybdenite. This alteration is associated with A-type granitoid, which intruded into the I-type granitoids. Therefore, post-depositional alteration are likely to be responsible for the inconsistent Re-Os age of the above molybdenite. Consequently, systematic analyses of molybdenites from various parts of the Riviera ore deposit allow us to determine the exact formation age of undisturbed molybdenites and to detect disturbance of Re-Os system of the molybdenite.

(To be submitted to G-cubed.)

The petrology and geochemistry of calc-alkaline andesites on Shodo-Shima Island, SW Japan: assessment for the origin of the continental crust

Tatsumi, Y. and Nakashima, T.

Petrographical and geochemical characteristics of calc-alkaline andesites on Shodo-Shima Island, SW Japan, having bulk compositions largely identical to the continental crust, are presented. The following petrographic observations suggest a role for magma mixing in producing such andesite magmas: (1) two types of olivine phenocrysts and spinel inclusions, one with compositions identical to those in high-Mg andesites and the other identical to those in basalts, are recognized in terms of Ni-Mg and Cr-Al-Fe^{3+} relations, respectively, (2) reversely zoned pyroxene phenocrysts may not be in equilibrium with Mg-rich olivine, suggesting the involvement of a differentiated andesite magma as an endmember component, and (3) the presence of very Fe-rich orthopyroxene phenocrysts, indicating the association of an orthopyroxene-bearing rhyolitic magma. Contributions from the above at least four endmember magmas to the calc-alkaline andesite genesis can also provide a reasonable explanation of the Pb-Sr-Nd isotope compositions of such andesites. Although differentiation of mantle-derived Mg-rich andesitic magmas has been proposed for explaining the characteristic compositions of bulk continental crusts, the present observations are nor consistent with this mechanism. (submitted to J. Petrology)

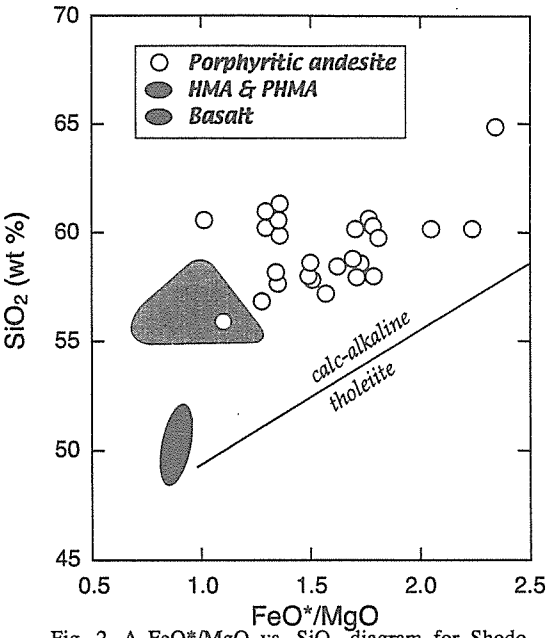

Fig. 2. A FeO*/MgO vs. SiO_2 diagram for Shodo-Shima volcanic rocks. Porphyritic andesites on this island exhibit a broad calc-alkaline trend based on Miyashiro's definition (1974).

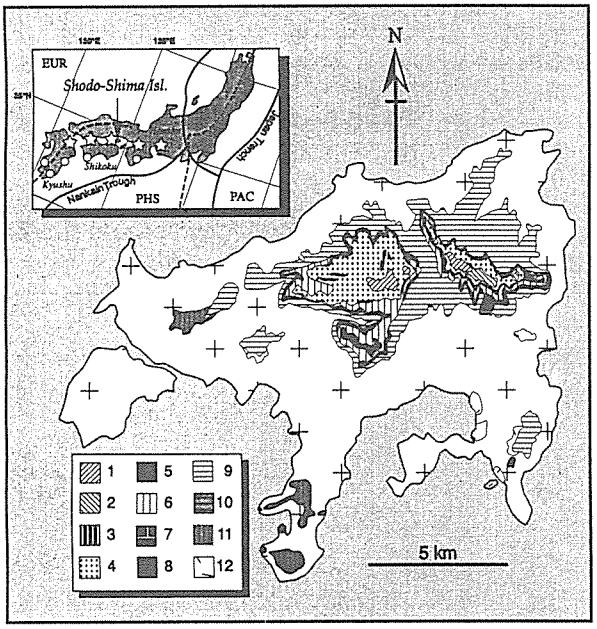

Fig. 1. Tectonic setting of the Setouchi volcanic belt and a simplified geologic map of Shodo-Shima Island after Tatsumi (1983b). The Setouchi volcanic rocks (open stars) and coeval felsic volcano-plutonic complexes (open circles) are distributed in the present forearc region, to the trench-side of the Quaternary volcanic front (hatched lines). Setouchi volcanic rocks on Shodo-Shima Island, which cover mainly granitic basements (cross), are divided into two groups, Kankakei (1-10) and Uchinomi (11) Formations in descending order. EUR, Eurasian plate; PHS, Philippine Sea plate; PAC, Pacific plate.

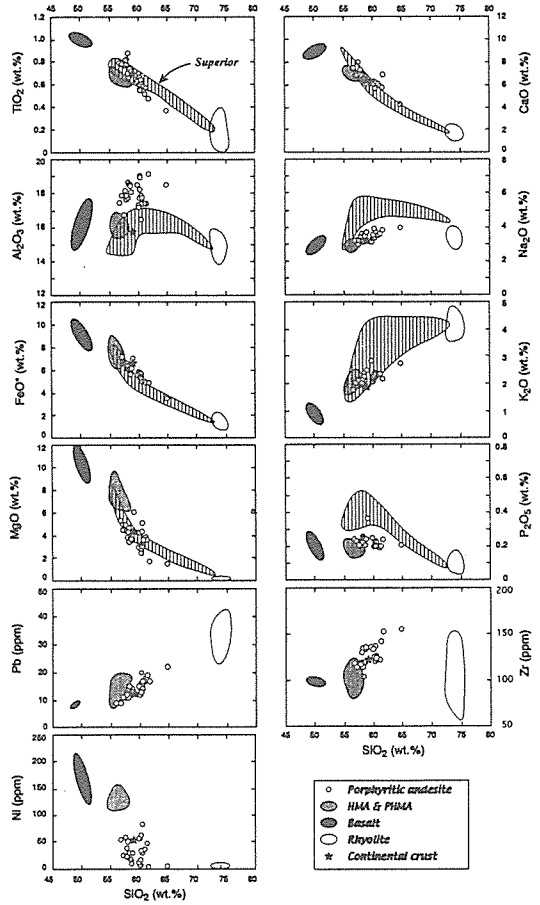

Fig. 3. SiO_2 variation diagrams for selected major and trace element concentrations in Setouchi volcanic rocks on Shodo-Shima Island. It should be stressed that Shodo-Shima andesites show chemical trends almost identical to those of monzonite-granodiorite suite in Superior Province (Shirey and Hanson, 1984; Stern et al., 1989; Stern and Hanson, 1991). Further, the bulk continental crust compositions (Rudnick, 1995) are plotted largely within the geochemical trend formed by Shodo-Shima andesites, except for the rather lower concentration of Al2O3 in the bulk continental crust.

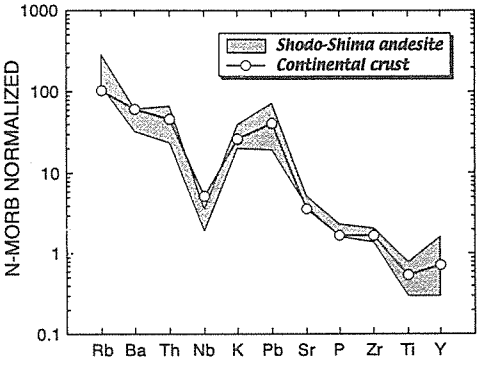

Fig. 4. N-MORB normalized (Sun and McDonough, 1989) incompatible element compositions of Shodo-Shima porphyritic andesites and the bulk continental crust (Rudnick, 1995). Both andesites show characteristics that typify subduction zone magmas.

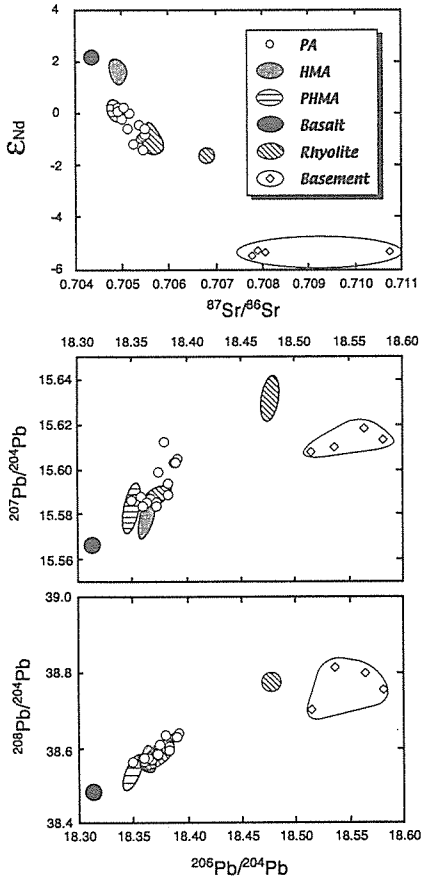

Fig. 5. Isotopic compositions of Setouchi volcanic rocks and basements on Shodo-Shima Island. Rhyolites in the Setouchi volcanic belt can be divided isotopically into enriched and less enriched groups, the latter having isotopic compositions largely identical to those of porphyritic andesites. It is suggested that mixing of basalt, HMA and enriched rhyolite magmas can produce porphyritic andesite (PA) magmas. On the other hand, the granitic basement may not be an endmember for such andesite magmas, as Pb isotope compositions of basement rocks do not lie on the extended trends for calc-alkaline andesites.

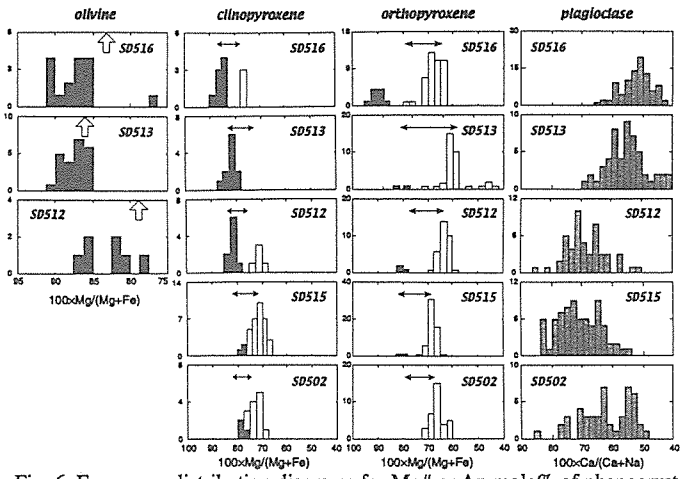

Fig. 6. Frequency distribution diagrams for Mg# or An mole% of phenocryst phases in cal-alkaline andesites on Shodo-Shima Island. Compositions of the phenocryst rims are shown with arrows. Filled and open boxes indicate compositions of normally and reversely zoned phenocrysts, respectively. Such clear zoning is not observed for plagioclase phenocrysts. Olivine compositions calculated by assuming Fe-Mg exchange partitioning between olivine and the bulk rock are shown by open arrows.

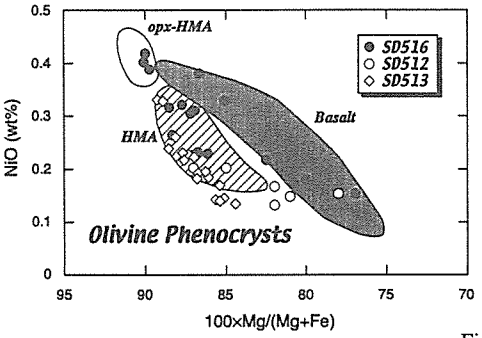

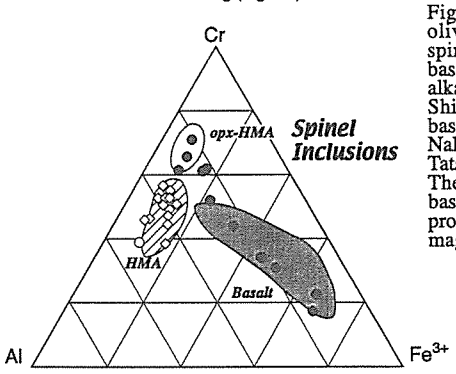

Fig. 7. Compositions of olivine phenocrysts and spinel inclusions in HMA, basalt, and porphyritic calc-alkaline andesites on Shodo-Shima Island. Data for basalts and HMAs are from Nakashima et al. (1999) and Tatsumi and Ishizaka (1981). The involvement of both basalt and HMA magmas in production of such andesite magmas is suggested.

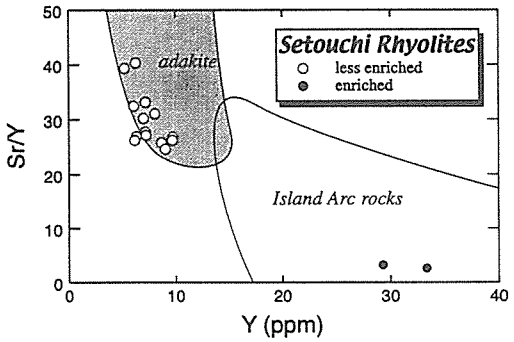

Fig. 8. Sr/Y vs. Y relations for adakites, arc rocks (Defant and Drummond, 1990) and Setouchi rhyolites (Shimoda and Tatsumi, 1999). Enriched rhyolites, which would be a possible felsic endmember component for calc-alkaline andesites, are characterized by lower Sr/Y ratios than less enriched rhyolites, suggesting a low-crust-origin, rather than a subducting-slab-origin for such rhyolitic melts.

Transition from arc to intraplate magmatism associated with backarc rifting: evolution of the Shikhote Alin volcanism

Tatsumi, Y., Sato, K., Sano, T., Arai, R., and Prikhodko, V.S.

K-Ar dates and chemical compositions of lavas in Shikhote Alin, Far East Russia, demonstrate marked secular variation in lava chemistry and suggest a linkage between magmatism and the major tectonic opening of the Japan Sea backarc basin. Lavas having typical arc magma chemistry were produced at 40-25 Ma in the eastern part of Shikhote Alin. A conspicuous volcanic hiatus is revealed in the region at 25-20 Ma, which is contemporaneous with the period of the major rifting of the backarc basin. Subduction-related magmatism may have been switched off by an oceanward retreat of the arc-trench system. In contrast, intraplate-type lavas with typical hotspot magma compositions have dominated magmatism in both the eastern and western Shikhote Alin since 20 Ma, and occupy the eastern margin of the Cenozoic intraplate magmatism in the NE Asian continent. (*submitted to Geophys. Res. Lett.*)

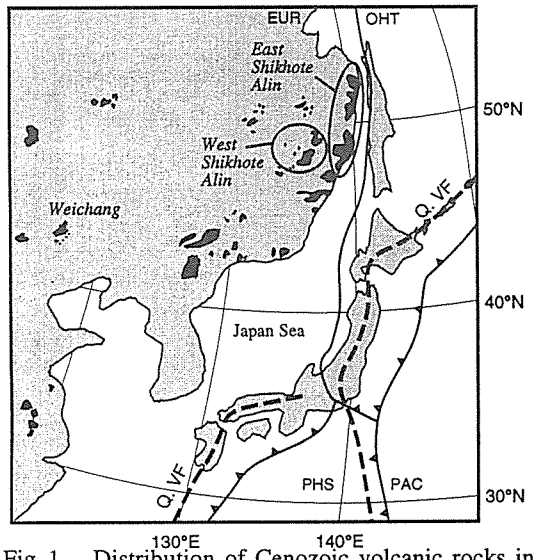

Fig. 1 Distribution of Cenozoic volcanic rocks in NE China and Far East Russia. Samples for dating and analysis were collected from two regions in Shikhote Alin and Weichang in NE China. Q. VF, Quaternary volcanic front; EUR, Eurasian plate; OHT, Okhotsk plate; PAC, Pacific plate; PHS, Philippine Sea plate.

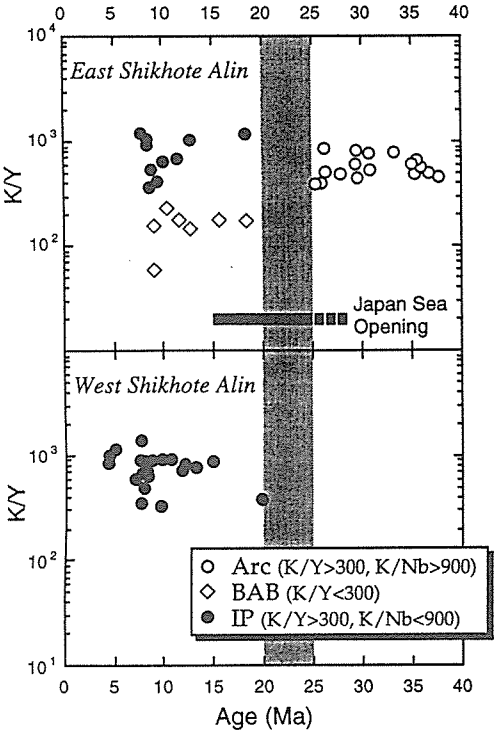

Fig. 2 Temporal variation in magma types for Shikhote Alin lavas. Identification of magma types, i.e., arc, BAB (backarc basin), and IP (intraplate) magmas, are based on K/Y-K/Nb relations in Figure 3. After the volcanic hiatus at 20-25 Ma, no arc-related magmatism took place.

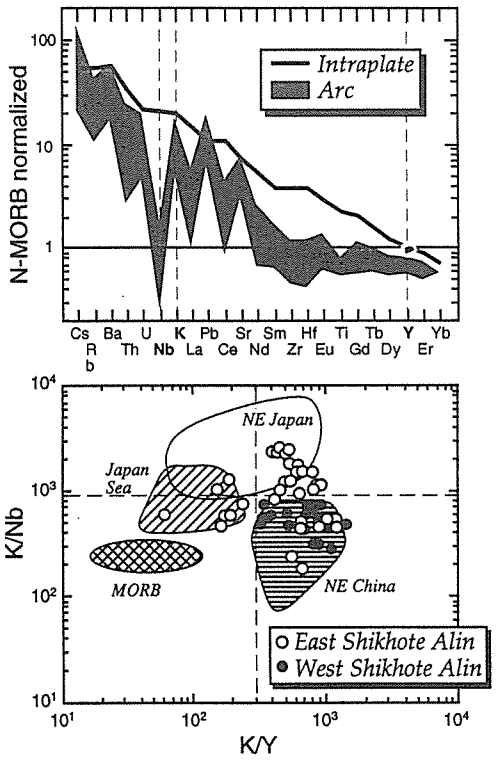

Fig. 3 Incompatible trace element characteristics of arc lavas [*Tatsumi and Eggins*, 1995}, intraplate and MORB [*Sun and McDonough* , 1989] on a spidergram (upper). The tectonic settings under which magma are produced can be more quantitatively identified in a K/Y-K/Nb diagram (lower). Lava compositions in NE Japan, Japan Sea and NE China are from *Sakuyama and Nesbitt* [1986], *Yoshida and Aoki* [1984], *Yamashita and Tatsumi* [1994], *Pouclet et al.* [1995], and *Tatsumi et al.* [1997].

Tectonic setting of high-Mg andesite magmatism in the SW Japan arc: I. K-Ar chronology of the Setouchi volcanic belt

Tatsumi, Y., Ishikawa, N., Anno, K., Ishizaka, K., and Itaya, T.

The Setouchi volcanic belt of SW Japan is characterized by the occurrence of andesites with an uncommonly high Mg concentration (HMAs, high-Mg andesites), which may have formed under unusual tectonic settings. A total of 50 new K-Ar ages for the Setouchi rocks confirmed that the magmatism took place within the short period of 13.2±0.4 Ma. This was synchronous with the major mode of opening of the Japan Sea backarc basin, which forced the initiation of subduction and melting of a young lithosphere of the Shikoku Basin beneath the arc. The volcanism was terminated by the cessation of this particular subduction. The eruption of HMA magmas may also be attributed to an extensional stress field in the Setouchi region, in contrast to the compressional stress regime documented for other regions of the SW Japan arc. (*submitted to Geophys. J. Inter.*)

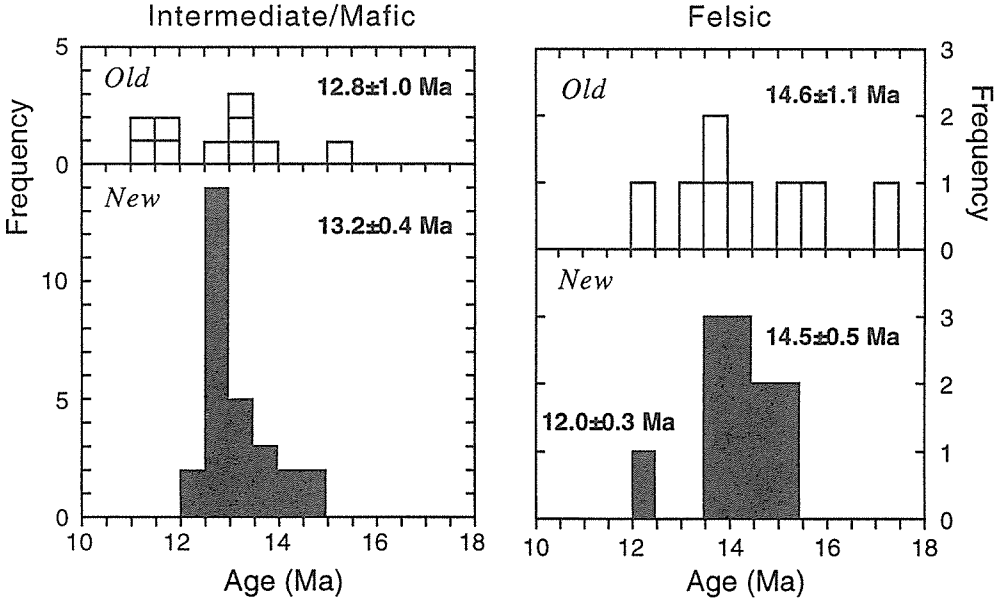

Figure 1. Frequency distribution diagrams for K-Ar ages of Setouchi volcanic rocks.

Tectonic setting of high-Mg andesite magmatism in the SW Japan arc: II. Paleomagnetism of the Setouchi volcanic belt

*Ishikawa, N., **Tatsumi, Y.**, Torii, M., and Yamazaki, T.*

The Setouchi volcanic belt of SW Japan, which is characterized by activity of high-Mg andesites, was formed in a short period between 15 and 12 Ma, coeval with the climax stage of opening of the Japan Sea backarc basin. Paleomagnetic data for the volcanic rocks, combining with K-Ar age data, demonstrated that the SW Japan arc was rotated between 15 and 13 Ma, and revealed that the volcanism opf intermediate to mafic compositions including high-Mg andesites took place during and immediately after the rotation of the arc sliver. It is thus likely that such short-lived magmatism was caused by effective subduction of the lithosphere of the Shikoku Basin beneath the SW Japan arc, which resulted from the obduction of the arc sliver onto the oceanic lithosphere. (*submitted to Geophys. J. Inter.*)

The piezomagnetic field considering the inhomogeniety of crustal magnetization.

Utsugi M.

In the present studies, the analytical solution of the piezomagnetic fields due to a spherical pressure source (which called the Mogi model in volcanology) has been obtained in the cases of the uniformly magnetized crustal model. However, it is self-evident that the earth's crust is inhomogeneously magnetized. In this study, we present the analytical method to evaluate the piezomagnetic field due to the Mogi model considering the inhomogeneity of crustal magnetization.

To evaluate the effect of the inhomogeneity of crustal magnetization, we consider the following situation as shown in Fig. 1: a cubic block V_1 within the crust is uniformly magnetized(1 A/m) and outside the cube is demagnetized (0 A/m). In general, the piezomagnetic field is expressed by the surface integral of displacement and strain over the boundary surface of the magnetized region of the crust. Then, in this case, the surface integral becomes finite one and cannot be solved analytically. However, using some mathematical techniques, we can transform this surface integral to one dimensional integral of the function which consists of the incomplete elliptic integrals of first and second kind. As for one dimensional integrals of analytic functions, there are some useful algorithms for numerical integration such as DEM (double exponential integral method). Then we can calculate the piezomagnetic field considering the inhomogeneity of the crustal magnetization accurately as well as rapidly.

In Fig. 2, we show the profiles of the total force of geomagnetic change along the y axis ($x = 0, z = 1$(m)). The case A in this figure is based on the uniformly magnetized crust: a layer $0 < z < H_C = 15$km (H_C indicates the Curie depth) is uniformly magnetized by 1 A/m. The case B is based on the inhomogeneously magnetized crust as shown in Fig. 1. The model parameters are given in Table 1. Through this calculations, it becomes clear that the seismomagnetic effect is enhanced around the edges of the cubic block (at $y_0 = 5$ and $y_0 = 15$ km). This is caused by the fact that, unlike a uniform medium, the magnetic fields arising from stress-induced magnetic dipoles do not cancel with one another around the edges.

Table 1. Model parameters.

Rigidity	μ	3.5×10^{11}	(cgs)
Poisson ratio	ν	0.25	
Moment of Mogi Model	$C = a^3\Delta P/2$	10^3	$(\mathrm{km}^3 \cdot bar)$
Source Depth	D	5	(km)
Geometry of the Cube	L, W, H	10, 10, 15	(km)
Stress Sensitivity	β	10^{-4}	(bar^{-1})
Curie Depth	H_c	15	(km)
Magnetic Inclination		45	(degree)
Magnetic Declination		0	(degree)

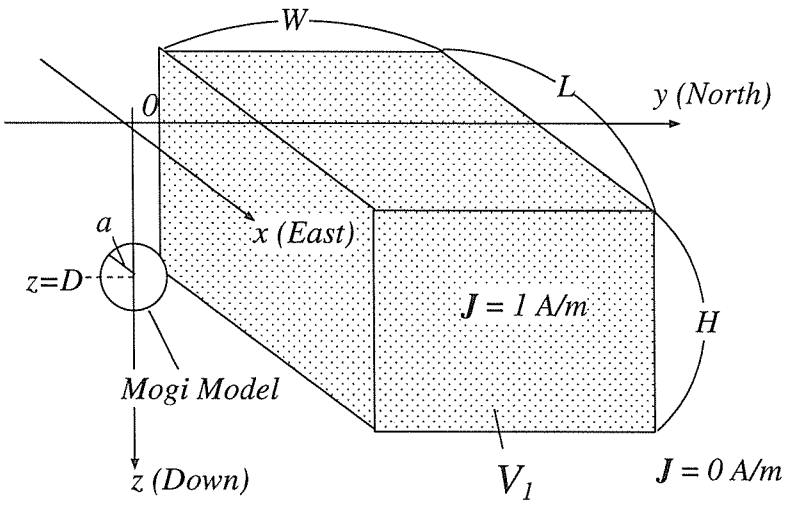

Fig. 1. Inhomogeneously magnetized crustal model.
A semi-infinite elastic medium occupies $z > 0$. The cubic block V_1 ($L \times W \times H\text{km}^3$) is uniformly magnetized and outside V_1 is demagnetized. In this medium, a spherical pressure source (Mogi model) is assumed.

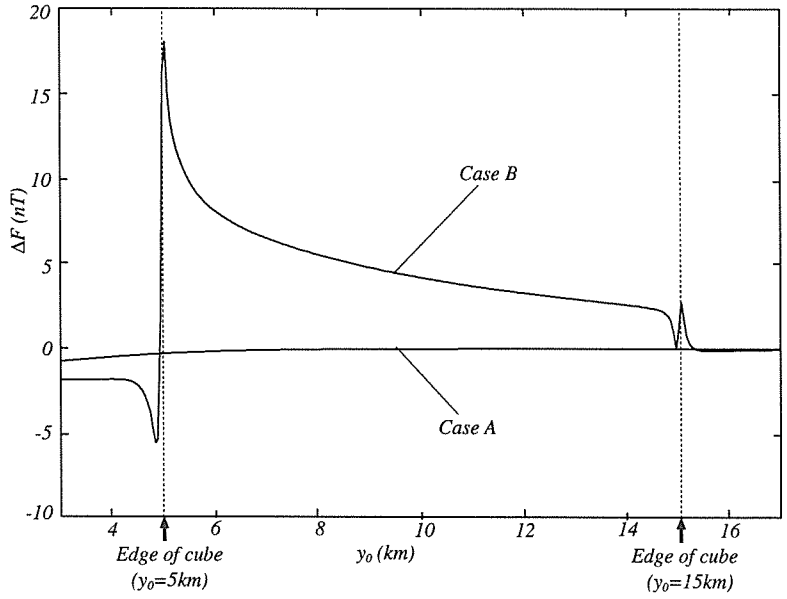

Fig. 2. Profiles of the total force of geomagnetic change along the y axis ($z =$ 1m).
The cases A and B indicate the geomagnetic changes based on an uniformly magnetized crustal model and a cubic model, respectively.

Detection of a Crack-like Conduit beneath the Active Crater at Aso Volcano, Japan

Mare YAMAMOTO, Hitoshi KAWAKATSU, Satoshi KANESHIMA,
Takehiko MORI, Tomoki TSUTSUI, Yasuaki SUDO, Yuichi MORITA

To constrain the source of long period tremors (LPTs), we deployed a very dence broadband seismic network consisting of totally twenty-four stations around the active crater of Aso volcano in Kyushu, Japan. The spatial varation of the observed sgna1 amplitudes reveals that the source of LPTs consists of an isotropic expansion (contraction) and an inflation (deflation) af an inclined tensile crack wlth a strike almost parallel to the chain of craters. The detected crack has a dimension of 1km and its center is located a few hundred meters southwest of the active crator, at a depth of about 1.8km. The extension of the crack plane meets the crater chain including the active fumarole at the surface, suggesting that the crack has played an important role in transporting gasses and/or lava to the craters from below. This work a.lso demonstrates a powerful usage of broadband seismometers as geodetic instruments to constrain subsurface structures at active volcanoes.

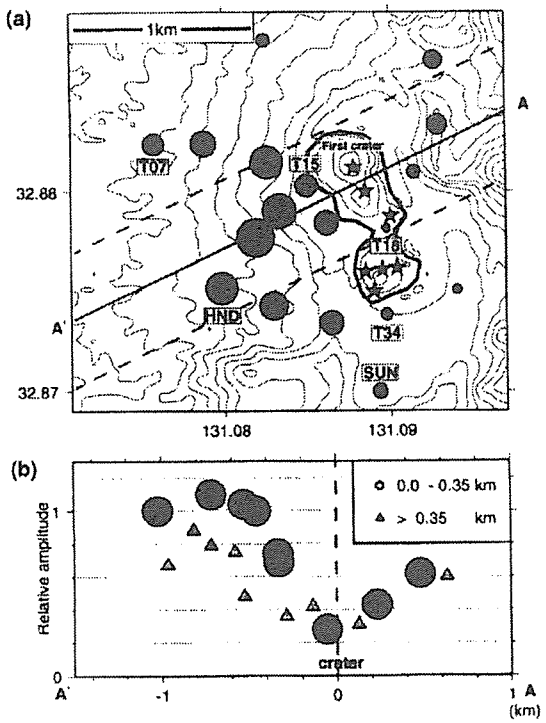

Figure 1. Spatial variation of LPT amplitudes (a): The solid circles indicate the stations used in our analysis and their radii are proportional to relative LPT amplitudes (black and gray circles represent the observed and the model predicted amplitude, respectively. See the text for the further information). The chain of craters of the Naka-dake consists of seven craters represented by stars (only the first crater is active at present). The contour lines represent 25 m contour intervals. (b): Two dimensional projection of the signal amplitudes along the line **A-A'**. Stations are classified into two classes according to the distance from the line.

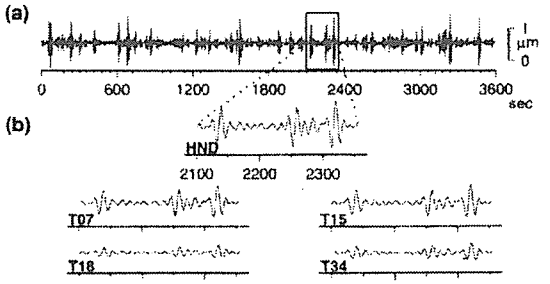

Figure 2. (a): Vertical component band-pass filtered (0.03-0.1Hz) displacement seismogram for one hour starting at 01:00 on Aug. 26, 1997 (JST).
(b): Examples of seismograms observed at different stations. All traces are drawn in the same scale for the same time window.

Chemical Separation of Rb and Sr from silicate rock samples

Yoshikawa, M. and Shibata, T.

Complete separation of Sr from silicate rock samples is required for isotope analysis of silicate rock samples with very low Sr concentration. For this purpose we adopted a combination of cation-exchange chromatography in H+ form and pyridinium form with DCTA complex. This procedure is essentially similar to the method discribed by Birck (1986) and Yoshikawa and Nakamura (1993).

Rough removal of major element. Rb and Sr separation from most of major element was done in 2.5M HCl with 1ml AG50W X8 resin. Collection of Sm and Nd can be made by 6M HCl after the Rb and Sr collection. The Rb and Sr fraction with small amounts of Ca and Mg was evaporated to dryness.

Purification of Rb and Sr. Purification of Rb and Sr was peformed on 0.3 ml AG50W X8 resin bed column. The resin bed was conditioned by pyridine. The dried sample obtained after the separation of major elements was converted to pyridinium chloride by adding pyridine and then dried. The dried sample was dissolved by DPE (0.06M DCTA in 0.5N pyridine) and this solution was loaded onto the column. DPE and water each were then successively added to the column to completely remove Ca and Mg. Rb and Sr was eluted by 2.5N HCl. Rb fraction slightly overlapped with the subsequent Sr fraction, because HCl concentration of this process was strong for perfect separation of Rb and Sr. Thus, the Sr appearing in Rb fraction could be removed to use more dilute HCl for Rb elution.

公表論文 Publications

〈査読有〉

Aizawa, Y., Tatsumi, Y. and Yamada, H. (1999) Element transport by dehydration of subducted sediments: implication for arc and ocean island magmatism, The Island Arc, 8, 38-46.

Furukawa, Y. (1999) Interplate coupling and deformation in the accretionary prism in the Southwest Japan subduction zone, Geophys. Res. Lett., 26, 3145-3148.

Furukawa, Y. and Tatsumi, Y. (1999) Melting of a subducting slab and production of high-Mg andesite magmas: Unusual magmatism in SW Japan at 13~15 Ma, Geophys.Res. Lett., 26, 2271-2274.

Garces, M., Iguchi, M., Ishihara, K., Morrissey, M., Sudo, Y. and Tsutsui, T. (1999) Infrasonic precursors to a Vulcanian eruption at Sakurajima Volcano, Japan. Geophysical Res. Lett., 26, 16, 2537-2540.

Handa,S. and Tanaka,Y.(1999) The Electric Low-resistivity Layer Beneath the Active Crater of Aso Volcano, Japan., Bull. Volcanol. Soc. Japan, 44, 191-200.

Hashimoto, T. (2000) Detection of Crustal Inhomogeneity in Nojima Fault Zone Using the Earth Current Noise, The Island Arc, in press.

Kumagai, I. and Kurita, K. (2000) On the fate of mantle plumes at density interface, Earth Planet. Sci. Lett., in press.

Mogi,T., Tanaka, Y., Kusunoki, K., Morikawa,T. and Jomori,N.(1998) Development of ground electrical source airbone transient EM(GREATEM), Exploration Geophysics, 29, 61-64.

Nishi, K., Ono, H. and Mori, H. (1999) Global positioning system measurements of ground deformation caused by magma intrusion and lava discharge: the 1990-1995 eruption at Unzendake volcano, Kyushu, Japan, J. Volcanol. Geotherm. Res., 89, 23-34.

Oguri, K., Shimoda, G. and Tatsumi, Y. (1999) Quantitative determination of gold and the platinum-group elements in geological samples using improved NiS fire-assay and tellurium coprecipitation with inductively coupled plasma-mass spectrometry (ICP-MS), Chem. Geol., 157, 189-197.

Ohgaki, S., Takenouchi, K., Hashimoto, T. and Nakai, K. (1999) Year-to-year Changes in Rocky-shore Malacofauna of Bansho Cape, Central Japan: Rising Temperature and Increasing Abundance of Southern Species, Benthos Research, 54-2, 47-58.

Ohsawa, S., Yusa, Y., Oue, K. and Amita, K. (2000) Entrainment of atmospheric air into the volcanic system during the 1995 phreatic eruption of Kuju volcano, Japan. J.

Volcanol. Geotherm. Res., 96, 33-43.

大沢信二、由佐悠紀、大山正雄 (2000) 噴気ガスの化学組成から得られる箱根火山の地熱情報. 温泉科学, 49, 151-161.

Shimoda, G. and Tatsumi, Y. (1999) Generation of rhyolite magmas by melting of subducting sediments in Shodo-Shima island, Southwest Japan, and its bearing on the origin of high-Mg andesites, The Island Arc, 8, 383-392.

Suzuki, K., Kagi, H., Nara, M., Takano, B. and Nozaki Y. (2000) Experimental alteration of molybdenite: Evaluation of the Re-Os system, infrared spectroscopic profile and polytype. Geochim. Cosmochim. Acta, 64, 223-232.

鈴木勝彦 (1999) 負イオン質量分析法による超高感度同位体分析とその地球化学・環境科学への応用, 地球化学, 33, 67-102.

Tatsumi, Y., Arai, R., and Ishizaka, K. (1999) The petrology of an melilite-olivine nephlinite from Hamada, SW Japan, J. Petrology, 40, 497-509.

Tatsumi, Y., Oguri, K., and Shimoda, G. (1999) The behaviour of platinum-group elements during magmatic differentiation in Hawaiian tholeiites, Geochem. J., 8, 38-46.

Tatsumi, Y., Oguri, K., Shimoda, G., Kogiso, T., and Barsczus, H.G. (2000) Contrasting behavior of noble-metal elements during magmatic differentiation in basalts from the Cook Islands, Polynesia, Geology, 28, 131-134.

Yamamoto, M., Kawakatsu, H., Kaneshima, S., Mori, T., Tsutsui, T., Sudo, Y. and Morita, Y. (1999) Detection of a crock-like conduit beneath the active crater at Aso volcano, Japan. Geophys. Res. Lett., 26, 24, 3677-3680.

Yoshikawa, M. and Nakamura, E. (2000) Geochemical evolution of the Horoman peridotite complex: Implications for melt extraction, metasomatism, and composotional layering in the mantle, J.Geophys.Res., 105, 2879-2901.

〈査読無〉

網田和宏・大沢信二・由佐悠紀（1999）噴気ガス化学組成の経時変化に関する研究. 大分県温泉調査研究会報告, 50, 27-32.

長谷英彰、田中良和、橋本武志、坂中伸也、森健彦、増田秀晴、吉川慎 (1999) 阿蘇火山構造探査における人工地震に伴う地電位変化、CA 研究会論文集、193-200.

橋本武志・田中良和・西田泰典・茂木透・山本圭吾・神田径・平林順一・石原和弘, 桜島火山の自然電位と熱水系（第２報） (1999) 京都大学防災研究所年報, 42, B-1, 19-25.

橋本武志・網田和宏・馬渡秀夫・田中良和 (1999) 九州地域におけるネットワークＭＴ観測（続報）, ＣＡ研究会論文集, 29-37.

橋本武志, 田中良和, 西田泰典, 茂木透, 山本圭吾, 平林順一, 石原和弘, 桜島火山の自然電

位（1999），京都大学防災研究所共同研究９Ｐ－５「桜島火山の地下水・熱水系に関する研究」報告書，65-101.

岩倉一敏・大沢信二・大上和敏・網田和宏・高松信樹・今橋正征・野津憲治・由佐悠紀 (1999) 長湯温泉の温泉遊離ガスの起源について. 大分県温泉調査研究会報告, 50, 19-25.

神田径・橋本武志・大島弘光 (1999) 諏訪之瀬島火山における自然電位分布，京都大学防災研究所年報, 42, B-1, 11-18.

神田径・森真陽・橋本武志・大島弘光 (1999) 諏訪之瀬島火山の自然電位，全磁力測定，第３回諏訪之瀬島火山の集中総合観測報告，41-53.

川本竜彦・佐野有司 (1999) 「揮発性元素の地球惑星科学」の特集にあたって、地球化学、33、４号巻頭.

火山研究センター〔火山噴火予知連絡会会報〕九重火山の火山活動について（1998 年 5 月～9 月），72，99-104，1999；阿蘇火山の最近の活動（1998 年 6 月～9 月），72，107-110，1999；九重火山の火山活動について（1998 年 9 月～1999 年 1 月），73，88-89，1999；阿蘇火山の最近の活動（1998 年 9 月～1999 年 1 月），73，92-97，1999.

茂木透，田中良和，長谷英彰，Arsadi, E.M., Widarto, D.S., 長尾年恭，上田誠也，スマトラ断層での地電位観測（２），(1999) ＣＡ研究会１９９９年論文集，179-186.

茂木透，橋本武志，神田径，田中良和，山本圭吾，大羽成征，大島弘光，佐波瑞恵，平林順一（1999），桜島における高密度電気探査，京都大学防災研究所共同研究９Ｐ－５「桜島火山の地下水・熱水系に関する研究」報告書，103-108.

佐野貴司（1999）LIPs の生成．月刊地球，21，228-235.

須藤靖明・吉川　慎・森　健彦・田中貴光（1999）火山活動と重力変化－活火山火口近傍における超伝導重力計観測．月刊地球，21，8，525-529.

田中貴光・竹本修三・福田洋一・東　敏博・小笠原志歩里・須藤靖明・吉川　慎（1999）超伝導重力計の観測に及ぼす海洋潮汐の荷重影響－京都・阿蘇・バンドンの比較．第９回超伝導重力計ワークショップ集録，1-7.

田中良和・橋本武志・長谷英彰・坂中伸也・増田秀晴 (1999) 阿蘇中央火口丘の自然電位(1)，ＣＡ研究会論文集，187-192.

巽好幸（1999）沈み込むプレートが融解して高 Mg 安山岩が生まれる，科学, 69, 537-545.

Yusa, Y. (1999) Natural Heat Pipe in Geothermal System. Proc. The 1999 Workshops, International Geothermal Days, Oregon 1999, 171-174.

学 会 発 表　Conference Presentations

相澤　義高、伊東　和彦、高温高圧下におけるオリビン多結晶体の P 波速度, 地球惑星科学関連学会合同大会（1999 年 6 月：東京代々木オリンピックセンター）

網田和宏・長谷英彰・坂中伸也・大沢信二・由佐悠紀, 鶴見火山における自然電位観測, 第 52 回日本温泉科学会（1999 年 8 月 29 日～9 月 1 日：群馬県草津町ホテルヴィレッジ）

阿蘇火山構造探査（人工地震）グループ・筒井智樹：阿蘇火山中央火口丘で観測された人工地震探について．地球惑星科学関連学会合同大会（1999 年 6 月：東京国立オリンピック記念青少年総合センター）

阿蘇火山構造探査（人工地震）グループ・森健彦：1998 年阿蘇火山人工地震探査観測網を利用した火山性微動の観測について．地球惑星科学関連学会合同大会（1999 年 6 月：東京国立オリンピック記念青少年総合センター）

阿蘇火山構造探査（人工地震）グループ・森健彦：阿蘇火山の短周期火山性微動発生モデル．1999 年度日本火山学会秋季大会（1999 年 10 月：神戸大学）

阿蘇火山構造探査（人工地震）グループ・筒井智樹：阿蘇火山中央火口丘の地震波速度構造－理論計算による速度構造モデルの検証－．1999 年度日本火山学会秋季大会（1999 年 10 月：神戸大学）

磐梯火山人工地震探査グループ：人工地震による磐梯火山構造探査(2) 3 次元浅部速度構造．地球惑星科学関連学会合同大会（1999 年 6 月：東京国立オリンピック記念青少年総合センター）

BOLFAN-CASANOVA N., KEPPLER H., KAWAMOTO T., RUBIE D.C.: " Water partitioning among mantle phases", Oral presentation, Gemeinschaftstagung DMG - MFT – Ö MG, Vien, 1999

BOLFAN-CASANOVA N., KEPPLER H., KAWAMOTO T., RUBIE D. C.: " Water partitioning among mantle phases", Processes and Consequences of Deep Subduction Workshop, Verbania, 1999

Gotoh,T., Shimizu,H., Utada,H., Tanaka,Y., Yumoto,K., Nikiforov,V., Palshin,N., Medzhitoh,R., Vanyan,L.(1999) Constraints on the electrical conductivity beneath the Japan sea by MT response of the japan sea cable(JASC), GA1.02/W/22-A2, 20July, poster, IUGG99

長谷英彰、阿蘇火山構造探査(人工地震)グループ、阿蘇火山構造探査における人工地震に伴う地電位変化、地球惑星科学関連学会合同大会 (1999 年６月８日～１１日：国立オリンピック記念青少年総合センター)

長谷英彰、田中良和、橋本武志、坂中伸也、阿蘇山における自然電位観測、日本火山学会秋季大会（1999 年１０月９日～１１日：神戸大学大学教育センター）

長谷英彰、田中良和、橋本武志、坂中伸也、阿蘇火山における自然電位観測(2)、地球電磁気・地球惑星圏学会講演会 (1999 年１１月９日～１２日：仙台市民会館)

長谷英彰、田中良和、橋本武志、坂中伸也、阿蘇山中央火口丘における自然電位観測、京都大学防災研究所研究発表講演会 (2000 年２月１７日～１８日：京都リサーチパーク)

橋本武志・田中良和・西田泰典・茂木透・山本圭吾・神田径・平林順一・石原和弘，桜島火山の自然電位分布と熱水系，地球惑星科学関連学会合同大会（1999 年 6 月 8 日～11 日：国立オリンピック記念青少年総合センター（東京））

橋本武志・網田和宏・長谷英彰・増田秀晴・小野博尉・坂中伸也・田中良和・半田駿・生駒良友・鍵山恒臣・小山崇夫・宗包浩志・小河勉・神田径・茂木透・ Djedi S. Widarto ・下泉政志，バイポール・ダイポール電気探査により推定される阿蘇火山の電気構造，日本火山学会秋季大会（1999 年 10 月 9 日～11 日：神戸大学教育センター（兵庫））

橋本武志・高倉伸一・坂中伸也・網田和宏・小川康雄・田中良和・長谷英彰，阿蘇火山の比抵抗構造（その２），地球電磁気地球惑星圏学会秋季大会（1999 年 11 月 9 日～12 日：仙台市民会館（宮城））

Hashimoto, T., Hase, H., Sakanaka, S., Tanaka, Y., Masuda, H., Amita, K., Kanda, W., Djedi S. W., Mogi, T., Ikoma, Y., Handa, S., Shimoizumi, M., Koyama, T., Ogawa, T., Kagiyama, T., and Masutani, F., Electrical Structure of Aso Volcano Inferred by Bipole-dipole Method, International Union of Geodesy and Geophysics (July 19-24, 1999: Birmingham University (UK)).

橋本武志・高倉伸一・坂中伸也・網田和宏・長谷英彰，ＭＴ法により推定される阿蘇火山中央火口丘の比抵抗構造，京都大学防災研究所研究発表講演会（2000 年 2 月 17 日～18 日：京都リサーチパーク（京都））

橋本武志，火山電磁気研究の現状と展望，ＣＡ研究会（2000 年 1 月 31 日～2 月 1 日：東京大学地震研究所）

Hashimoto, T., Resistivity Structure of the Central Cones of Aso Volcano, Japan, VIIth International Meeting of Colima Volcano (March 6-10, 2000: University of Colima (Mexico))

家森俊彦，能勢正仁，竹田雅彦，田中良和，松本浩志，住友則彦（ポスター）地磁気脈動自動検出による地磁気変換関数推定の安定性，地球惑星科学関連学会合同大会（１９９９年６月８日～１１日，国立オリンピック記念青少年総合センター（東京））

岩倉一敏・大沢信二・大上和敏・網田和宏・野津憲治・高松信樹・今橋正征・由佐悠紀，炭素ヘリウム同位体組成から見た長湯温泉の遊離ガスの起源，第 52 回日本温泉科学会（1999 年 8 月 29 日～9 月 1 日：群馬県草津町ホテルヴィレッジ）

神田径・橋本武志・大島弘光，諏訪之瀬島火山における自然電位分布－第３回諏訪之瀬島火山集中総合観測－，地球惑星科学関連学会合同大会（1999 年 6 月 8 日～11 日：国立オリンピック記念青少年総合センター（東京））

神田径・網田和宏・長谷英彰・橋本武志・増田秀晴・小野博尉・坂中伸也・田中良和・半田駿・生駒良友・鍵山恒臣・小山崇夫・宗包浩志・小河勉・茂木透・ Djedi S. Widarto ・下泉政志，阿蘇火山における TDEM 法電磁気構造探査，日本火山学会秋季大会（1999 年 10 月 9 日～11 日：神戸大学教育センター（兵庫））

川勝均・金嶋聡・須藤靖明・筒井智樹・橋本武志・森健彦・吉川慎他多数：ASO98++：阿蘇山における稠密広帯域＋短周期地震計アレイ観測．地球惑星科学関連学会合同大会（1999 年

6月：東京国立オリンピック記念青少年総合センター）

川本竜彦、Hans Keppler、バセット型外熱式水熱合成ダイアモンドアンビルセル：含水マグマの高温度高圧力条件下でのその場観察をめざして，地球惑星科学関連学会（1999 年合同大会：東京）

川本竜彦、バセット型外熱式ダイアモンドアンビルセルを用いたマグマのその場観察，第 40 回高圧討論会（1999 年：福岡市）

熊谷一郎、栗田敬、プルームの取り込みに関する粘性比の影響について，1999 年地球惑星科学関連学会合同学会（1999 年 6 月：東京）

Londono,J., 須藤靖明, Sannz,L.,Osorio,J. : The use of spectral analysis for identification of spatial seismic sources in Nevado del Ruiz Volcano, Colombia. 1999 年度日本火山学会秋季大会（1999 年 10 月：神戸大学）

Londono,J., 須藤靖明, Franco,E. : Analysis of the temporal and spatial variation of the seismic activity and the Vp/Vs ratio of volcano-tectonic earthquakes at Nevado del Ruiz Volcano, Colombia (1986-1996). 1999 年度日本火山学会秋季大会（1999 年 10 月：神戸大学）

茂木透・橋本武志・田中良和・大羽成征・神田径・山本圭吾・大島弘光・佐波瑞恵・平林順一，桜島における高密度電気探査，日本火山学会秋季大会（1999 年 10 月 9 日～11 日：神戸大学教育センター（兵庫））

Mogi,T., Tanaka,Y., Arsadi,E.M., Widarto,D.S.(1999) Geoelectric potential variation monitoring in southern Sumatra, Indonesia- co-seismic variation, JSA15/E/02-A5, poster, 23July, IUGG99

Mogi,T., Widarto,D.S., Arsadi,E.M., Tanaka,Y., Nishimura,S.(1999) Tectonic setting and crustal resistivity structure in the Indonesia island arc, GA1.02/E/29-A2, 20Jujy, poster, IUGG99

中坊真・小野博尉・迫幹雄・橋本武志・須藤靖明，九重火山の地熱活動に伴う地盤変動，日本地熱学会（1999 年 12 月 1 日～3 日：福岡ソフトリサーチパーク（福岡））

中坊真・小野博尉・橋本武志・迫幹雄・須藤靖明：九重火山の地熱活動に伴う地盤変動．地球惑星科学関連学会合同大会（1999 年 6 月：東京国立オリンピック記念青少年総合センター）

大沢信二・由佐悠紀・大山正雄，噴出ガスの化学組成から得られる箱根火山の地熱情報，第 52 回日本温泉科学会（1999 年 8 月 29 日～9 月 1 日：群馬県草津町ホテルヴィレッジ）

大沢信二・由佐悠紀・大山正雄，噴出ガスの化学組成から得られる箱根火山の地熱情報，日本地熱学会（1999 年 12 月 1 日～3 日：福岡ソフトリサーチパーク（福岡））

大上和敏・大沢信二・由佐悠紀，高温湖沼堆積物を用いた熱水系の変遷の復元,第 52 回日本温泉科学会（1999 年 8 月 29 日～9 月 1 日：群馬県草津町ホテルヴィレッジ）

坂中伸也・田中良和・橋本武志・小野博尉，九重火山噴気地帯における地磁気変化，京都大学防災研究所研究発表講演会（2000 年 2 月 17 日～18 日：京都リサーチパーク（京都））

Santos, R. A., Suzuki, K., Takano, B., Tatsumi, Y., Miyata Y. and Nozaki Y., Re and Os System in Ophiolitic Complexes: Implications for Chromitite Formation and Ophiolite Paragenesis. 11th V. M. Goldschmidt Conference (1999 年 8 月, Boston, USA)

Santos, R. A., Suzuki, K., Takano, B., Tatsumi, Y., Miyata Y. and Nozaki Y., Re and Os System in Ophiolitic Complexes: Implications for Chromitite Formation and Ophiolite Paragenesis, (1999 年 12 月, AGU Fall Metting, San Francisco, USA)

Santos, R. A., Suzuki, K., Takano, B., Tatsumi, Y., Miyata Y. and Nozaki Y., Re - Os Isotope Systematics in the Chromitite Producing System: the case of Two Philippine Ophiolite Complexes, 日本地球化学会 (1999 年 10 月, 筑波)

佐野貴司・福岡孝昭・長谷中利昭・米沢仲四郎・松江秀明・澤畑浩之，大陸洪水玄武岩および大陸リソスフェア中のホウ素含有量，地球惑星科学関連学会合同大会（1999 年 6 月：東京代々木オリンピックセンター）

佐野貴司・長谷中利昭・福岡孝昭・米沢仲四郎・松江秀明・澤畑浩之，岩手火山の火山岩中のホウ素含有量（地球惑星科学関連学会合同大会，1999 年 6 月：東京代々木オリンピックセンター）

佐野貴司・福岡孝昭・長谷中利昭・島岡晶子，東北日本弧の火山フロントに噴出した溶岩と日本海溝の堆積物中のホウ素含有量の比較（日本地球化学会年会，1999 年 10 月：地質調査所）

Sasai,Y., Johnston,M., Mueller,R., Tanaka,Y., Zlotnicki,J., Gotoh,T.(1999) Modeling expected and observed piezomagnetic field changes in the Long Valley caldera, California, JSA15/E/38-A4, poster, 22Jujl, IUGG99

笹井洋一，田中良和，上嶋誠，後藤忠徳，Malcom,J.S., Robert,M.,Jacques,Z.,ロング・バレー・カルデラの電磁気共同観測（２），第１０６回地球電磁気・地球惑星圏学会講演会（１９９９年１１月９日～１２日、仙台市民会館）

下泉政志，半田駿，網田和宏，田中良和，茂木透，鈴木貞臣（ポスター），北西九州の電気伝導度構造，２０００年度ＣＡ研究会（平成１２年１月３１日～２月１日、東京大学地震研究所）

周藤正史，Eddie Listanco，石川尚人，田上高広，鎌田浩毅，巽好幸，K-Ar 年代から見たフィリピン島南西部マコロード回廊地域の第四紀火山活動地球惑星科学関連学会合同大会（1999 年６月８日，東京）

須藤靖明・阿蘇火山構造探査（人工地震）グループ：1998 年阿蘇火山人工地震探査について．地球惑星科学関連学会合同大会（1999 年 6 月：東京国立オリンピック記念青少年総合センター）

鈴木勝彦，巽好幸，J-シリーズはレニウムーオスミウムの標準になりうるか？日本地球化学会 (1999 年 10 月，筑波)

鈴木勝彦，硫化物鉱物の Re-Os 年代測定法の確立 -日本地球化学会奨励賞受賞講演- 日本地球化学会 (1999 年 10 月，筑波)

高倉伸一・橋本武志・小池克明・小川康雄，阿蘇カルデラの深部熱水系の比抵抗構造，日本地熱学会（1999 年 12 月 1 日～3 日：福岡ソフトリサーチパーク（福岡））

Tanaka, Y., Hase, H., Hashimoto, T., Electrical Self-Potential on the Central Cones of Aso Volcano, International Union of Geodesy and Geophysics (July 19-24, 1999: Birmingham University (UK)).

田中良和・長谷英彰・橋本武志・坂中伸也，阿蘇中央火口丘の自然電位（１），ＣＡ研究会（1999年１月25日～26日：京都大学防災研）

田中良和，橋本武志（口頭）地磁気変化から推定される火口浅部でのマグマと水の相互作用，地球惑星科学関連学会合同大会（１９９９年６月８日～１１日，国立オリンピック記念青少年総合センター（東京））

田中良和，笹井洋一，上嶋誠，後藤忠徳，Johnston,M.，Mueller,R.，Zlotnicki,J., Yvetot, P.（ポスター）ロングヴァレーカルデラにおける電磁気総合観測，２０００年度ＣＡ研究会（平成１２年１月３１日～２月１日、東京大学地震研究所）

巽好幸，大陸地殻と EM1 貯蔵庫の同時形成メカニズム，地球惑星科学関連学会合同大会（1999年６月８日，東京）

Tatsumi, Y., Continental crust formation by crustal delamination in subduction zones, and complementary accumulation of EMI component in the mantle, Goldschmidt Congerence (1999年８月30日，ボストン)

巽好幸，OD21 における科学目標と研究体制，ODP 成果報告会（2000 年１月 13 日，東京大学海洋研究所）

Uyeda,S., Nagao,T., Orihara,Y., Takahashi,I., Yamaguchi,T., Mogi,T., Tanaka,T., Widarto,D.S., Arsadi,E.M.(1999) Preseismic and coseismic geoelectrical potential changes, JSA15/E/17-A3, oral, July 21, IUGG99.

安田龍司・大川恵・戸田茂・須藤靖明・筒井智樹他多数：阿蘇中岳における反射法地震探査（速報）．地球惑星科学関連学会合同大会（1999 年 6 月：東京国立オリンピック記念青少年総合センター）

Yusa, Y. : Natural Heat Pipe in Geothermal System. International Geothermal Days. Oregon 1999 (1999年10月：Klamath Falls, USA)

吉川美由紀・須藤靖明・田口幸洋・筒井智樹：九重北西部の地熱地域における Vp/Vs 比とその変動．地球惑星科学関連学会合同大会（1999 年 6 月：東京国立オリンピック記念青少年総合センター）

吉川美由紀・筒井智樹・須藤靖明・田口幸洋：九重火山周辺部の地熱地帯における地震活動の特徴について．資源地質学会第 49 回年会講演会（1999 年 6 月：東京）

吉川美由紀・須藤靖明・筒井智樹・増田秀晴・吉川慎・外輝明・迫幹雄・田口幸洋：大岳・八丁原地熱地帯における地震活動．日本地熱学会平成 11 年福岡大会（1999 年 12 月：福岡）

吉川美由紀・須藤靖明・筒井智樹・田口幸洋：九重火山周辺部地熱地帯における地震活動．平成 11 年度京都大学防災研究所研究発表講演会（1999 年 2 月：京都）

Zlotnicki,J., Gotoh,T., Johnston,M., Tanaka,Y., Sasai,Y.(1999) Hydrothermal system and faulting in Long Valley Caldera inferred by self-potential mapping, JSA15/E/27-A4, poster, 22 July, IUGG99

共同研究　Collaboration

国内

橋本武志　高速サンプリングデータロガーを使った阿蘇火山における自然電位連続観測　参加機関：地質調査所地殻熱部.

橋本武志、田中良和、坂中伸也、網田和宏　中部九州における長周期ＭＴ探査　参加機関：地質調査所地殻物理部.

橋本武志、坂中伸也、長谷英彰、網田和宏　阿蘇中央火口丘の広帯域ＭＴ法探査　参加機関：地質調査所地殻物理部，熊大工.

大沢信二　京都大学防災研究所研究担当（山地斜面の地下水に関する研究）

大沢信二　福島県裏磐梯・五色沼水系の青色湖水の呈色機構に関する研究　参加機関：東邦大学理学部.

大沢信二、由佐悠紀　長湯温泉の温泉遊離ガスの研究　参加機関：東邦大学理学部，東京大学地殻化学実験施設.

田中良和、長谷英彰、橋本武志、坂中伸也　岩手火山における地磁気・自然電位調査　参加機関：東北大.

阿蘇火山火山性微動観測ＡＳＯ９９　11 月 22 日-30 日（震研・東工大，川勝・大湊・山本・金嶋・須藤・橋本・森・中坊・吉川・吉川・迫・外・増田）.

阿蘇火山古坊中における「空中電磁および空中磁気探査（電力中央研究所受託研究）平成１２年２月２４日～２６日（茂木、石川、楠、海江田、城森、藤光、松嶋（＋学生２名）、田中、小野、坂中、宇津木、長谷、増田）

雲仙掘削に関る千本木周辺の電磁気調査（地質調査所受託研究）平成１２年２月２７日～３月６日（田中、坂中、宇津木、増田）.

田中良和　理化学研究所併任（地震国際フロンティア研究プログラム）京都大学超高層電波研究センター「地磁気日変化と電離層電場、風の関係」

巽好幸　京都大学防災研究所研究担当（姶良カルデラにおける大規模火砕流マグマの成因）

巽好幸　岡山大学固体地球研究センター嘱託研究員（沈み込み帯における物質循環）

国際

田中良和　ロングバレーカルデラの電磁気観測（米国地質調査所），１９９９年８月１７日～８月３１日

田中良和　インドネシア、スマトラ島リワ地域の地電位観測（インドネシア科学院），１９９９年４月１３日～２１日

巽好幸　インドネシアサンギヘ火山弧の岩石学的研究（日本学術振興会）

教育活動　Education

学位・授業　Academics

学位審査

大沢信二	（審査員）大上和敏	（博士	京都大学大学院理学研究科）
	（審査員）中崎宏昭	（修士	京都大学大学院理学研究科）
	（審査員）岩倉一敏	（修士	東邦大学大学院理学研究科）
須藤靖明	（審査員）小笠原志歩里	（修士	京都大学大学院理学研究科）
	（審査員）岸本優子	（修士	京都大学大学院理学研究科）
巽　好幸	（主査）　可児智美	（博士	京都大学大学院理学研究科）
	（審査員）相澤義高	（博士	京都大学大学院人間・環境学研究科）
	（審査員）中島　剛	（博士	京都大学大学院人間・環境学研究科）
	（審査員）佐藤佳子	（博士	京都大学大学院理学研究科）
	（審査員）大上和敏	（博士	京都大学大学院理学研究科）
	（審査員）志藤あずさ	（修士	京都大学大学院理学研究科）
由佐悠紀	（審査員）中崎宏昭	（修士	京都大学大学院理学研究科）
	（主査）　大上和敏	（博士	京都大学大学院理学研究科）
	（審査員）可児智美	（博士	京都大学大学院理学研究科）

授業・実習

科目	担当教官
学部授業	
地熱学	古川善紹、大沢信二、須藤靖明、田中良和、巽　好幸、由佐悠紀
陸水物理学	由佐悠紀（分担）
地球惑星科学Ⅰ	巽　好幸（分担）
大学院（修士）授業	
水圏地球物理学Ⅱ	大沢信二、由佐悠紀（分担）
地球熱学・地熱流体学Ⅰ	大沢信二、田中良和、由佐悠紀
地球熱学・地熱流体学Ⅱ	古川善紹、須藤靖明、巽　好幸（分担）
応用地球電磁気学	田中良和（分担）
環境地球科学Ⅱ	巽　好幸（分担）
ゼミナール（修士・博士）	
水圏地球物理学Ⅲ	大沢信二、由佐悠紀（分担）
地球熱学・地熱流体学Ⅰ	川本竜彦、大沢信二、田中良和、由佐悠紀

地球熱学・地熱流体学Ⅱ　古川善紹、橋本武志、小野博尉、須藤靖明、巽　好幸、筒井智樹

応用地球電磁気学　橋本武志、田中良和（分担）

環境地球科学Ⅱ　巽　好幸（分担）

実習

地熱学野外実習（７月２６日～７月３１日）

古川善紹、須藤靖明、田中良和、巽　好幸、由佐悠紀

地球電磁気学３回生野外実習

橋本武志、田中良和

講義（他大学）ほか

大沢信二　大分大学非常勤講師（教養教育後期「大分の水」）

橋本武志　京都大学技官研修講師（理学部）２月２５日

巽　好幸　東京大学海洋研究所教授（併任）

集中講義：東北大学，大阪府立大学，金沢大学

田中良和　京都大学技官研修講師（理学部）２月２５日

由佐悠紀　集中講義：九州大学工学部，大分県立芸術文化短期大学

セミナー　Seminars

地熱学セミナー

１９９９年

６月２５日　網田和宏「別府地域鍋山噴気ガスの化学成分の連続観測」
小野博尉「雲仙普賢岳 1990 - 95 年の噴火活動における地盤変動」

７月２７日　鈴木勝彦「Re - Os　system：Introduction, analysys and application to molybdenite dating 」
森　健彦「阿蘇山の短周期火山性微動について－98 年構造探査データから－」

１０月１日　大上和敏，相澤義高，中坊真，網田和宏，長谷英彰，吉川美由紀「地球科学に関する談話会」

１０月２９日　大上和敏，相澤義高，中坊真，網田和宏，長谷英彰「地球科学に関する談話会」

火山研セミナー

１９９９年

９月１０日　長谷英彰「阿蘇の自然電位－湯ノ谷～南郷谷のデータから－」
森　健彦「モーメントテンソルについて」
吉川美由紀「トモグラフィーについて」

１０月６日　火山学会予聴会

１０月２０日　坂中伸也「逆解析による磁気双極子の大きさ・位置の決定」

１１月４日　吉川美由紀「九重北西部のＰ波速度構造」

１１月３０日　地熱学会予聴会

１２月２０日　中間研究発表

１２月２２日　高倉伸一（地質調査所）「阿蘇カルデラ深部熱水系の比抵抗構造」

２０００年

１月１７日　宇津木充「ピエゾ磁気効果に基づく地震・地磁気効果」

１月２４日　鴨川　仁（早稲田大学大学院理工学研究科）「地震に関する大気電磁・発光現象」

２月１４日，１６日
平成１１年度防災研究所研究発表講演会予聴会

ＢＧＲＬセミナー

１９９９年

５月１７日　可児智美「Geochronology and Geochemistry of Limestones and Greenstones from

Accretionary Prisms in SW Japan」

6月18日　真島英壽（九州大学理学研究科地球惑星科学）「九州北西部松浦玄武岩類の発生と進化」

7月2日　佐藤　佳子（京都大学大学院理学研究科地球惑星科学専攻）「北部シホテアリン地域の漸新世以降の火山活動史」

山下　茂（岡山大学固体地球研究センター）「珪酸塩メルトへの水の溶解度測定実験と溶解度の熱力モデリングについて」

9月10日　大上和敏「D論の発表予行」

11月12日　Iskandar Zulkarnain「PETROGRAPHY AND ROCK CHEMISTRY OF PRE-AIRA CALDERA VOLCANICS SOUTHERN KYUSHU, JAPAN; Its Implication for the Rock Genesis」

11月15-16日　マントルプルームセミナー

佐野貴司「LIPs の Overview　～どこまでが確実な情報か？～　LIPs の全体像（体積・年代・岩石学的な特徴など）と個別（デカン）のお話」

山岸保子・小川佳子・栗田敬（東大大学院理学研究科地球惑星物理専攻）「地球外天体におけるプルームの証拠　～問題提起あるいはモデル化の対象の提示～」

巽　好幸「プルームは何処からやってくるのか？～モデル化～マントル脈動事件」

鈴木勝彦「プレートのリサイクル：オスミウム同位体比で何が分かるか」

並木敦子（東大大学院理学研究科地球惑星物理専攻）「流体力学的にみた、対流におけるプルームの位置の決定機構」

柳沢孝寿（東大大学院理学研究科地球惑星物理専攻）「大陸が作る対流パターン」

柳川智彦（九州大学理学研究科地球惑星科学）「大陸の分布に依存するマントル対流のパターンが決める外核からの熱流出」

由佐悠紀「南極バンダ湖における熱塩現象」

久利美和（地質調査所）「二層対流系での取り込みと混合」

高嶋晋一郎（東大大学院理学研究科地球惑星物理専攻）「Porous Media における重力不安定とダイアピル生成」

川本竜彦「上部マントルの融解温度とマグマの化学組成」

柳沢孝寿（東大大学院理学研究科地球惑星物理専攻）「小型携帯磁力計で何が見えるのか？：別府（温泉）では使えませんか？」

熊谷一郎「プルーム運動から予測されるもの（化学・サイズ・時間間隔など）」

12月22日　中島　剛（京都大学人間・環境学研究科）「博士論文の発表予行」

相澤義高（京都大学人間・環境学研究科）「博士論文の発表予行」

２０００年

１月２５日　ジョン・マシューズ「Montoring Unzen pyroclastic flow deposits using JERS-1 SAR interferometry」

１月２８日　松下 忍（愛媛大学大学院理工学研究科生物地球圏科学専攻地球進化学講座）「Pyrolite-CO2 系における高圧溶融実験」

２月４日　Rogel A. SANTOS（東京大学大学院総合文化研究科広域システム科学系）「The ophiolitic chromitite genesis: constraints from Re-Os isotope systematics」

２月１８日　田村　芳彦（金沢大学理学部地球学科）「大山火山と南西インド洋海嶺のカンラン石玄武岩：斑晶はカンラン石だけというマグマも実は奥が深いという例」

田中康博（金沢大学理学部地球学科）「経ヶ岳火山の岩石学的研究：福井県奥越セ地方法恩寺山火山岩類について」

電磁気学ゼミ

１９９９年

４月２７日　橋本武志・長谷英彰『3 次元電場計算プログラム（大羽，修士研究，1998）について』

坂中伸也『TDEM 法（Time Domain Electromagnetic Method）について』

網田和宏『地下水流動計算プログラム（由佐，1983）について』

由佐悠紀『地熱流体流動の基礎理論』

７月９日，８月２４日，１０月１４日，１１月４日

橋本武志・長谷英彰『3 次元電場計算プログラムについて』

坂中伸也『TDEM 法について』

網田和宏『地下水流動計算プログラムについて』

９月１４日　橋本武志・長谷英彰『3 次元電場計算プログラムについて』

坂中伸也『TDEM 法について』

２０００年

２月１３日　橋本武志・長谷英彰『3 次元電場計算プログラムについて』

坂中伸也『TDEM 法について』

網田和宏『地下水流動計算プログラムについて』

その他

橋本武志「自然電位法の原理と応用について」（１９９９年１０月１３日，京大防災研究所地震予知研究センター）

Takeshi Hashimoto「Electromagnetics in Volcanic Fields」(March 3, 2000, Escuela Politecnico Nacional, Equador)

John P. Matthews「Lecture on Interometric SAR to members of Depatment of Geophysics, Kyoto University」（Feb １６，２０００）

John P. Matthews「Lectures to staff of Kyushu University on HF rader and Inetrferometric SAR techniques」（March １５+１６，２０００）

特別講義

１９９９年

７月１２，１３日　笹井洋一（東京大学地震研究所）「地殻活動電磁気学～ピエゾ磁気の理論と実践を中心に～」

研 究 費　Funding

科学研究費補助金

奨励研究（A）古川善紹「初期地球の沈み込み帯ダイナミクス：地球の化学的進化の解明に向け」900 千円

奨励研究（A）橋本武志「地下浅部に貫入したマグマの冷却過程の解明」1,100 千円

奨励研究（A）川本竜彦「水を含んだマグマの構造の実験的解明」1,700 千円

基盤研究（A）橋本武志、須藤靖明、筒井智樹（分担）「阿蘇山の火口直下に存在する圧力源の実体と噴火活動における役割の解明」代表者：川勝均

基盤研究（B）須藤靖明「活動火口におけるマグマ熱水系構造探査法の実用化実験」1,200 千円

基盤研究（B）田中良和（分担）「３次元深部地殻構造電磁探査システムの研究」4,100 千円　代表者：茂木透

基盤研究（B）巽好幸・川本竜彦「含水珪酸塩溶融体の高温高圧下におけるその場観察：マントルの融解過程における水の役割の解明」1,200 千円

基盤研究（C）大沢信二・由佐悠紀「火山体土壌空隙を介しての火山ガスと大気の相互作用」2,000 千円

基盤研究（C）田中良和、橋本武志「海底電線を用いた九州西部海域の地殻電気構造の研究」2,200 千円

基盤研究（C）田中良和（分担）「九州北西海域下の電気伝導度構造の研究」代表者：半田駿、1,100 千円

受託研究

大沢信二「火山体水理構造のマグマ活動への影響の解明」1,849 千円

巽好幸「スーパープリュームの岩石学的研究」13,584 千円

その他

日米科学協力事業共同研究　田中良和（分担）「ロングバレーカルデラの電磁気共同観測」代表者：笹井洋一、1780 千円

京都大学学術研究奨励金　鈴木勝彦　「玄武岩，カンラン岩のオスミウム同位体・白金族元素存在度から地球内部地図を作る試み」　1,000 千円

奨学寄付金：伊藤科学振興会　須藤靖明　700 千円

学会活動　Activities in Scientific Societies

受賞

鈴木勝彦　日本地球化学会　奨励賞

委員

川本竜彦

客員編集委員：日本地球化学会「揮発性元素の地球惑星科学」特集号

須藤靖明

会計監査：日本火山学会

田中良和

運営委員：地球電磁気・地球惑星圏学会

委員：地磁気観測作業委員会

巽　好幸

編集委員長：The Island Arc

編集委員：G-Cubed

評議員：日本火山学会・日本地質学会

学会賞選考委員：日本岩石鉱物鉱床学会

由佐悠紀

編集委員：日本温泉科学会

学会賞選考委員：日本陸水学会

評議員：日本陸水学会，日本温泉科学会，日本地熱学会

運営委員長：陸水物理研究会

社会活動　Public Relations

大沢信二

大分県温泉地保全検討会委員（大分県生活環境部）

地熱開発促進調査辻之岳地域検討会委員（新エネルギー財団）

地熱開発促進調査委員会辻之岳ワーキンググループ特別委員（NEDO）

新エネルギー財団地化学技術検討会委員

須藤靖明

測地審議会臨時委員

火山噴火予知連絡会委員

阿蘇火山ガス安全対策専門委員会委員

くじゅう山系（硫黄山）防災協議会委員

民放労連九州地連青年協議会　講演　（1999 年 7 月）

熊本市竜田地区地域公民館研修会　講演　（2000 年 2 月）

巽　好幸

ODP 国内研究連絡会委員

OD21 国内連絡委員会委員

OD21 科学計画策定 WG 長

OD21 陸上施設検討 WG 委員

IODP Scientific Planning Working Group 委員

大分県環境保全審議会委員

由佐悠紀

資源エネルギー庁環境審査顧問

地熱開発促進調査委員会委員

大分県環境審議会委員

大分県自然環境保全審議会委員（温泉部会長）

大分県土地利用審査会委員

大分県温泉地保全検討委員会委員長

大分県温泉管理検討懇話会座長

地熱発電所環境保全実証調査委員会委員

地熱構造モデル構築スタンダード作成調査検討委員会委員長

温泉影響予測手法導入調査検討委員会委員長

日本温泉協会学術部委員

日本保健物理学会第 34 回研究発表会特別講演講師（1999 年 5 月）

歴史と自然を学ぶ会土曜講座講師（1999 年 6 月）

（社）宅建協会別府支部研修会講師（1999 年 7 月）

第 50 回地方衛生研究所全国協議会総会特別講演講師（1999 年 10 月）
別府市国際交流懇話会講師（1999 年 11 月）
大分地方気象台職員研修会講師（1999 年 12 月）。
別府子供たちセミナー「温泉と火山のはなし」講師（2000 年 3 月）

来訪者　Visitors

阿蘇

１９９９年

4月8日　吉井雅彦（環境庁事務所次長）：渡辺武他１名（長陽村農政課）

１７日　Marie Angendre（仏）

１９日　小川康夫（地調）

２１日　佐藤伸雄（久木野村企画課）

２６日　山田（愛教大）

３０日　岡野（環境庁事務所）

5月6日　丸田晴男（NHK 情報）

１１日　金嶋　聡・山本　希（東工大・震研：13 日まで）

１２日　茂木透（九大：13 日まで）

１３日　熊本地方裁判所司法修習生 13 名：西岡光俊他１名（阿蘇町観光課）

１７日　ＪＩＣＡ研修生一行（１８日まで）

１８日　山下・J.Barint（Phoenix Geophysics），高倉伸一（地調）（３０日まで）

１９日　中山雅文（九地建立野ダム）

２０日　平林順一他３人（東工大：２１日まで）

２７日　笠原稔・Gordev（北大），V.Zobin（Colima 大：29 日まで）

３１日　成井（理・司計：５月１日まで）

6月１４日　平田（西技）

7月1日　古川信雄・研修生（建研・ザンビア）

１２日　笹井洋一（震研：１４日まで）

２４日　戸田茂他６名（愛教大：２８日まで）

8月5日　金嶋　聡・山本　希（東工大・震研：９日まで）

７日　神沼忠克・金尾（極地研），戸田（愛教大：１２日まで）

１２日　重富（防災研）

２６日　三菱重工 20 人

8月　田口幸洋（福岡大）

9月2日　倉橋他５名（九地建立野ダム）

９日　長崎（理・人事：１０日まで）

１１日　秋山豊寛

１８日　穀田昇一・松本良浩他２名（水路部・研修生フィジー・韓国）

１０月5日　古関・東辻・大江・岸田・木村（理・司計・施設，本部施設：６日まで）

６日　倉橋他３名（九地建立野ダム）

１２日　九州保安協会６人

１５日　黒田徹（地科研）

１１月９日　長陽村農政課・建設課・水道課
１０日　筒井和男（Ｍ１）
２２日　大湊・山本・川勝（震研：２９日まで）：金嶋他３人（東工大：２９日まで）
２５日　丸岡政雄・石橋安雄他１名（施設部）：一色博（経理部）：村田和喜（財務局）：川崎浩次（理）（２６日まで）
２９日　前野正世他４名（理：３０日まで）
１２月１日　平林順一他２名（東工大：２日まで）
３日　田中日出雄・柴田・伊藤（熊本電波高専・文学部）
８日　横江正己・本辻秀明・前本康央・小野敦・増池正和（施設部）
２０日　石原和弘他６名（桜島観測所：２１日まで）
２１日　倉橋他３名（九地建立野ダム）
２２日　宮縁（森林総研）：本座（熊本大），高倉伸一（地調）
２４日　志賀美英・洪他３名（鹿児島大・中国地震局）
２０００年
1月２６日　島原・西野（理・庶務）
２８日　電気通信管理局
2月１１日　望月英志（地磁気観測所）
１５日　早川知宏（文部省学術課）：増池（経理部）
２３日　中谷・河野・青山・前野（経理部：24日まで）
2月　長陽村役場２名
3月2日　倉吉・古閑・東辻（理事務長・司計・施設）
３日　丸山正樹（理研究科長）
９日　西田宏他２名（総合人間学部事務長補佐）
１５日　太田隆・西山幸夫（経理部管財課長・第２管財掛長）

別府

１９９９年
4月6日　御沓稔弘（大分県生活環境課）
８日　安部（大分合同新聞）
９日　中崎宏昭・筒井和男（京大大学院）
１２日　川野田実夫（大分大学福祉教育学部）及び学生
１５日　田原廣信（大分県立湯布院青年の家）
１６日　片岡裕一郎（SBC テクノ九州）
5月１０日　Rogel A. Santos（１８日まで）
１１日　挾間健（大分県別杵速見地方振興局）
１４日　甲斐倫明（大分県立看護科学大学）

３１日　横山真二（京大理・用度掛）
6月7日　廣瀬俊治・八坂悦朗（大分県水資源・土地対策局長）
９日　松山尚典・有吉俊光（応用地質）
１４日　小堀（別府市民），多田正明（地球科学総合研究所）
１６日　宮川和則（宅建協会別府支部）
１８日　秋山雄介・田代公明（熊本県生活環境課）
7月1日　山下　茂（岡山大学固体地球研究センター：４日まで）
１５日　後藤淳一（大分朝日放送）
7月28日　Rogel A. Santos（８月７日まで）
２９日　中本雅文・清水功（電源開発豊肥地熱事務所）
３０日　山本達二（読売新聞）
8月2日　筒井和男（京大大学院）
１８日　北岡豪一（岡山理科大：24 日まで），山田誠（大阪教育大大学院：２３日まで），
河野　忠（日本文理大学），手嶋修一（別府市温泉課）
１９日　野口哲男（別府市議会議員）
２１日　山口一裕（岡山理科大）
２３日　宮坂恵次（映像新社），堀江正治（京大名誉教授）
２４日　テレビ大分取材
２７日　高島・山本（別府市教育センター）
8月29日　手話サークルにじ一行
9月7日　高松信樹・岩倉一敏・半谷亜有美（東邦大学：10 日まで）
１３日　牧野芳大（大分県衛生環境研究センター），宮坂恵次（映像新社）
２５日　竹村恵二（京大院理）
２７日　栗田典年（大分県教育センター）
10月21日　中野義幸（別府市国際交流推進室）
２８日　福田道博（九大工学研究科）及び地熱研修コース一行（10 名）
11月8日　淡路敏之・根田昌典（京大理学研究科）
１２日　栗田敬他７名（東大・九大・地調：１７日まで）
１５日　韓国済州文化放送取材班一行（８名）
２２日　Rogel A. Santos（28 日まで）
２９日　熊谷公生（九重町）
12月1日　小西喜久男・伴佳英・島田裕美・藤澤雅章・中村守（京大施設部）
１０日　太田幸憲・御沓利弘（大分県生活環境課）
１７日　NHK 取材班
２０日　伊藤笙・牧ヶ野英生（キューバス）
２１日　清水・池田（電源開発）

２４日　Paul Stradins 博士夫妻

２０００年

１月２０日　林昌治（別府青年会議所），牧ヶ野英生（キューバス）

２４日　井本雅昭・永田裕美・小玉明彦・布施智美（京大経理部）

２７日　松下 忍（愛媛大学大学院理工学研究科生物地球圏科学専攻地球進化学講座：２９日まで）

３０日　本松利郎（出光大分地熱）

２月４日　Rogel A. Santos（8 日まで）

２月１１日　村岡洋文・浦井稔（地質調査所），Ir. Kastiman Sitorus （インドネシア火山調査所）ほか１名

１５日　早川知宏（文部省学術国際局学術課・学術振興係），増地公一（京大経理部）

１７日　坂田節子・大川昌治（京大木質科学研究所），田村　芳彦（金沢大学理学部地球学科：１８日まで），田中　康博（金沢大学理学部地球学科：１８日まで）

２４日　東山邦雄・濱田慎二（施設部）

２８日　細川紀子（読売新聞）

３月２日　丸山正樹（京大理学研究科）

６日　高松信樹・岩倉一敏（東邦大学：８日まで）

９日　西田宏・松井規至・金川智子（京大総合人間学部）

１３日　三浦・中野（別府ケーブルテレビ），牧ヶ野英生（キューバス），林昌治（別府青年会議所），中川一郎（京大名誉教授）

２３日　北岡豪一（岡山理科大：25 日まで）

２７日　鎌田浩毅（京大総合人間学部）ほか

２８日　東辻保男（京大理学部施設掛）

３１日　金庫検査；小池正一・森田勇二（京大経理部），成井明徳（京大理学部）